UTILIZATION OF*MUSA PARADISIACA* LEAF EXTRACT-BASED INHIBITORFOR CORROSION PROTECTION OF CARBON STEEL IN 3.5% NaCl

BY

IDEMA, OSUANI FYNEFACE (B.Eng.; M. Eng. FUTO)

ACEFUELS/21/PhD/11000119

A DISSERTATION SUBMITTED TO ACE-FUELS, POSTGRADUATE SCHOOL, FEDERAL UNIVERSITY OF TECHNOLOGY, OWERRI

IN PARTIAL FULFILMENT OF THE REQUIREMENTS FOR THE AWARD OF THE DEGREE OF DOCTOR OF PHILOSOPHY (Ph.D.) IN CORROSION TECHNOLOGY

OCTOBER, 2025

CERTIFICATION

This is to certify that this work "**Utilization of *Musa paradisiaca* leaf extract-based inhibitor for corrosion protection of carbon steel in 3.5% NaCl"** is an original work carried out by **Idema Osuani Fyneface (ACEFUELS/21/Ph.D/11000119)** in partial fulfilment of the requirements for the award of the Degree of Doctor of Philisophy in Corrosion Technology in the African Centre of Excellence in Future Energies and Electrochemical Systems (ACE-FUELS) Post Graduate School, Federal University of Technology, Owerri (FUTO), Imo State, Nigeria.

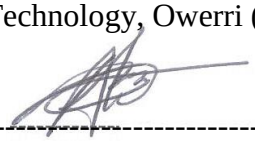

27/10/25

Dr. I.O. Arukalam **Date**
(Supervisor)

28-10-25

Dr. E. Ekeke **Date**
(Co-Supervisor)

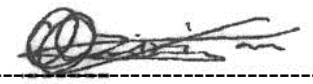

29/10/25

Dr. C.N. Njoku **Date**
(Co-Supervisor)

Dr. Christopher Akalezi **Date**
(Programme Coordinator)

Prof. E.E. Oguzie **Date**
(Centre Leader, ACE-FUELS)

Prof. J.N. Nwosu **Date**
(Dean, Postgraduate)

29/10/25

Date

(External Supervisor)

DEDICATION

This dissertation is dedicated to God Almighty on whose benevolence my sustenance depends on.

ACKNOWLEDGEMENTS

I wish to sincerely appreciate the Almighty GOD for his kindness and enablement to successfully carry out this research work.

Most importantly, let me whole heartedly acknowledge the unwavering support and unfettered mentorship I enjoyed from the Centre Leader Prof. E. E. Oguzie for his untiring and very personal approach he deliberately adopted in attending to the academic challenges of all students of the center which I also benefitted.

I wish to also express my unalloyed delight to Prof. A. Madu, the deputy centre leader who always made sure to be present in all of my progress report presentations to offer intelligent contributions that helped in a great deal to shape this project work in this present form.

Worthy of note is the undivided attention I enjoyed from my supervisory team who are made up of the following eminent Academics and members of faculty such as, Prof. M. Abdulwahab, Dr. I. O. Arukalam, Dr.I.C. Ekeke, Dr. N.C. Njoku, Dr. I. B. Onyeachu and Dr. C. N. Anyiam in no particular order, whose faculty and invaluable contributions shaped this research work to this present form. I'm indebted to each and every one of them.

My warmest gratitude goes to Prof. S. O. Onyekuru…the PhD research coordinator; Dr. C. Akalezi…the corrosion technology programme coordinator; Dr. I. I.Ayogu…webinar coordinator; Mrs C. A. Appiah…the administrative team lead; and Mr J. O. Anyanwu…the senior research laboratory attendant whose critical contributions made the project a success.

Furthermore, may I express my sincere appreciation to Prof. J. N. Nwosu, the Dean of post graduate school, FUTO for her tireless efforts, dignified and graceful manner in which she adopted as chairperson of this project's internal defense review committee in diligently proffering scholarly debate and constructive inputs that heralded the overall improvement of this project work.

Likewise, let me also appreciate the contributions of Mrs U. Prisca in typing and formatting the thesis which gave me the leverage for more time for research activities, her tenacity and zeal in doing whatever she was directed and suggested to was examplary.

In a very prominent way, may I acknowledge the following persons Prof. O. Oguoma; Prof. A. C. Okoronkwo; Prof. B. Okafor and Prof. J. Igbokwe of blessed memory for their mentorship during my undergraduate days that gave me the tenacity to pass through the often academically charged and tensed FUTO learning environment while having the flexibility for all the valuable experiences passing through me. Infact, the very idea of Africa Centre of Excellence for Future Energies and Electrochemical Systems was brought to my notice

during one of our fruitful conversations by Prof. O. Oguoma who directed Prof. A.C Okoronkwo to recommend me for the program, I remain indebted to them.

May I also recognize the contributions of Pst. O. W. Itari and family, my resident pastor who often joins his faith with mine in prayers and supplications to God for my safety and enablement throughout this project work due to my ugly kidnap experience in 2017 on the Port Harcourt/Owerri road that saw me spend two grueling weeks in the kidnapper's den, his sacrifices mean the world to me.

I wish to also acknowledge my parents Mr and Mrs F. Idema whose inspiration kept me on my toes to see to the final completion of this research work, their consistent calls and inquiry on what challenges I was encountering in course of this project was highly encouraging.

May I also gratefully appreciate my Wife, Mrs L. S. Idema and children whose endless sacrifices and moral support gave me reasons to continue inspite of obvious family challenges during the period of this research work as a result of my frequent physical absence.

Finally, my profound regards go to everyone who has in one way or the other contributed to the successful completion of this research work. I thank you all and wish that God almighty attend to every of your need.

TABLE OF CONTENTS

LIST OF TABLES

LIST OF FIGURES

ABSTRACT

The utilization of *musa paradisiaca* leaves (MPL) extract-based inhibitor on carbon steel protection in marine environment has been studied using gas chromatography mass spectroscopy (GC-MS), Fourier transform infrared spectroscopy (FT-IR), gravimetric method (GM), Atomic force microscopy (AFM), Contact angle measurement (θ), potentiodynamic polarization (PDP), electrochemical impedance spectroscopy (EIS), density functional theory (DFT) and molecular dynamics (MD) simulations. Firstly, the GC-MS analysis showed the presence of compounds with heteroatoms in the MPL inhibitor. Likewise, the FT-IR analysis showed the presence of polar functional groups. The GM showed MPL extract-based inhibitor having optimum inhibition efficiency of 91% at a concentration of 100g/L and immersion time of 120 hours which led to a decrease in corrosion rate from 0.8817 mm/y to 0.0823 mm/y. Also, the weight loss experienced by the test specimen decreased from 0.0986g to 0.0091g. AFM morphology revealed thin film adhesion showing firm adsorption of Langmuir films on the metal/inhibitor interface, with root mean square roughness values for uninhibited and inhibited substrates 71.2722Rq and 33.6773Rq respectively. Likewise, contact angle measurement showed high contact angle of 152.42$^{\bullet}$with a hydrophobic metal/inhibitor interface for inhibited substrate hence not prone to corrosive species and low contact angle of 76.20$^{\bullet}$ for the uninhibited substrate with hydrophilic surface which is prone to invasive corrosive species. The potentiodynamic polarization (PDP) via Tafel plots showed a cathodic slope capable of controlling both activation (oxidation) and diffusion (oxygen reduction) reactions. Also EIS via Nyquist, Bode plots and Phase angle showing high polarization resistance thereby reducing corrosion rate. Further, Density functional theory (DFT) analysis correlated the results by affirming the contributions of the isolated compounds of the MPL inhibitor molecule to the inhibition efficiency of 91%. In addition, MD results showed planer orientation of MPL inhibitor molecules over the surface of the substrate as such enhancing larger surface coverage, hence better inhibition effectiveness. Also, the high adsorption energy of -184.954cal/kJ is indicative of chemisorption. Radial distribution function (RDF) showed presence of short bond lengths of between 2.97-3.49 atom thick, confirming the presence of strong covalent bonding. Test of adsorption isotherms reveal conformance of the Langmuir model.

Keywords: Adsorption sites, carbon steel corrosion, electrochemical measurements, Gravimetric method, Langmuir isotherm, Musa paradisiacal leaf, organic corrosion inhibitors, Plant extract, Surfactant, Surface interaction, theoretical and computational studies

CHAPTER ONE

INTRODUCTION

1.1 Background Information

Corrosion is the deterioration, degradation and loss of a material and its critical engineering properties as a result of its interaction with the surrounding environment. When a metal reacts with oxygen, hydrogen, electrical current, dirt and bacteria, corrosion could emanate. Also, when metals are exposed to external environmental factors such as moisture, acid rain, acids, bases, harmful gases and chemicals which include, NH_3, Cl_2, sulfur oxide and hydrogen oxide, the phenomenon of corrosion sets in (Fonseca, Tagliari, Guaglianoni, Tamborim, Borges., 20240; Chatterjee, Bose & Roy., 2001). To state succinctly, corrosion is a spontaneous thermodynamic process in which a metal in its thermodynamic unstable but refined state gradually returns back to its originally crude but stable state when exposed to its immediate environment.

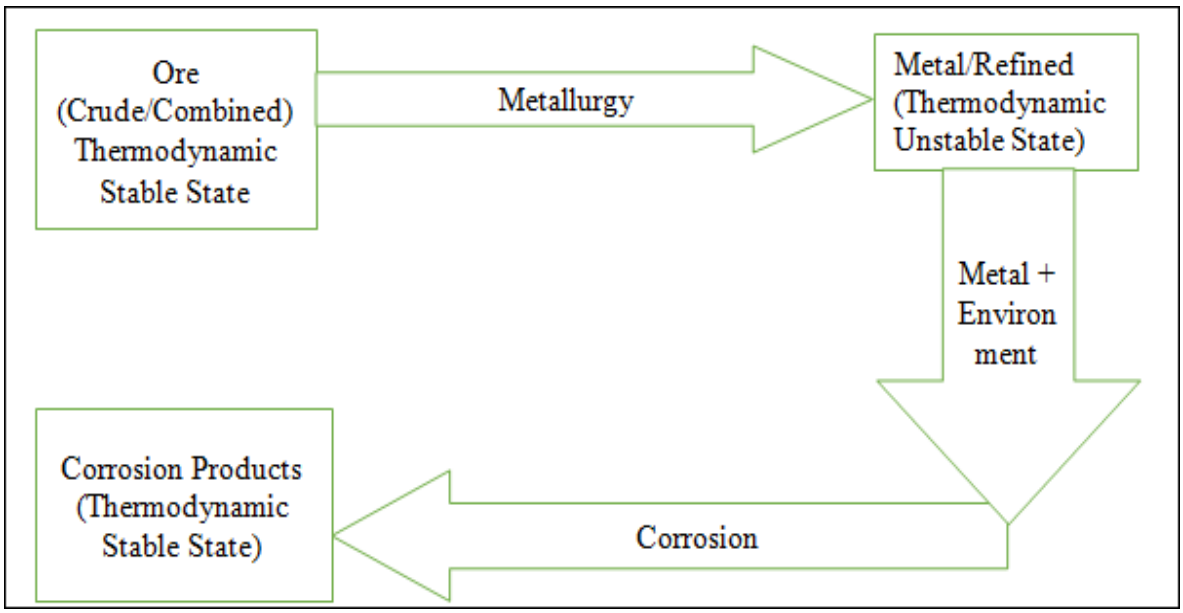

Figure 1.1: A typical corrosion process

Corrosion is destructive and could lead to catastrophic consequenceswith huge human and economic costs. The financial implications of corrosion are huge. According to the national association of corrosion engineers (NACE), the cost of corrosion's debilitating effects is estimated at 2.5 trillion US dollars each year and this is about 3% of global GDP (Verma,Ebenso, Quraishi, & Hussain, 2021). Because of this huge economic effect; prevention, control and mitigation of corrosion have been advocated and have been the practice. In fact, NACE estimated that implementing best practices in corrosion prevention could result to significant cost savings of up to about 875 billion US dollars yearly (Verma et al., 2021).

The methods of implementing these best practices include:

1. Selection of materials
2. Application of inhibitors
3. Application of coatings
4. Cathodic protection
5. Design

However, the application of inhibitors will form the basis of this work.The application of corrosion inhibitors is widely used in companies, commercial processes, and industrial environments. Originally, rusting and anodic corrosion of metals could be addressed by applying a chromate layer on a metal surface. Corrosion inhibitors like oxygen scavengers react with dissolved oxygen in the environment and prevent cathodic corrosion. They function by deactivating the corrosivity of corrodents, and then adsorb on the metal or alloy surfaces to form a protective layer (Kaczerewsk et al., 2018; Verma, Quraishi and Ebenso, 2018a).

Basically, corrosion inhibitors may be categorized as cathodic, anodic, or mixed type depending on the cathodic or anodic reaction of the corrosion process or both, respectively. The inhibition of anodic corrosion reactions could be due to reduction in the corrosion of active surface area of metal while inhibition of cathodic corrosion is due to a change in the activation energy of the oxidation or reduction in the corrosion process (Gan, 2023). The synergism of cathodic and anodic corrosion inhibitors often produces improved protection. The inhibition process is followed by formation of protective film, which may be of three different types: passivating, precipitating, and adsorption types.

Based on this, several corrosion control methods have been formulated. Among them is the use of inorganic compounds mainly nitrites, chromates, borates, molybdates, silicates, and zinc salts (Verma et al., 2021). The effectiveness of these compounds is the formation

of passive film over metal surfaces (passivation) through their adsorption as such they are known as passivators. However, as time progressed, they were replaced by more economical alternatives such as phosphonic acid, gluconates, polyacrylates, surface active chelates, polyphosphates, poly phosphonates, phosphonates, and carboxylates which were the common corrosion inhibition strategy during 1960-1980 (Verma et al., 2021). Overall, these compounds are precipitated at the metal/electrolyte interface and therefore they are called precipitating inhibitors (precipitators). Further, due to adverse environmental effects of most of the precipitating corrosion inhibitors, they were substituted by eco-friendly natural alternatives, such as biopolymers, bio-surfactants, plant and animal extracts. This approach came into full effect during 1980-1995. From 1995 to present, more environment-friendly and durable approaches such as the use of rare earth metals (REM), polyfunctional compounds, the synergism of organic/inorganic compounds using REM, and the encapsulation of inhibitors became the main areas of focus (de Damborenea, Conde & Arenas, 2014). These alternatives have demonstrated durable and high protection effectiveness with very low, or no toxicity.

Recent research studies in corrosion inhibition are now focused on the design, synthesis, development, and consumption of sustainable inhibitors. This is in line with global sustainable development goals (SDGs) which are anchored on materials sustainability and environment protection. Thus, various environment-friendly materials derived from biomass resources such as biopolymers, plant extracts (oils, exudate gums, phytochemicals), herbal drugs, *etc*., are widely used (Verma, Obot, Bahadur, SherifEbenso, 2018c). Interestingly, various biopolymers in their pure and modified forms are extensively utilized as sustainable corrosion inhibitors (Imai, Shiraishi, Saito, &Otagiri., 1991; Singla& Chawla, 2010; Guo et al., 2007; Portes, Gardrat, Castellan, & Coma, 2009). Additionally, compounds derived through multicomponent reactions (MCRs), microwave (MW) and ultrasound (US) irradiations are also regarded as sustainable inhibitor alternatives (Verma et al., 2018b). Moreso, ionic liquids (ILs) which possess low vapor pressure are also considered environment-friendly materials (Ardakani, Kowsari & Ehsani., 2020). Again, chemical blends involving green solvents such as water, ILs (ionic liquids) and supercritical CO_2 are regarded as sustainable inhibitor systems.

In view of the above, sustainable organic corrosion inhibitors have been confirmed as one of the most effective and facile methods of corrosion inhibition because of their association with E4 (efficiency, economy, ecology, and environmental-friendliness) factors (Verma et al., 2018b; Alhaffar, Umorem, Obot, & Ali, 2018; Kaczerewsk et al.,2018). These organic corrosion inhibitors find applications in various industrial operations. For instance, organic

corrosion inhibitors are used extensively in oil exploration and drilling operations, crude oil refining operations, petrochemical plants, chemical storage tanks, etc. In addition, corrosion inhibitors are commonly added to coolants, fuels, hydraulic fluids, boiler water, engine oil and many other fluids used in the industry. They are also embedded in organic coatings to improve protection performance.Inthe case of industrial processes like oil-well acidification, acid descaling, acid pickling, and acid cleaning processes, corrosive species are introduced into such systems which eventually result to corrosion. Therefore, corrosion inhibitors are used to mitigate the corrosive effects. The degradation of infrastructural materials leads to maintenance downtime and severe failure of structures, environmental flora and fauna are also impacted such that hazards and injury to living organisms are rife. To state clearly, the huge cost associated with the corrosion of materials and infrastructures such as cooling systems, refinery units, pipelines, oil and gas production units, boilers, water processing units, paints, pigments, and lubricants can be reduced when they are protected from corrosion using corrosion inhibitors (Kaczerewsk et al.,2018). Figure 1.2 shows some industrial application of corrosion inhibitors.

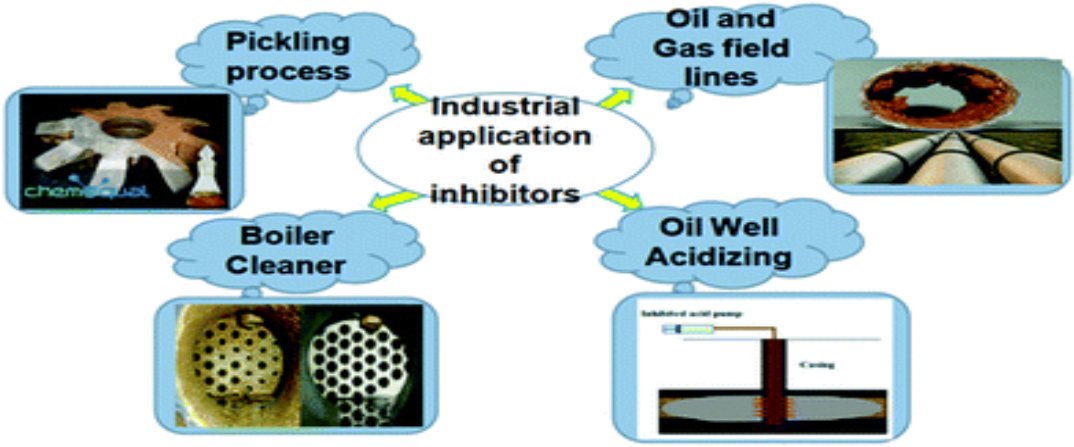

Figure 1.2: Industrial application of corrosion inhibitors (Verma et al., 2021)

In this work, *Musa Paradisiaca* L. (MPL) extract was used as organic inhibitor because it is known to contain hydrophilicpolar functional groups in its molecular structure.Generally, plant extracts are considered to be an abundant source of naturally derived chemical compounds that can be extracted from several parts of plants, such as leaves, stem, root, bark, fruits, fruit peel, seeds, flowers, husks, and nuts, which contain phytochemicals and organic compounds like alkaloids, flavonoids, heteroatoms, tannins, and nitrogen-based compounds. They are easily extracted, inexpensive, and environmentally friendly.

They are also widely available and naturally biodegradable. These benefits explain why plant extracts and their byproducts are used as corrosion inhibitors for metallic materials and alloys in various environments. Plant extracts are rich in polar molecules with oxygen, sulfur,

phosphorus and nitrogen, as well as nonpolar compounds with aromatic rings, aliphatic chains, heterocyclic rings, and functional moieties. These are thought to promote the adsorption of inhibitors on the surfaces of metals and form a protective film on metallic surface without affecting the surroundings and hence decrease the rate of corrosion. Methanol, ethanol, acetone or any other suitable aqueous solvent is used to extract the majority of plant extracts. Based on their chemical compositions and properties, phytochemicals are thought to be the cause of the corrosion inhibition. So, it is crucial to identify the chemical components in plant extracts in order to have a foreknowledge of how effective they would perform in inhibiting corrosion. The phytochemical components in plant extracts can be examined and identified chemically and with the use of characterization techniques.

1.1.1 Key Concepts

The following are some of the key concepts considered in the design of corrosion inhibitors:

- Synergism
- Wettability and Contact Angle
- Hydrophobicity
- Hydrophilicity
- Lewis Acid-Base Theory
- Frontier Molecular Orbitals Theory.

1.1.2 Synergism

Synergism is the interaction of two or more substances to produce a combined effect greater than the sum of their separate effects. Synergism is described by as a tendency in which the combined action of compounds is greater than the sum of the individual effects of the compounds (Pezzani et al., 2019). For corrosion inhibitor systems, synergism arises either as a result of interaction between components of the inhibitor formulation or due to interaction between the inhibitor and one of the species present in the aqueous medium. In fact, synergism is of considerable interest in corrosion protection because the phenomenon boosts corrosion inhibition when a proper combination of inhibitors is used, that is., the resulting mixture displays superior corrosion inhibition performance compared to individual compounds in the mix. Many examples of synergistic blends are known, ranging from organic to inorganic compounds as well as combinations of organic compounds with halides other anions, rare earth salts and metal cations (Pezzani et al., 2019).

1.1.3 Wettability and Contact Angle

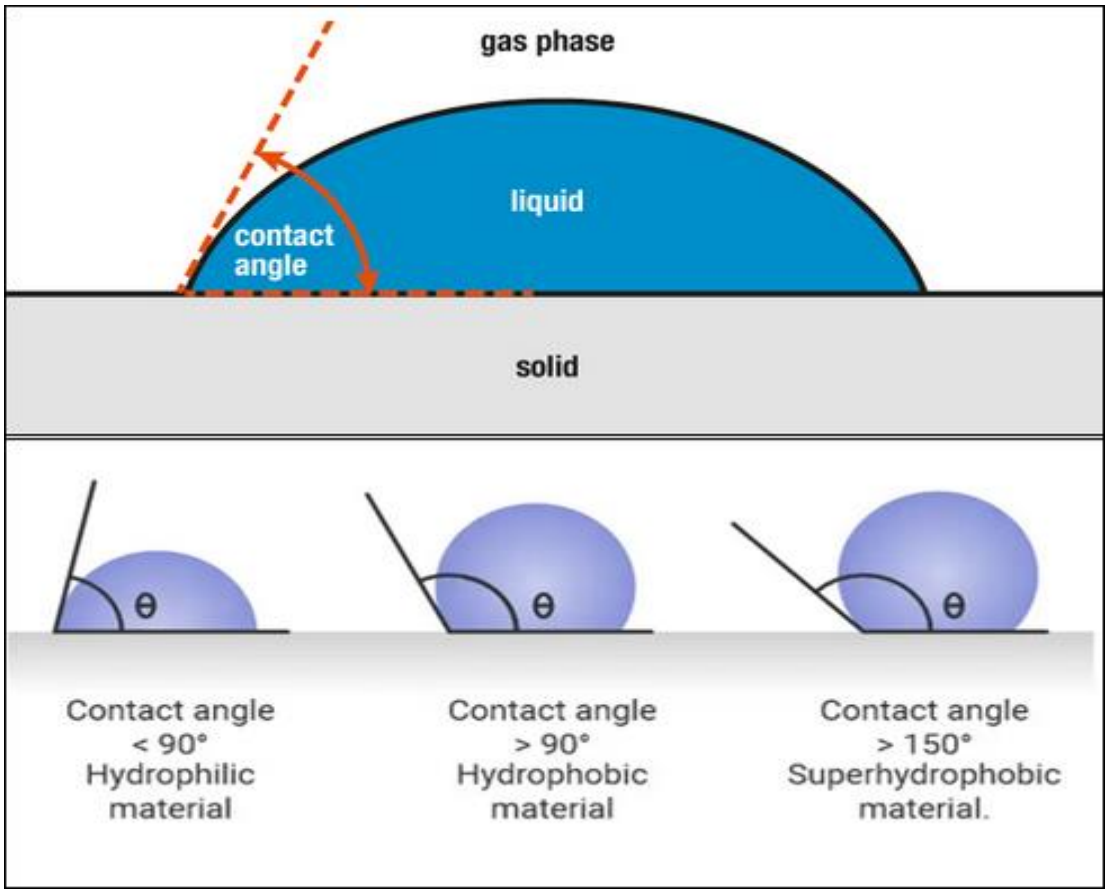

Figure1.3: Showing contact angles (Giridhar, Manepalli&Apparao, 2017)

Wetting is a very important property to understand the bonding and adherence strength of a solid surface or any two materials. The adhesive force in the liquid helps in spreading across a solid surface whereas the cohesive forces in the liquid avoid the liquid from spreading on a solid surface. The contact angle is one of the qualitative ways of measuring the wettability of the liquids and it determines if the solid surface is favorable or unfavorable to wetting. If the contact angle is less than 90 degrees then it is called the low contact angle which indicates that the surface is favorable to wetting (Giridhar, Manepalli & Apparao, 2017). If the contact angle is greater than 90 degrees then it is called high contact angle indicating that the surface is unfavorable to wetting. This is represented by Figure 1.3. In the case of water, this interaction on the solid surface can be termed as the hydrophilic and hydrophobic nature of the material surface. The type of solid surface on which the liquid interacts and spreads over causes different wettability hence it is important to understand the type of solid surface it interacts with. There are mainly two types of solid surfaces interacting with the liquid. They are high-energy and low-energy solid surfaces (Giridhar, Manepalli & Apparao, 2017)

High energy solid surface**:** Solid materials such as metals, ceramics, glasses, and others which have very strong chemical bonds such as covalent and ionic bonding are very strong. When there is an interaction of liquid on these surfaces then there is a need for larger forces to break the bonding and the liquids attain complete wetting on these surfaces.

Low energy solid surface**:** The solids with weaker molecular bonding such as hydrocarbons or fluorocarbons where their molecules are bonded by van der Waals forces or hydrogen bonding are termed as low energy solid surfaces. The wetting on these surfaces depends on the type of liquids and it may be partial wetting or complete wetting.

1.1.4 Hydrophobicity

Hydrophobic surface**:** A surface is called hydrophobic surface if it repels the water, in this case, the water does not spread over the surface. The wettability of the surface is considered to be not good with high contact angle. The cohesive force is dominating this liquid-solid interaction. Hydrophobic surface is characterized by Young contact angle, for any liquid, that is larger than or equal to 90° (Giridhar, Manepalli & Apparao, 2017).

1.1.5 Hydrophilicity

Hydrophilic surface**:** A surface is called hydrophilic surface if it attracts the water, in which the water droplets spread on the surface. The wettability of the surface is very good with a low contact angle. The adhesive force between the liquid and solid is high in this case. Hydrophilic surface is characterized by Young contact angle, for any liquid, that is smaller than 90° (Giridhar, Manepalli & Apparao, 2017).

1.1.6 Lewis Acids and Bases

A. Lewis Acid

Lewis acid accepts electron lone pair and they are electrophilic meaning that they are electron attracting. When bonding with a base the acid uses its lowest unoccupied molecular orbital or LUMO as in Figure 1.4.

Various species can act as Lewis acids. All cations are Lewis acids since they are able to accept electrons, for example; Cu^{2+}, Fe^{2+}, Fe^{3+}.An atom, ion, or molecule with an incomplete octet of electrons can act as Lewis acid, for example; BF_3, AlF_3. Also, molecules where the central atom can have more than 8 valence shell electrons can be electron acceptors, and thus are classified as Lewis acids, for example, $SiBr_4$, SiF_4. Furthermore, molecules that have multiple bonds between two atoms of different electronegativities are thought to be Lewis acids, for example CO_2, SO_2 (Larsen, 2023).

B. Lewis Bases

On the other hand, Lewis bases have lone pair electrons to share and thus occupy a higher energy level. They donate an electron pair. They are nucleophilic, meaning that they "attack" a positive charge with their lone pair. They utilize the highest occupied molecular orbital or HOMO as in Figure 1.4. An atom, ion, or molecule with a lone-pair of electrons can thus be a Lewis base. Each of the following anions can "give up" their electrons to an acid. For example: OH^-, CN^-, CH_3COO^-, NH_3, H_2O, CO. Lewis base's HOMO (highest occupied molecular orbital) interacts with the Lewis acid's LUMO (lowest unoccupied molecular orbital) to create bonded molecular orbitals. Both Lewis acids and bases contain HOMOs and LUMOs but only the HOMO is considered for bases and only the LUMO is considered for Acids (Larsen, 2023).

1.1.7 Amphoteric Substances

It has been observed that acids and bases are two separate things. However, some substances can be both an acid and a base. Water has shown this unique characteristic, which can act as an acid or a base. This ability of water to do this makes it an amphoteric molecule. Water can act as an acid by donating its proton to the base and thus becoming its conjugate acid, OH- as shown in Equation 1.1. However, water can also act as a base by accepting a proton from an acid to become its conjugate base, H_3O^+ as in Equation 1.2.

Water acting as an Acid: $H_2O+NH_3 \rightarrow NH^{+4}+OH^-$ 1.1

Water acting as a Base: $H_2O+HCl \rightarrow Cl^-+H_3O^+$ 1.2

It is important to note that the degree to which a molecule acts depends on the medium in which the molecule has been placed in. Water does not act as an acid in an acid medium and does not act as a base in a basic medium. Thus, the medium which a molecule is placed in has an effect on the properties of that molecule. Other molecules can also act as either an acid or a base (Larsen, 2023).

1.1.8 Frontier Molecular Orbitals Theory

The frontier molecular orbitals of a compound are at the "frontier" of electron occupation—the highest-energy occupied and lowest-energy unoccupied molecular orbitals (the HOMO and LUMO). The HOMO is logically viewed as nucleophilic or electron donating, while the LUMO is electrophilic and electron accepting. Frontier orbitals, that is, the highest occupied molecular orbital (HOMO) and the lowest unoccupied molecular orbital (LUMO), are important indicators for the effect of adsorption on a metal (Larsen, 2023). It is important to mention that the interaction of organic corrosion inhibitors with the metallic surface involves the donor–acceptor (charge sharing) phenomenon, as in Figure 1.5.

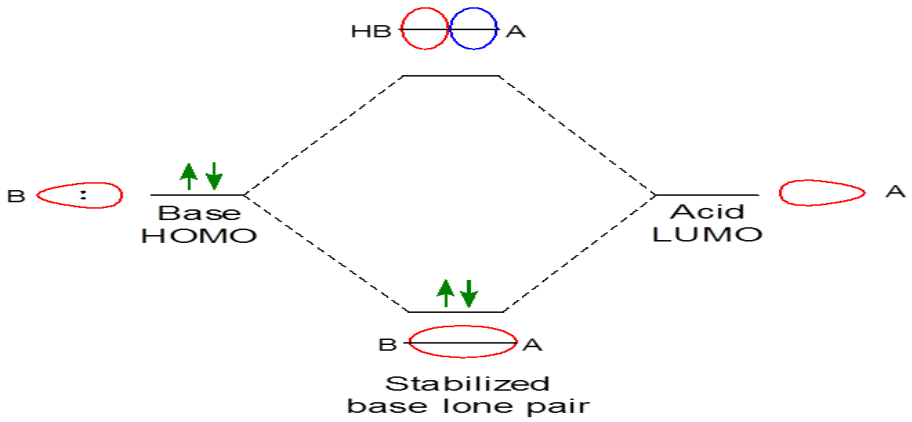

Figure1.4: Generalized frontier orbital picture for adduct formation between a Lewis base (B) and a Lewis acid (A) (Larsen, 2023).

1.2 Statement of the Research Problem

There are numerous challenges of using organic inhibitors for corrosion protection. Some of these challenges are low specific gravity, thermal decomposition, reacting with resins, prolonged cement setting time and limited solubilty. However, limited solubility has been a major challenge, especially in polar electrolytes. Organic corrosion inhibitors are used in a variety of ways in the oil and gas industry such as in drilling fluids to protect drilling equipment and organic acid production to minimize damage to carbon steel surfaces that are often used in the oil and gas industry. To solve this problem, current research studies in corrosion science and engineering are oriented towards the development of corrosion inhibitors that contain hydrophilic polar functional substituents in their molecular structures, which have the ability to be soluble in polar electrolyte.

Hence, in this studythe use oforganic compound containing hydrophilic polar functional substituents in its molecular structure, namely; MPL, for the corrosion protection of carbon steel in order to mitigate corrosion in the oil and gas industry is highlighted.

1.3 Objectives of Study

The main objective of this work is to evaluate the utilization of *musa paradisiaca* leaf (MPL) extract-based inhibitor for the protection of carbon steel corrosion in 3.5 wt. % NaCl. This main objective was achieved through the following specific objectives:

i. determination of the chemical compounds presents in the MPL extract using GC-MS
ii. extraction and characterization of MPL extract using FT-IR
iii. evaluate the corrosion rate of the carbon steel specimen in 3.5wt% NaCl, the inhibition efficiency of the MPL extract and the MPL concentration for effective corrosion inhibition of carbon steel using GM.

iv. evaluate the surface morphology of the carbon steel specimen with and without MPL in 3.5wt% NaCl solution using AFM.

v. determine the contact angles of the carbon steel surface in 3.5wt% NaCl solution with and without the MPL inhibitor using optical tensiometer.

vi. determine the Tafel plots, Nyquist plots, Bode and Phase angle curves of the carbon steel in 3.5wt% NaCl with and without MPL inhibitor in various concentrations using electrochemical measurements.

vii. determine HOMO-LUMO and other global quantum chemical descriptors of the compounds in MPL molecule and molecular interfacial interaction of MPL/substrate using DFT and MD.

viii. determine the adsorption phenomenon on the adsorption site of the metal/MPL extract interface by test of isotherms

1.4 Justification of the Study

With an inhibition efficiency of 91%, a large surface coverage of 0.91 and presence of Langmuir films, MPL has demonstrated the qualities of a very good corrosion inhibitor for carbon steel in 3.5% NaCl. Also, the presence of hydrophilic substituents and polar functional groups have shown that it is highly soluble in water and organic electrolytes, again another unique property and exceptional quality of a good organic corrosion inhibitor. Because of its solubility, it has the ability to sequester corrosive ions and oil molecules. In addition, the presence of hydrophobic substituents in its molecule makes it function like a typical SURFACTANT. Consequently, surface active agents (surfactants) are a group of very important substances for various industrial applications for corrosion mitigation. Further, they are used extensively in all stages of oil industry for corrosion control contributing significantly in various processes from oil drilling and well completions to enhanced oil recovery. Meanwhile, inorganic surfactants are expensive and also have environmental safety concerns. Therefore, currently research is oriented towards organic substances such as plant extracts. Most importantly, plant extracts are inexpensive, environment-friendly and the use of these eco-friendly inhibitors aligns with the growing emphasis on sustainability in industrial practices, offering a promising opportunity for corrosion management without compromising environmental and health standards. Hence, this study has contributed significantly to the body of knowledge in identifying MPL as a biosurfactant.

1.5 Scope of the study

This research is restricted to the use of GC-MS, FT-IR, experimental methods (gravimetric and electrochemical measurements), surface roughness measurements, contact angle

measurements and theoretical/computational methods (density functional theory (DFT) and molecular dynamics simulation (MD) from material studio). It involves the determination of hetero-atoms, polar functional groups, weight loss, corrosion rate, inhibition efficiency, test of adsorption isotherms and surface coverage. It is followed by surface characterization, surface wetness determination and confirmatory analyses using DFT and MD. Also, global molecular descriptors and interfacial/atomic level interaction are determined. In addition, Origin software is used for results presentation.

CHAPTER TWO

LITERATURE REVIEW

2.1 Conceptual Literature

The use of energy is generally taken as an index of standard of living. We use energy in the form of firewood, electricity and fossil fuels (Shreir, 2010). In order to utilize energy, infrastructures are needed, designed to enable its extraction, transportation, distribution and use. Most often, the infrastructure needed are designed with engineering materials which are exposed to corrosion. Therefore, the viability and functionality of such infrastructures are determined by how well they are protected from corrosion.

Corrosion is generally viewed as a universal phenomenon (Fernandes &Monternor, 2015). Engineering materials can be metallic or nonmetallic. In the case of non-metallic materials, the term corrosion invariably refers to their deterioration from chemical causes, but a similar concept is not necessarily applicable to metals. Many authorities are of the view that the term metallic corrosion embraces all interactions of a metal or alloy (solid or liquid) with its environment, not minding whether this is deliberate and beneficial or unplanned and damaging (Hoar, 1961; Ceciia& Carrizo, 2022). This definition of corrosion, which is for convenience sake will be referred to as the transformation definition, will include, for example, the deliberate, anodic dissolution of zinc in cathodic protection and electroplating as well as the spontaneous gradual wastage of zinc roofing sheet due to atmospheric exposures.

On the other hand, Uhlig (2011) defined corrosion as the undesirable deterioration of a metal or alloy. This definition which will be referred to as the deterioration definition, is also applicable to non-metallic materials such as glass, concrete, etc. and embodies the concept that corrosion is always damaging. However, the restriction of the definition to undesirable chemical reactions of a metal results in anomaly which will become apparent from a consideration of the following instances.

When steel is exposed to an industrial atmosphere, it reacts to form the reaction product rust, of approximate composition $Fe_2O_3.H_2O$, which being loosely adherent does not form a protective barrier that isolates the metal from the environment; the reaction thus proceeds at an approximately linear rate until the metal is completely consumed. Copper, on the other hand forms an adherent green patina, corresponding approximately with bronchantite, $CuSO_4.3Cu\ (OH)_2$ which is protective and isolates the metal from the atmosphere. Copper roof installed 200 years ago are still performing satisfactorily, and it is apparent that the formation of bronchantite is not damaging to the function of copper roofing material-indeed,

in this particular application it is considered to enhance the appearance of the roof, although a similar patina formed on copper water pipes would be aesthetically objectionable (Shreir, 2010).

The rapid dissolution of a vessel constructed of titanium in hot 40% H_2SO_4 with the formation of Ti^{4+} aquo cations meets the requirement of the two definitions of corrosion, but if the potential of the metal is raised (anodic protection), a thin adherent protective film of anatase TiO_2, is formed, which isolates the metal from the acid so that the rate of corrosion is enormously decreased (Shreir., 2010). The formation of this very thin oxide film on titanium, like that of the relatively thick bronchantite film on copper, clearly meets the requirement of the transformation definition of corrosion but not the deterioration definition, since in these examples the rate and extent of the reaction is not significantly detrimental to the metal concerned (Shreir, 2010).

Also, is the case of magnesium, zinc or cathodic protection of steel structures, as these metals are clearly not required to be so maintained as such, their consumption in this particular application cannot according to the deterioration definition, be regarded as corrosion. Furthermore, corrosion reactions can be of advantage in technological processes such as pickling, etching, chemical and electrochemical polishing and machining. According to Sheir (2010), the examples, already discussed lead to the conclusion that any reaction of a metal with its environment must be regarded as a corrosion process irrespective of the extent of the reaction or of the rates of the initial and subsequent stages of the reaction. It is not illogical, therefore, to regard passivity, in which the reaction product forms a very thin protective film that controls rate of the reaction at an acceptable level, as a limiting case of a corrosion reaction. He further stated that both the rapid dissolution of active titanium in 40% H_2SO_4 and the slow dissolution of passive titanium in that acid must be regarded as corrosion processes, even though the latter will not be detrimental to the metal during the anticipated life of the vessel.

Fontana and Staehle (2013) on their part, stated that corrosion will include the reaction of metals, glasses, ionic solids, polymeric solids and composites with environments that embrace liquid metals, gases, non-aqueous electrolytes and other non-aqueous solutions, thereby extending the scope of the term corrosion even further (Fontana &Staehle, 2013).

Vermilyea (1972) who has defined corrosions as a process in which atoms or molecules are removed one at a time, considers that evaporation of a metal into vacuum should fall within the scope of the term, since atomically it is similar to other corrosion processes (Vermilyea., 1972).

Evans (1948) on his part considers that corrosion may be regarded as a branch of chemical thermodynamics, of kinetics as the outcome of electron affinities of metals and non-metals, as short-circuited electrochemical cells, or as the demolitions of the crystal structure of a metal.

The above considerations from the various authorities lead to the conclusion that there is probably a need for two definitions of corrosion, which depend upon the method adopted such as;

-Definition of corrosion in the context of corrosion science, to the effect that; the reaction of a solid with its environment is known as corrosion.

-Definition of corrosion in the context of corrosion engineering, to the effect that; the reaction of an engineering material with its environment with a subsequent deterioration in properties of the material is known as corrosion.

2.1.1 The Phenomenon of Corrosion

Although corrosion is fundamentally associated with metallic materials, however, non-metallic materials can also corrode. For instance, ceramics also corrode through selective dissolution. In as much as it cannot be completely eliminated from existence, corrosion is a major happening that every individual hopes to overcome as its effect is never ever a favorable experience. Lowering of the system's Gibbs free energy has been found to be the major cause of all forms of corrosion (Saranya, et al., 2016). The atmosphere where corrosion arises may be air, gas or hybrid water-based. Such conditions are referred to as electrolytes because they possess their own conductivity for the flow of elections. The corrosion cycle requires a minimum of two reactions in a semi-corrosive atmosphere. Such reactions are called anodic and cathodic (Alemayehu &Birahane, 2014). Then metal oxidation occurs by anodic reaction and reduction occurs by cathodic reaction. For example, in this work steel was considered. Hence, the anodic and cathodic half cell reactions are as shown in Equations 2.1, 2.2 and 2.3:

Anodic: $Fe \rightarrow Fe^{2+} + 2e^{-}$ 2.1

Cathodic: $O_2 + 2H_2O + 4e^{-} \rightarrow 4OH^{-}$ 2.2

Overall reaction (Redox): $2Fe + O_2 + 2H_2O \rightarrow 2Fe(OH)_2$ 2.3

Every corrosive reaction is naturally electrochemical and in this case, ferrous ions are on the anodic site which is the iron's surface. While cathodic reactions occurs for the non-atoms, where electrons are released with a build-up of negative charges that would prevent further corrosion reaction from the anodic site of the metal (Chigondo & Chigondo., 2016). On a corroding system, corrosion involves a reduction reaction and oxidation reaction that generates several metallic electrons and ions. These electrons in the reduction reactions are

then consumed. However, for a moist environment with a certain amount of moisture content in the air, the conservation of water and oxygen to hydroxide ions literally consumes the electrons (Cinitha, Umesha&Iyer, 2014).

Corrosion usually starts at the external material surface. Corrosion resistance of metals and alloys is a basic property related to the easiness with which these materials react with the given environment. This is a natural process that seeks to reduce the binding energy in metals and is electrochemical in nature (Parashar & Parashar., 2015).

Metals and their alloys tend to make a chemical reaction with the elements of a corrosive medium so as to form stable compounds that are similar to those found in nature. When this happens, loss of metal occurs and the compound formed is referred to as corrosion products (Parashar & Parashar., 2015).

According to Shreir (2010), any fundamental approach to the phenomena of corrosion must therefore involve consideration of the structural features of the metal, the nature of the environment and the reactions that occur at the metal / environment interface. He further stated, that the more important factors involved may be concisely put as follows;

- Metal-composition, detailed atomic structure, microscopic and macroscopic heterogeneities, stress (tensile, compressive, cyclic), etc.
- Environment-chemical nature, concentrations of reactive species and deleterious impurities, pressure, temperature, velocity, impingement etc.
- Metal/environment interface-kinetics of metal oxidation and dissolution, kinetics of reduction species in solution, nature and location of corrosion products, film growth and film dissolution, etc. It should be appreciated that the decision to use a particular metal or alloy in preference to others in a given environment or to employ a particular protective system is based usually on previous experience and empirical testing rather than on the application of scientific knowledge. The technology of corrosion is without doubt in advance of Corrosion Science and many of the phenomena of corrosion are not fully understood (Shreir, 2010). Thus, the phenomenon of passivity which was first observed by Faraday in 1836 is still a subject of controversy. The specific effect of certain anions in causing stress-corrosion cracking of certain alloy systems is not fully understood and dezincification of brasses can be prevented by additions of arsenic (or other elements such as antimony or phosphorus) but no adequate theory has been submitted to explain the action of these elements (Shreir 2010). According to Shreir, the understanding of the basic principles of the science of metallic corrosion is clearly important for corrosion control and knowledge of the subject that advances the application of scientific principles rather than empirical

approach may be used for such purposes as the selection of corrosions inhibitors, formulation of corrosion-resisting alloys, etc.

2.2 Types of Corrosion

The broad classification of corrosion reactions into wet and dry is now generally accepted, and the nature of the process is frequently made more specific by the use of an adjective that indicates type or environment, e.g. concentration-cell corrosion, crevice, bimetallic, atmospheric, localized or pitting, high temperature, sea-water corrosion, etc.

One of the most insidious types of corrosion is pitting. According to Li, Feng, Bai, Zhu & Zheng (2007), this type of corrosion is a dangerous form because metals are punctured without warning of signs or growth in pits. Active metals undergo pitting attacks due to local external circumstances, such as holes in the coatings. It is a local type of corrosion, which forms deep, narrow pits on the surface of the metal, thus puncturing the material over time. This usually occurs when there are inclusions on the metal surface or when the surface is rough, resulting in local failure of the passive film (Li et al., 2007). It is considered to be very dangerous compared to uniform corrosion damage because it is difficult to predict its appearance in the design system. Passivated metals are mainly attacked by pitting corrosion, which occurs in solutions containing chlorides, iodide etc.

Uniform corrosion happens when there is metal waste at the same rate in large areas of the metal surface. It uniformly spreads across the surface and occurs when the two areas of the metal-anode and cathode, respectively at the surface of the metal exchange positions that extend continuously. Uniform corrosion occurs more frequently than other forms of corrosion. Metals undergo uniform corrosion due to their uniform chemical composition and microstructure that allow the corrosive medium to access the surface of the metal. The uniform corrosion rate depends on the most important parameter such as temperature, because high temperature reduces the oxygen present in the aqueous solution, which influences the rate of corrosion (Roy, Karfa, Adhikari & Sukul, 2014).

According to Liu, Haixian & Yuxuan (2020), galvanic corrosion is an accelerated corrosion attack when two metallic materials having dissimilar compositions are electrically coupled in the presence of an electrolyte. It is also known as bimetallic corrosion. Apparently, different metals tend to corrode and when two different metals are joined together, the electrons move from the most reactive (anodic site) to the least reactive (cathodic site). The formed galvanic couple has the tendency to accelerate corrosion of the anode and slow down or completely stops the corrosion at the cathode. The corrosion rate becomes even severe when the metals are far apart on the galvanic potential (Roy et al., 2014). A small anode

coupled to a large cathode will result in increased corrosion rate at the anodic site and high current density.

Han, Zhang & Carey (2011) stated that crack corrosion occurs mainly in areas where the space is wide enough to allow the liquid to penetrate the crack and narrow enough to allow stagnation of the liquid. According to them, oxygen being restricted in the crack, a differential aeration is established between the crack and the surface (Han et al., 2011). This kind of corrosion mechanism is visible within the connection regions of flange joints, screw heads and lap joints, between tube plates and their tubes in the heat exchangers (Anwo, Ajanaku, Fayomi, Olanrewaju., 2019). This is known as crevice corrosion, a situation whereby a crevice, crack or overlap of the surface of metals prevents corrosive species and oxygen from entering or leaving the formed enclosure, thereby facilitating, rapid corrosion leading to the cracks of metallic materials. The phenomenon of cavitation and erosion corrosion is a unique form of corrosion which enhances degradation, resulting in building up and collapsing bubbles inside liquid near the metal surface. This has been attributed to chemical and mechanical effects due to bubbles on the protective film, causing the newly exposed metal surface to corrode (Anwo et al., 2019). The reformed film then gives rise to a new cavitation formation at the same spot. Cavitation corrosion can be prevented with the aid of fluid pressure gradients and pressure drops limitation (Chandler & Richer, 2000). Alteration of environment, coating and cathodic protection are main preventive ways to combat this form of corrosion. Its appearance leads to participating groves, gullies, waves, rounded holes and valleys, which develop on the surface film as resistance to corrosion. Also, selection of materials of better resistance to this form of corrosion inputs, designs, environmental changes, coatings and cathodic protection are ways to minimize damages or depletion due to erosion corrosion (Heakal & Elkholy, 2017).

The phenomenon of stray current corrosion occurs at the outward pipeline surface which affects stray passage currents along the pathway of pipelines. It results in metal degradation in the form of localized or pinholes corrosion. The surface make-up of stray corrosion behaves like a localized form of corrosion. Its corroding strength can be as a result of rapid perforation of pipelines. As for a foreign pipeline, it acts as a reverse current pathway for the cathodic protection system. In rare cases, rectifiers of cathodic protection are connected backwards in a way that direct current is discharged from the pipeline and anode of impressed current, can be retrieved rather than discharging current (Eddy, 2009).

Microbial influence corrosion phenomenon (MIC) involves the activities of microbes which lead to the dissolution of metals. The microbial in this form of corrosion can be clarified using a classical and modern form of mechanisms (Anwoet al., 2019). According to the

classical mechanism, chemicals are produced from microorganism's activities which are enhanced through an electrochemical reaction. The aids of sulfate-reducing, Iron-reducing, non-oxidizing and acid producing bacteria are the four main microbial species that accelerate the influence of MIC (Heak & Elkholy, 2017). The stepwise reaction of sulfate-reducing bacteria requires the consumption of hydrogen atom to convert sulfate into sulfide, sulfate-reducing bacteria activeness speed up the cathodic reaction and thereby increases the corrosion rate. During the anodic reaction, ferrous ion produced combine with sulfide ions to produce iron sulfide (Anwo et al, 2019). Modern mechanism, mostly results in localized corrosion having the formation of a biofilm at the initial stage which comprises of several species of bacteria. Some of these activities reduce oxygen content within the biofilm, making the surface of the metal covered by biofilm to become anaerobic, having the solution as aerobic. The biofilm creates a pathway area for bacteria to thrive and influence corrosion may be controlled by cleaving the surface to remove the biofilm or applying biocides to control the bacterial activity in the solution, and increasing cathodic protection potent (Hubbell, Price & Heidersbach, 1985).

A difference in the concentration of impurities in the presence of galvanic elements is the major cause of inter-granular corrosion. Generally, metals solidify with unique forms of grains consisting of crystalline units. Moreover, the irregularities of the grains, at the grain boundaries has resulted in the more susceptible dissolution of the metallic surface because of their reduction in mechanical properties and ductility of the substrates due to welding and stress cavitation (Anwoet al., 2019). A typical example is the nitric acid test for stainless steels where more than 12% Chromium is needed to make stainless steel, thereby increasing the corrosion resistance of chromium towards the grain boundary.

Weld decay can also cause inter-granular corrosion. Time and temperature effects provide one reason electric arc welding is used more than gas welding for stainless steels. The former produces higher and more intense heat within a short interval. The Latter would keep metal in a broad zone sensitizing range for a long duration, which means greater carbide precipitation. Employing high-temperature solution heat treatmentthat is solution-quenching and rapid cooling, are viable solutions to prevent inter-granular corrosion on austenitic stainless steel (Hubbell, Price & Heidersbach, 1985).

2.3 Chemical factors Affecting Corrosion

2.3.1 Dissolved Oxygen

Fontana and Staehle (2013) captured the effect of dissolved oxygen on metal substrate which brings about degradation of protective hydrogen film that oxidizes dissolved ions into insoluble form (metal precipitates), he also deduced that parts of dissolved gases (oxygen,

nitrogen, carbon dioxide, ammonium, sulfurous gases) which support aquatic life are also responsible for corrosiveness of such water towards metal and volumetric ratio of oxygen in water which aids photosynthesis. He reported that this challenge could be prevented or minimized by mechanical action and chemically scavenging the remainder. The mechanical approach makes use of vacuum de-gasifiers to reduce the oxygen level to less than 0.5-10 mg/L orde-aerating heater to reduce oxygen concentration to the range of 0.005-0.010mg/L. Chemical approach involves the use of hydrazine and sulfite. Using Sodium sulfite as an effective scavenger has a confined system operating limit about 1000 psi forming corrosive, hydrogen sulfide and sulfur dioxide shutdown occurrence. Hydrazine is more efficient to eliminate the residual oxygen by reacting with oxygen to give water and gaseous nitrogen, which are quite recognized as toxic substances.

2.3.2 Chloride lons

According to Fontana and Staehle (2013), the effect of some chemical substances such as sodium salts (chloride, sulfates, nitrates, bicarbonate, salts of heavy metals, silica etc. which are part of mineral constituents occurs in the presence of chlorideion at a temperature of over 300°F (180°c) and forms a unique type of corrosion, which can grow under porous iron sulfide layer on the corroding steels. It was ascertained that the corrosive nature of carbon dioxide act as a function of forming hydrogen ion which enables the anodic reaction to continue having hydrogen as products which are known as hydrogen embrittlement. When carbon dioxide dissolves in water its effectlowers the pH and increases the corrosion rate. Relatively, oxygen as predominant corrosive gas in the oil sector has a severe corrosive effect at a concentration of 50 ppb alongside any other acid gases.

2.3.3 Effect of Temperature

Generally, the corrosion rate increases with increasing temperature up to a maximum point. Ebenso et al. (2008) also posited that it is difficult to establish the formation of a $FeCO_3$ surface layer at a temperature below 70°F (20°C). For a temperature range of 70 and 100°F (20°C and 40°c), the surface layer formed is not adherent enough and can easily be wiped off using cloth (Ebenso et al., 2008). However, in the range between 140 and 300°F (60°C and 150°C) it is found that the surface layer is hard, adherent and protective. The negative aspect of temperature change reveals that at 70°F (20°C) there is the non-uniform, fragile surface layer. Cosequently, pitting corrosion is mostly subjected to this form of effects. As both the pit density and pit depth decreases, the temperature increases, leading to the formation of adherent and protective surface layer on the substrates.

2.4 Some Historical Examples of Catastrophic Effects of Corrosion

Based on research and statistical data, it is possible to estimate and state evidently that corrosion in all its forms such as; general corrosion, pitting corrosion, crevice corrosion, stress corrosion cracking, corrosion fatigue, contributes to failure with about 42% when considering the frequency of failure mechanisms in engineering structures. Even in aircraft structures, where the largest numbers of failure were as a result of fatigue, corrosion is the cause of about a quarter of the total number of failures (Findlay& Harrison, 2002).

In 1973, an aluminum heat exchanger failed catastrophically leading to the explosion of an LNG plant at the Skikda natural liquefied gas plant in Algeria, killing many people and inflicting injuries to a lot more (Chalkidis, Jampaiah, Hartley, Sabri, & Bhargava, 2020). The explosion resulted in a further 56 none fatal injuries and $900 million loss (Ouddai, Chabane, Boughaba&Frah, 2012). Investigations determined that mercury corrosion caused the failure. After the Skikda failure, a study on Groningen fields in Holland revealed similar corrosion in the gas gathering system. CO_2 was initially thought to be the culprit, but investigation pointed to mercury with concentrations ranging from 0.001 to180 µg/Nm²(Ouddai et al.,2012). Although the concentration of Mercury in natural gas may be considered extremely low, it observes that its affect is cumulative as it amalgamates (forming alloys). Elemental mercury forms an amalgam with the surface layer of the metal it contacts. With aluminum, the corrosion problems occur when Mercury comes into contact with an aluminum metal Surface, where aluminum diffuses from the interface into the mercury droplet and it is rapidly converted to Al_20_3 by reaction with air or water. By this mechanism, metallic mercury actually, bores into the aluminum leaving brittle layer of Al_20_3. To initiate aluminum corrosion, the tightly adhering aluminum oxide layer on the surface of the aluminum must be removed. The mercury aluminum amalgam process removes this oxide layer in the presence of a catalyst or an aqueous electrolyte. The aqueous corrosion cell forms aluminum hydroxide and gaseous hydrogen, through Equations 2.4 and 2.5:

$$Al + Hg \longrightarrow AlHg \qquad 2.4$$

$$2AlHg + 6H_2O \longrightarrow 2Al(OH)_3 + 3H_2 + 2Hg \qquad 2.5$$

These reactions leave the previously amalgamated mercury free to form additional amalgam with the base metal in a continuous process. Metal corrosion does not start at a significant rate if the equipment is maintained below the melting point of mercury (-29°C).

This problem is clearly shown in the natural gas liquefying processes (LNG), and greatly affects the processing equipment (vessels / pipes) specifically the aluminum heat exchangers used to liquefy the gas (Chalkidis et al., 2020). As described above, elemental mercury forms an alloy with aluminum (amalgam). This amalgam (which is much weaker than the metal

itself) reacts with moisture to form a metal oxide plus free mercury, which can continue the corrosion process. Consequently, the mercury can damage the aluminum used in these exchangers and must be completely removed to no detectable levels in upstream equipment. This explosion was the worst accident at an LNG site in nearly 30 years ago where it destroyed three out of six production trains (Chalkidis et al., 2020).

Another catastrophic failure that was caused by corrosion was the Mexico Analco Guadalajara Sewer explosion of 1992. A series of ten explosions took place on April 22, 1992, in the downtown district of Analco Colonia Atlas in Guadalajara city, Jalisco State, Mexico. Numerous gasoline explosions in the Sewer System and fires over four hours, destroyed 13 kilometers of streets, killed more than 200 people and damaged 1224 buildings (Divine, 2016). And about 1,500 people were hospitalized, 25,000 people had to be evacuated, above 500 persons were missing, 637 vehicles were destroyed and the total damage was estimated at between $300 million and $1 billion (Divine, 2016).

It was reported that 8 days before the disaster, a loss of pressure in a 12inches pipeline which carried the gasoline from the Salamanca refinery to the Guadalajara depot of the petroleum company was detected, and it was discovered that the loss in pressure was the result of the perforation of the pipeline, leading to a leak of gasoline. The leak was localized in Alamo industrial area, less than 1 km from the storage tanks of the petroleum company (Divine, 2016)). Town water pipes probably made of copper coated with Zinc - installed five years had been installed close to the steel hydrocarbon pipeline without respecting standards for protection, provoking the corrosion and then the perforation of the pipeline. The gasoline thus poured out into the ground, infiltrating to a great depth (3 to 4metres) before running into the drainage network as far as the next main drain, following the natural slope of the terrain.

In another incident, according to Chris (2001), for thirty-nine years the Silver Bridge stood, allowing passage across the Ohio River. Narrating further, Chris stated “With the previous inspections, no one conceived that the structure might fail and collapse into the riverbed, however, on that fateful day, December 15, 1967 at about 5:00pm, tragedy struck. Within seconds, the Silver Bridge had collapsed killing and injuring many individuals” (Chris, 2001).After extensive studies of the broken structural members, the cause of failure was determined and was attributed to a cleavage fracture in the lower limb of eye-bar 330 at a joint C13N of the north eye-bar suspension chain in the Ohio side span. The fracture emanated from a minute crack formed during the casting of the steel eye-bar. Over the years, stress corrosion and corrosion fatigue allowed the crack to grow, causing the failure of the entire structure (Chris, 2001). Consequently, the catastrophic failure was as a result of a

combination of stress corrosion cracking due to the formation of brittle cracks in a corrosive environment and corrosion fatigue due to cyclic stresses in a corrosive environment.

In yet another incident, before the 19thMay, 2015, Santa Barbra/California oil spill, the Santa Barbara/CaliforniaRiver has been a case of recurring oil seeps. The 2015 oil spillin which there was a discharge of 540m^3 of crude oil destroying environmental flora and fauna was just another case. Investigations indicated the presence of serious corrosion. In the lower quadrant of the pipeline, the thickness of which was reduced by 45% due to corrosion, there was crack propagation (Lorenson et al., 2011).

On April 28, 1988 an Aloha Boeing 737 plane crashed. The structural damage to the plating on the Boeing 737 aircraft, operated by the US airline Aloha Airlines, undoubtedly contributed to the creation of awareness of aircraft aging. This aircraft suffered very serious damage caused by explosive decompression during flight. At 8,000m above the ground, a large segment of the upper fuselage was literally torn off and it made a big hole in the passenger cabin (Miller, 1990). The crew landed the plane safely on the Island of Maui in Hawaii. One flight attendant got killed, while 65 out of 94 survivors sustained injuries. In the remaining structure of the aircraft, in several lap joints of the fuselage body, in the holes of the upper row of fasteners, subsequent investigation discovered more cracks caused by fatigue (Wildey, 1990). The report of the National Committee for Traffic Safety, made after the completion of the investigation, attributed the incident to maintenance program and detection of damage from corrosion. It was the NLR – Netherlands Aerospace Centre (Nederlands Lucht- enRuimtevaartcentrum) department of Structures and Materials that was responsible for investigating the components connecting engine No. 3pylon on the right wing. It turned out that these components were the key to explaining this complicated accident (Wanhill, Molent, Barter, 2021). After this accident report, Boeing introduced several changes for the pylon-to-wing connection including a newly designed safety pin made ofcorrosion-resistant stainless steel.

In May 1974, the helicopter Sikorsky S-EIN PH-NZD crashed into the North-sea and six people were killed. All the main rotor blades were broken, but blade No. 3 was an exception because of low deformations at the fracture. The spar No. 3 blade was made of aluminum alloy AA 6061-T6. The spar is adhesively bonded to the sheeting in the form of a ribbed aluminum pocket. It was found that the fractographic analysis determined the phases of the spar fracture and their order. The first phase was high-cycle fatigue initiated by corrosion pits on the spar lower surface under the bonded area (Wanhill et al., 2021).

On August 19, 2000, a 76 cm diameter natural gas transmission pipeline operated by the El Paso Natural Gas Company (EPNG) ruptured adjacent to the Peco River near Carlsbad, New

Mexico. The incident, according to the company costs $998.296. The explosion created a crater 16 meters wide and blew out three large pieces of the pipeline. All three pieces showed evidence of internal corrosion damage, but one of the pieces showed significantly more corrosion damage than the other two. Corrosion pits were visible on the inside surface of this piece, and the pipeline wall was significantly thinned at several locations, a perforation of the wall visible at one location. No significant corrosion damage was visible on the outside surfaces of the three pieces or on the two ends of the pipeline remaining in the crater (National Transportation Safety Board, 2003).

On August 15, 2014, the landing of a Jetstream resulted to an accident whereby the landing gear was affected. Immediately after landing, the left leg of the landing gear separated from the shackles. The aircraft slid off the runway into the grass. The results of the investigation showed that the failure had been caused by stress corrosion (Zoran, 2016).

On June 24, 2013 in England an Airbus A330 running at the airport in Manchester, at a speed of 190 km/h, the right caught fire. The investigation revealed that there had been a fracture of one of the turbine blades. The blade failed due to high cyclic fatigue initiated by pitting corrosion (Zoran, 2016).

On 12 December 1999, an oil tanker by the name Erika broke into two and sank in the Bay of Biscay, France. There were no casualties. However, the oil spill led to a great environmental disaster. The main cause of the accident after investigation was attributed to significant corrosion of the internal structure of the vessel (Zoran, 2016).

Next was the April 10, 1992 EL AL Boeing 747 crash in the Netherlands. After a takeoff, engine No 3 separated from the right wing and hit motor No. 4. The reason for the separation of the two right engines was damage on an internal safety pin in the compound of Engine No 3 Carrier and the middle spar of the right, wing, caused by pitting and fatigue corrosion (Zoran, 2016).

On March 12 in 1984 in Bhopal India, toxic gas was released into the atmosphere from the Union Carbide India Limited (UCIL) pesticide plant in Bhopal in the state of Madhai Pradesh. The official death toll was 2,259, while unofficially the number was much higher about 8,000. After investigating the cause of the accident, it was revealed that the main culprit was corrosion (Zoran, 2016). From the foregoing, the need for corrosion protection of engineering systems can’t be overemphasized and as such is highly recommended in order to reduce the enormous cost associated with corrosion failures.

2.5 Theoretical Literature

2.5.1 Theory of Electrode Kinetics

The theoretical considerations of the three laws governing electrode kinetics of corrosion of some metals were discovered some decades ago. The logarithmic law was really discovered in 1922, a year before the discovery of the linear and parabolic laws, but it was not until after its rediscovery in 1939 that explanations became available for an increasing number of discrepancies (Miley, 1942). An electrochemical interpretation of the ionic theory provides a basis for developing the equations of these laws. The diffusion theory had never provided an adequate explanation of the parabolic law. The ionic theory postulates the movement of cations and electrons outward and of anions inward across the growing film, and the electrochemical interpretation of this theory makes it theoretically possible for a continuous film to obey two or more of these laws in turns (Miley, 1942). The growing film may be compared with a current-producing cell, the requirements for changing a parabolic growth rate to a logarithmic rate being provided by polarization. The critical film thickness, beyond which polarization may be expected, is influenced by all of the factors that affect the perviousness of the film. The linear law may be obeyed sometimes when the resistance of the film is small enough to permit the mechanics of the film building process to control the rate of growth (Miley, 1942). These theories are termed the electrode kinetics theories.

2.5.1.1 Linear Rate law

The linear rate law corresponds to a surface reaction being rate limiting, the surface reaction possibly being the adsorption or adsorption reaction of hydrogen on the metal surface. According to the parabolic law, the resultant stress at the interface increases and eventually the oxide layer can fail either by fracture parallel to the Interface or by a shear or tensile fracture through the layer (Smallman & Ngan, 2014). In these regions the oxidation rate is then increased until the build-up in stress is again relieved by local fracture of the oxide scale. Unless the scale fracture process occurs at the same time over the whole surface of the specimen, the repeated parabolic nature of the oxidation rate will be smoothed out and an approximately linear law observed. This breakaway parabolic law is sometimes called para-linear and is common in oxidation of titanium when the oxide reaches a critical thickness. In some metals, however, the linear rate with an interface reaction converting a thin protective inner oxide layer to a non- protective porous oxide (Smallman & Ngan, 2014).

2.5.1.2 Parabolic Rate law

According to this law, the rate of oxide-scale formation is inversely proportional to time, which means that as time increases, the rate of scale formation continuously decreases. From the standpoint of oxidation of engineering alloys, the parabolic law is of great importance.

Here the oxide growth occurs with a continuing decreasing oxidation rate. Most metals and engineering alloys follow parabolic kinetics at elevated temperatures. The oxide growth process is usually governed by the diffusion of ions or electrons through the initially formed oxide scale (Khanna, 2002).

2.5.1.3 Logarithmic Rate law

The logarithmic rate laws are observed for thin films growing at low temperatures. The law predicts the quick initial reaction, followed by almost no reaction. Based upon how slowly the rate subsides after initial fast reaction, the logarithmic kinetics can have direct or inverse behavior of scale thickness versus time (Khanna, 2002). The mechanism of growth involves electric fields localized very close to the metal surface. Adsorbed oxygen atoms acquire electrons from the metal atoms, creating large electric fields across the thin film between positive metal ions and negative oxygen ions. Metal atoms are pulled by the electric field through the oxide film. In such cases the growth rate varies inversely with time. It is important to understand that these three laws determine the Kinetic behavior of metals and alloys (Khanna, 2002).

2.5.1.4 Thermodynamics of Corrosion

It has been reported in literature that thermodynamics give the change in energy state, also predicts the direction of a reaction. For Spontaneous reactions, the systems must decrease their Free-energy and move to a lower energy state (Popov, 2015).

It is observed, that corrosion reactions inevitably involve electron transfer. For this reason, the reactions may be considered electrochemical in nature. Thermodynamics can provide a basis for the understanding of the energy changes associated with the corrosion reaction. It can in general, predict when corrosion is possible. Thermodynamics cannot predict corrosion rates. The rate at which the reaction proceeds is governed by kinetics (Popov, 2015)

2.5.2 Nernst Theory of Electrode Potential

According to Hemant, Nernst in 1889 gave his theory of electrode potential. An electrode is a couple of active elements, and its ionic solution. When metal is immersed in its salt solution it shows two opposite tendencies called de-electronation (oxidation) and electronation (reduction) (Hemant, 2019). Metal have the tendency to pass into solutions as cations and liberate electrons. This process is oxidation or de-electronation. The tendency of a metal to pass into its salt solution in the form of cations liberating electrons is called the solution pressure of the metal (Ps). There is a reverse tendency of cations to deposit on the electrode by taking electrons. This process is called electronation or reduction. The tendency of the ions in the solution to be deposited back on the surface of the metal by taking electrons is called osmotic pressure (P_o). Nernst suggested the mechanism of the establishment of the

difference of potential in a cell. His theory is based on the theory of electrolytic dissociation and his ideas of solution pressure and formation of the electrical double layer (Hemant, 2019).

2.5.3 Electrolytic Dissociation Theory

The main idea of the theory of electrolytic dissociation is that when an electrolyte dissolves in water, it disintegrates into two charged parts, one part carrying a positive charge, cations, and the other carrying a negative charge, anions, and these charged particles are the current carriers responsible for the conductivity of the electrolytic solution.

According to Wilder (2002), when an electrolyte is dissolved in water, it is separated into two types of changed particles: one with a positive charge and the other with a negative charge. In its modern form, the theory assumes that solid electrolytes are composed of ions that are held together by the electrostatic forces of attraction (Wilder, 2002).

2.5.4 Mixed Potential Theory

The mixed potential theory explains metal corrosion as a reaction of two or more electrodes working simultaneously at the interface of the given metal surface and electrolyte.

According to Frankel (2016), in a corrosion cell (electrolyte, anode, cathode and a metallic path), multiple reactions occur. The metal constitutes a multi-electrode, because at least two different reactions occur on its surface simultaneously, one oxidation and the other reduction (Frankel, 2016). It is used to predict the rate of corrosion of metals and alloys in a given environment.

According to reports, mixed potential theory has two basic assumptions such as;

a. Electrochemical reactions are composed of two or more partial anodic and cathodic reactions.
b. There cannot be any accumulation of charges.

Typical corrosion process involves one or more cathodic reactions and one or more anodic reactions (Perez, 2004). According to mixed potential theory any electrochemical corrosion process reaches a mixed potential such that the sum of all anodic reaction rates equals the sum of all catholic reaction rates, taking into consideration the reaction areas, A. Moreover, there is no net electrical charge accumulation. This open circuit potential is a kinetically and thermodynamically determined mixed potential that can be measured experimentally against reference Scale (Perez, 2004).

2.5.5 Theories of Passivity

Theories of passivity are ideas developed to explain the usefulness of certain active metals in the galvanic series towards having certain corrosive resistance when exposed to

passivating environments or polarization (Popov, 2015). This means that, active metals can be made passive, so that they corrode less as compared to their origin at state, which corrodes rapidly. This is achieved by reducing the anodic reactions that occur at the surface of the metals. Theories of passivity explain how protection is achieved in certain structures by the development of passive films on the surface of the metallic material.

According to Popov (2015), theories of passivity are based on the formation of oxide films on the surface of the material that is in a passive state. Through anodic polarization, certain metals like iron can become passive, thus demonstrate some corrosion resistance. The oxide films can exist when certain metals have pronounced corrosion tendencies, but produced lesser reactions with the surrounding environment. As they undergo these passive states, their potential approaches those of noble metals which do not react easily, such as platinum (Popov, 2015).

The theories of passivity also explain how adsorption works in the reduction of reaction activity of active metals. The oxygen adsorption on the surface of these metals prevents further anodic reactions thus protecting the material from degradation (Popov, 2015).

2.5.6 Cabrera and Mott Theory

This theory has been widely accepted and extended to a wide range of systems such as nano particles, nanowires and liquid metals, which significantly inspired the continuous studies of oxidation mechanisms and oxidation-based material synthesis methods (Goffet al., 2021; Laboureur, Glabeke&Gouriet, 2021;Cysteret al., 2021; Gorobez, Maack, &Nilius, 2021).

2.5.7 Wagner's Theory of oxidation

Wagner's theory is anchored on the growth of oxide film on a metal by thermal oxidation. The theory states that oxidation rate of a metal is controlled by the transport of ions across the oxide film under the combined effects of concentration gradients and electric fields (Gesmundo, 1992). The theory has many assumptions, such as:

1. The scale growing on the metal surface is compact in its entirety.
2. Diffusion of reagents in the scale takes place in the form of ions and electrons through point defects in the crystalline lattice of the reaction product.
3. The scale formation process is determined by diffusion, the rate of which is lower than that of chemical reactions at the interface.
4. Electronic and ionic defects in the crystalline lattice of the scale travel due to ambipolar diffusion.
5. Diffusion of reagents in the scale proceeds under the influence of a lattice detect gradient caused by the oxide chemical potential gradient.

6. Point defect concentrations are established at the scale interfaces, to which the oxidation process proceeds according to the parabolic law.
7. There is a state close to thermodynamic equilibrium at the scale interfaces (Gasmundo, 1992; Kofstad, 1989; Khanna, 2002)

2.5.8 Theory of Polarization Resistance

This theory states that whenever the potential of an electrode is forced away from its value at open circuit, this is called polarizing the electrode. When electrode is polarized, it can cause current to flow through electrochemical reactions that occur at the electrode surface (Cigna et al, 1993).

All polarization resistance techniques such as linear, potentiodynamic, cyclic etc. can be employed to evaluate the corrosion kinetics of coatings systems and the coating thicknesses achievable as a function of time. Current density is the main parameter used to measure the efficiency of protective coating kinetics; the high the current density, the poorer the electrochemical behavior. Moreover, higher corrosion rates are characterized by a small passive potential range and a lower pitting potential, thereby implying the presence of defects and pores in the coating that allow electrolyte diffusion, and thus, promoting the failure of the protective coating.

According to Papavinasam & Revie (2008), because polarization resistance method has the advantage of providing corrosion rate measurement within minutes and it does not affect the ongoing corrosion rates, this method is the most widely used in the field (Papavinasam & Revie, 2008).

2.5.9 Faraday's law of electrochemistry

This law states that when current produced at anodic areas are known, it is possible to calculate the rate of corrosion penetration or corresponding mass loss. The law relates to electrolysis and how electrochemical reaction current is associated with the moles of elements under reaction (Bagotsky, 2005). The rate of dissolution of the anode is governed by Faraday's law of electrolysis. According to the law, the rate of anodic dissolution is directly proportional to the amount of current passed through the electrolyte (Lefrou, Fabry & Poignet, 2012). Faraday’s law is used to determine corrosion rates according to the kinetics of the cathodic and anodic reactions or the oxidation-reduction. Using this law, along with Tafel plot, industries are able to predict whether a certain setup is likely to lead to corrosion. It also takes into consideration how fast the rate of corrosion will be in a given setup, making this law significant in corrosion testing and control.

2.6 Empirical Literature

2.6.1 General Empirical Literature on Corrosion

In the past decades, the corrosion rate of steel reinforcements in reinforced concrete Structures under chloride- prone environments has been widely investigated and the key methodologies adopted in modelling the corrosion rate were, empirical, kinetics and equivalent electrical circuit modelling (Siamphukdee, Collins & Zou, 2013). The study focuses on the empirical models of corrosion rate developed from field data and/or experimental results (Otieno, Beushausen, & Alexander, 2011; Raupach, 2006) which are based on assumed direct relationships between the corrosion rate of the steel reinforcement and the basic properties and parameters of concrete such as water-to-content (W/C) ratio, cover depth, concrete resistivity, type of binder and the exposure conditions considering chloride content, corrosion duration, relative humidity and ambient temperature. Currently, there are several empirical models for predicting the rate of chloride-induced corrosion of Steel reinforcement in RC (reinforced concrete) structures (Ahmad, Basavaraja& Bhattacharjee, 2000; Liu & Weyers, 1998; Lu, Liu, Gao, Xing & Wang, 2008; Morinaga, 1988; Pour-Ghaz, Isgor & Ghods, 2009; Rodriguez, 1996; Vu & Stewart, 2000).

Nguyen & Dang (2020), did an empirical study to predict the corrosion rate in RC. In this study, several empirical models were used to predict the corrosion rate and their limits of application. The predicted values of steel corrosion rate using four empirical models were compared with the measured values of a series of 55 experimental samples collected from the literature. The results showedthat the empirical models overestimated the experimental corrosion rate. Using a model proposed by Liu& Weyers (1998) provided the best agreement with the experimental data (Nguyen& Dang, 2020).

In a similar study Vanmarcke (2010), studied experimental data on corrosion rate from literature and did a comparative analysis. Seven empirical models for predicting the corrosion rate were studied using the data collected. From their investigation, a new empirical model was proposed for predicting the corrosion rate in corrosion-affected reinforced Concrete structures considering parameters such as concrete resistivity, temperature, relative humidity, corrosion duration and concrete chloride content (Vanmarcke, 2010).

Ali & Fulazzaky (2020), carried-out an empirical study with the aim of developing new empirical models based on the experimental data of testing 25 samples immersed in five different environments for predicting weight change and corrosion rate of low-carbon steel at the limited chloride ion concentration.

Ali&Fulazzakyfurther carried out a study to develop a simple model for predicting weight loss of mild steel due to corrosion in NaCl Solution. For this purpose, 25 samples of 80 x 24 x 3mm Sized coupons were prepared and the measurements of weight loss were carried out on the specimens for 10, 20, 30, 40, 50, 60 and 70 days, respectively by total immersion of the samples in NaCl solution of 2, 3, 4 and 5 wt.% with one treated in distilled water. The results showed that NaCl concentration significantly influenced the corrosion rate for all variations with average weight loss value of 1.38 mg/cm² and corrosion rate value of 25×10-5 mm/year.They concluded, that the proposed empirical model ($WL = 0.001 + 1.34^{\alpha} + t^{0.87}$) was successfully established.

In a study carried out by Ekuma&Idenyi (2007), they did a statistical analysis of the influence of environment on prediction of corrosion from its parameters. In this study, they analyzed the corrosion characteristics of Al-2.5% Zn binary alloy system. The set up were allowed to stand for 480 hours with a set withdrawn 120-hourly for corrosion rate characterization. The model equation developed using regression technique revealed that the model could be used for effective and accurate determination of corrosion trend in seawater and atmospheric environments as it showed good correlation with the experimental data (Ekuma&Idenyi, 2007).

In a study carried-out by Kaushal & Najafi (2021), they investigated microbiologically influenced corrosion of concrete in sanitary sewers. The results showed Variation in corrosion rates and other empirical inputs obtained on and through laboratory studies due to different testing procedures (Kaushal & Najafi, 2021).

Umoren, Solomon, & Saji (2022), analyzed polarization based on the identification of the partial currents of the single electrochemical reactions involved and investigated the relationship between the gradient of polarization curves, and the corrosion rate in uninhibited corrosion processes. The analysis of polarization curves was explained and two methods of using polarization curves in corrosion studies were compared. The conditions for stability of the active and the passive states were specified for application in anodic and cathodic protection (Umoren, Solomon & Saji, 2022).

Brown, Darr, Morse & Laskowski (2012) on their part, presented the theory and experimental validation of analatom's structural health management (SHM) system for monitoring corrosion. Corrosion measurements in this experiment were acquired using a micro-sized linear polarization resistance (µLPR) sensor. A series of experiments were conducted to validate the µLPR sensor for AA 7075-T3. At the end of the experiment, pit-depth due to corrosion was computed for each sensor from the recorded LPR measurements

and compared to the average pit-depth measured on the control coupons. The results demonstrate the effectiveness of the sensor as an efficient means to measure pit- depth for AA 7075-T3 (Brown et al., 2012).

An investigation on the corrosion behavior of steel embedded in basic magnesium sulfate concrete (BMSCC) was carried out by Tan, Yu & Wu (2020). In this investigation, linear polarization resistance and electrochemical impedance spectroscopy (EIS) were used to study the corrosion behavior of steel bars in different strength grades of basic magnesium sulfate cement concrete in seawater. The LPR and EIS results showed that the corrosion potential and polarization resistance of steel bars in BMSCL decreased with the immersion time in the seawater environment (Tan et al., 2020).

In a study to examine the effect of applied potential on the microstructure, composition and corrosion resistance evolution of fluoride conversion film on AZ31 magnesium alloy carried-out by Wu et al (2018), AZ31 magnesium (Mg) alloy was potentiostatic polarized in 0.1 M de-aerated KF solution with pH 7.5 from -0.4V to -1.4V with an interval of -0.2V. The polarization process was described by the potentiostatic current delay and the results demonstrated that the deposited film included a Mg $(OH)_2/MgF_2$ containing inner layer and a $Mg(OH)_2/Mg\ F_2/KMgF_3$ comprising outer layer (Wuet al., 2018).

In another study to investigate the degradation mechanism at the bone - implant interface of different degrading magnesium alloys in bone and to determine their effect on the surrounding bone (Witteet al., 2005). The results showed that metallic implants made of magnesium alloys degrade in vivo depending on the composition of the alloying elements. The results further showed high mineral opposition rates and an increased bone mass around the magnesium rods, while no bone was induced in the Surrounding soft tissue. It was therefore concluded that a high magnesium ion concentration could lead to bone cell activation (Witteet al, 2005).

A study on nano-indentation and corrosion characteristics of ultrasonic vibration assisted stir-cast AZ 31-Wc -graphite nano-composites carried-out by Banerjee, Poria, Sutradhar& Sahoo (2021) reveals that incorporation of I wt.% Gr has improved corrosion resistance but further addition of graphite nanoparticles results in decrease in the corrosion resistance (Banergeeet al, 2021).

According to Saifi et al (2019), in a study of electrochemical behavior investigation of cysteine on nickel corrosion in acidic medium, the surface observation by scanning election microscope corroborates that the addition of cysteine has no significant improvement of the

surface morphology of nickel electrode in 0.5M H_2SO_4. The results obtained by different methods corroborate each other.

2.6.2 Empirical Literature on Corrosion Inhibition

In a study by Kim et al (2015), to examine the corrosion inhibition mechanism of nitrite ion on the passivation of carbon steel and ductile cast iron for nuclear power plants,a corrosion and inhibition mechanism were proposed for iron to be added in other for nitrite to oxidize such that nitrogen compounds can be reduced and these compounds may be absorbed on the surface of graphite. Since nitrite ion needs to oxidize, the surface matrix needs to passivate the galvanic corroded area and since it is absorbed on the surface of graphite, a greater amount of corrosion inhibitor needs to be added to ductile cast iron compared to carbon steel. The passive film of carbon steel and ductile cast iron formed by $NaNO_2$ addition showed N-type semi-conductive properties and its resistance is increased; the passive current density is thus decreased and the corrosion rate is then lowered. In addition, the film is mainly composed of iron oxide due to the oxidation by ion; however, regardless of the alloys, nitrogen compounds (not nitrite) were detected at the outermost surface but were not incorporated in the inner oxide (Kimet al., 2015).

In another study by Solomon, Gerengi&Umoren (2017), to boost the inhibition efficiency and stability of carboxymethyl cellulose (CMC), this objective was achieved by incorporating silver nanoparticles (AgNPs) generated in-situ by reduction of $AgNO_3$ using natural honey into CMC matrix. Characterization of CMC/AgNPs composite was done using transmission electron microscope (TEM), Fourier transform infrared (FTIR) spectroscopy, ultraviolet–visible spectroscopy (UV-vis), scanning electron microscope (SEM), and energy dispersive x-ray spectroscopy (EDS), Weight loss, electrochemical (dynamic electrochemical impedance spectroscopy, electrochemical impedance spectroscopy, and potentiodynamic polarization) supported by surface assessment (SEM, atomic force microscope, and FTIR) techniques were deployed for the anticorrosion studies of CMC/AgNPs on St37 specimen in 15% H_2SO_4 medium. CMC/AgNPs performs better than CMC. At 25^oC, optimum inhibition efficiency of 93.94% was afforded by 1000 ppm CMC/AgNPs from DEIS method. Inhibition efficiency of 96.37% has been achieved from weight loss method at 60^oC. CMC/AgNPs was found to retard both the anodic and cathodic reactions and the adsorption is explained using Langmuir adsorption isotherm. AFM and SEM graphics reveal smoother surface for St37 sample in the acid solution containing inhibitor than in the solution without the inhibiting agent. FTIR and EDS results show that CMC/AgNPs molecules were adsorbed on the metal surface (Solomon et al., 2017a; Solomon, Gerengi, Kaya & Umoren, 2017b).

Incomprehensive macroscopic/microscopic level explorations using integrated experimental /theoretical approaches were applied to fundamentally evaluate the impact of non-toxic rare earth cerium (III) ions addition to the chicory leaves extract (CLE) on mild steel (MS) corrosion mitigation in saline solution. Surface studied confirmed the cerium oxides/hydroxide (CeO_2 and $Ce(OH)_3$) as well as $CLECe^{3+}$ and $CLEFe^{2+}$ complexes formation on MS surface. Results demonstrated that in the presence of the mixture of CLE (400 mg/L) and Ce^{3+} ions (400 mg/L) the anodic/cathodic reactions were remarkably affected. The corrosion resistance of the MS sample subjected to CLE (400 mg/L)-Ce^{3+} ions (400 mg/L) significantly increased, yielding 94% efficiency. Additionally, the microscopic level (i.e., electronic/atomic) theoretical assessments (density functional theory (DFT), molecular dynamics (MD), Monte Carlo (MC)) were adopted to basically probe the mixed green organic-inorganic adsorption affinity and local adsorption and reactivity on the steel base adsorbents. (Ramezanzadeh, Bahlakeh&Ramezanzadeh, 2019a).

Also, the corrosion inhibition of a new benzimidazole derivative, 6-(dodecyloxy)-1*H*-benzo[*d*]imidazole (DBI), for mild steel in 1 M HCl was investigated by Zhang et al. (2016a). Computational chemistry was performed to explore the adsorption of DBI on metal surface. Inhibition performance of DBI was attributed to both the direct interaction of benzimidazole segment with iron surface and the barrier effect of the non-polar long chain against aggressive solution. Compared to the protonated form, the molecular form of DBI could more tightly interact with iron surface. These results show that the long-chain alkyl-substituted benzimidazole derivative is of great potential application as corrosion inhibitor (Zhanget al., 2016a).

In a study, some quantum chemical parameters were calculatedusing Hartree–Fock (HF) approximation, density functional theory (DFT/B3LYP) and MøllerPlesset perturbation theory (MP3) methods at LANL2DZ, LANL2MB and SDD levels in gas phase and water for dichromate ($Cr_2O_7^{2-}$), chromate (CrO_4^{2-}), tungstate (WO_4^{2-}), molybdate (MoO_4^{2-}), nitrite (NO_2^-) and nitrate (NO_3^-) which are used as inorganic corrosion inhibitors. All theoretical results and experimental inhibition efficiencies of inhibitors were subjected to correlation analyses. In a summary, MP3/SDD level in water was found as the best level. In this level, the inhibition efficiency ranking was found as; $CrO_4^{2-} > WO_4^{2-} > MoO_4^{2-} > CrO_7^{2-} > NO^{2-}$ ~ (Sayin&Karacas, 2013).

In a theoretical study, molecular dynamics (MD) simulation and density functional theory (DFT) were performed to evaluate the adsorption process and the synergistic effects between nettle leaf extract (NLE) and zinc nitrate (ZN). Electrochemical analyses results confirmed

effective synergistic inhibition between organic inhibitors existed in NLE and zinc cations. A 96% inhibition efficiency was obtained when 400 ppm NLE was combined with 400 ppm Zn $(NO_3)_2$. The theoretical results evidenced that all considered organic-inorganic inhibitors adhered to steel surface, reflecting their corrosion inhibition effect (Ramezanzadeh, Bahlakeh & Ramezanzadeh, 2019b).

In another study of the corrosion of iron exposed to H_2S saturated solution at pH 4 using electrochemical impedance spectroscopy, weight loss coupons and surface analysis, hydrogen permeation was also used as indirect means of evaluating the intensity of the proton reduction reaction leading to hydrogen entry into the metal. Since corrosion in this type of test solution results in the rapid build-up of a conductive and highly porous iron sulfide scale, a specific contribution of the film had to be considered. An impedance model was thus proposed. The faradaic anodic impedance consists of a two-step reaction with charge transfer and adsorption – desorption. An additional contribution, associated with the conductive and highly porous iron sulfide film was added in parallel. This contribution, mostly visible in the low frequency domain, presents a 45° tail associated with a porous electrode behavior. This model was well adapted to describe impedance diagrams measured at various exposure times, up to 620 h. Charge transfer resistance determined from impedance analysis allowed calculating the evolution with time of the corrosion current density. A very good correlation was found between this corrosion current density and the hydrogen permeation current density. As expected, permeation efficiencycloser to 100% was demonstrated. Corrosion rate of 490 μm/year was measured by weight-loss specimens, confirming the validity of the impedance analysis, which resulted in a calculated corrosion rate of 530 μm/year (Ayagouet al., 2018).

In a study to evaluate different types of inhibitors for corrosion protection on metal surfaces the inhibitors were classified as cathodic, anodic and/or mixed-type inhibitors, which were based on the active inhibitor molecules that retard the corrosion process, silicate, nitrites, molybdates, phosphates, zinc salt and cerium salt were used as inorganic inhibitors while many organic compounds were been widely utilized as inhibitors. Corrosion protection was achieved by various mechanisms such as physisorption, chemisorption, barrier protection, thin-film formation and electrochemical processes (Ma, Ammar, kumar, Ramesh, K & Ramesh, 2022a).

In this study, a sodium zinc phosphate pigment synthesized by using a co-precipitation method and characterized by x-ray diffraction was investigated for its corrosion inhibition

activity in comparison with the commercial zinc phosphate using EIS in a 3.5% NaCl solution. A mild steel surface analysis after exposure to the test solutions was conducted using scanning electron microscope, energy dispersive x-ray and infrared spectroscopies. The results indicated that the corrosion inhibitive performance of the synthesized pigment was higher than that of the commercial zinc phosphate. This can be the result of the synthesized pigment's relatively high solubility, which affects the precipitation of a phosphate layer onto the mild steel surface and the modification of the crystalline structure of the corrosion products in the presence of the inhibitive pigment. The salt spray and wet pull-off tensile strength results revealed an improved corrosion protection of the coatings formulated with SZP (Alibakhshi, Ghasemi & Mahdavian, 2014).

In a study toward understanding the adsorption mechanism of large size organic corrosion inhibitors on an Fe (110) surface using the DFTB Method, density functional based tight binding (DFTB) approach was used to investigate the adsorption properties of three large size inhibitors (*i.e.*, chalcone derivatives) on an iron surface. The molecular activity of free chalcone derivatives was studied by means of frontier molecular orbital theory. The growth characteristics of α-Fe habits were observed using the "morphology" software. Some adsorption parameters such as charge density difference, density of states, and changes of molecular orbital were described in detail. The present study is helpful to understand the anticorrosive mechanism of similar organic inhibitors and provides a feasible way to develop novel corrosion inhibitors (Guoet al., 2017)

The synthesis and characterization of a novel organic corrosion inhibitor (4-(3-mercapto-5,6,7,8-tetrahydro-[1,2,4] triazolo[4,3-b][1,2,4,5]tetrazin-6-yl)phenol), for mild steel in 1 M hydrochloric acid (HCl) was successfully reported for the first time. The inhibitor was evaluated as corrosion inhibitor for mild steel in 1 M of hydrochloric acid solution using electrochemical impedance spectroscopy (EIS), and electrochemical frequency modulation (EFM) measurement techniques. Changes in the impedance parameters suggested an adsorption of the inhibitor onto the mild steel surface, leading to the formation of protective films. The results showed that the inhibition efficiencies increased with increasing the concentrations of the inhibitors and decreased with increasing temperature. The maximum inhibition efficiency was up to 67% at the maximum concentration 0.5 mM. This shows that those inhibitors are effective in helping to reduce and slowing down the corrosion process that occurs on mild steel with a hydrochloric acid solution by providing an organic inhibitor for the mild steel that can be weakened by increasing the temperature. The adsorption process of the synthesized organic inhibitor depends on its electronic characteristics in addition to

steric effects and the nature of metal surface, temperature degree and the varying degrees of surface-site activity. The synthesized inhibitor molecules were absorbed by metal surface and follow Langmuir isotherms (Othmanet al., 2018).

In this study, the inhibition effect of sodium molybdate (Na_2MoO_4) on the corrosion of aluminum in 1.0 M H_3PO_4 solution was studied by weight loss, potentiodynamic polarization curves and electrochemical impedance spectroscopy (EIS) methods. The results show that Na_2MoO_4 is a good inhibitor, and the inhibition efficiency obtained by three methods is higher than 84% at 20 mM. The adsorption of Na_2MoO_4 obeys Freundlich isotherm at lower concentrations (1–7 mM), while Langmuir isotherm at higher concentrations (7–20 mM). Polarisation curves indicate that Na_2MoO_4 acts as an anodic inhibitor. EIS spectra exhibit three loops (two capacitive loops and one inductive loop) (Li, Deng & Fu, 2011a)

According to Verma, Ebenso & Quraishi (2017), in the last decade, metallic corrosion inhibition using ionicliquids has attracted considerable attention due to their interesting properties such as low volatility, non-inflammability, non-toxic nature, high thermal and chemical stability and their ability to adsorb on the metallic surface. The review covers on ionic liquids as "green corrosion inhibitors" for different metals and alloys such as mild steel, aluminum, copper, zinc, and magnesium in several electrolytic media. The ionic liquids are promising, noble, green and sustainable candidates to replace the traditional volatile corrosion inhibitors and can be effectively adsorbed on metallic surface (Verma et al., 2017b). Several ionic liquids have been used successfully as corrosion inhibitors for mild steel; however, their use as corrosion inhibitors for non-ferrous metals is scarce.

In this work, the inhibition effect of ionic liquid (IL) 1-ethyl-3- methylimidazolium thiocyanate $(EMIM)^+(SCN)^-$ on the corrosion of API 5L X52 steel in 0.5 M H_2SO_4 solution at different temperatures were studied, using gravimetrical, electrochemical, spectroscopic and simulation methods. The highest efficiency and the optimal concentrations were 90.1% and 75 ppm of the IL, respectively. Scanning electron microscopy characterization reveals less surface damage in the corroded samples confirming the effectiveness of the IL, while X-ray photoelectron spectroscopy analysis evidenced the formation of an interfacial protective layer, composed by the inhibitor molecules and corrosion products. Polarization measurements showed that the IL is a mixed-type inhibitor, retarding the dissolution of mild steel and hydrogen evolution reactions, enhancing its efficiency as a function of its concentration; besides a minor influence of the temperature in the inhibition efficiency is recorded by weight loss, potentiodynamic polarization, and electrochemical impedance

spectroscopy techniques. A competitive chemisorption process is observed on steel obeying a Langmuir isotherm. Ultraviolet-visible spectroscopy confirmed chemical interaction between IL and metal surface. The density functional theory and molecular dynamic (MD) simulation were used to correlate with the experimental results and determine the adsorption energy of the inhibitor in different substrate's crystallographic planes (Lunaet al., 2019).

In a study to evaluate the environmentally friendly anticorrosive pigment for alkyd primer, an alkyd formulation containing zinc phosphate (10 wt.%) was prepared and subsequently modified replacing the latter anticorrosive additive by a very low concentration of conducting polymer. Specifically, three modified paints, which contain polyaniline emeraldine base (undoped form), polyaniline emeraldine salt (doped form) and an eco-friendly polythiophene derivative (partially oxidized), were formulated. The properties and corrosion resistance of the four alkyd coatings have been characterized. Among the three modified paints, the one containing polythiophene shows the best adherence and the highest corrosion resistance. This has been attributed to the fact that the miscibility of the polythiophene derivative with the alkyd formulation is better than that of polyaniline. Furthermore, accelerated corrosion assays and electrochemical impedance spectroscopy measurements revealed that the corrosion resistance of the paint with polythiophene is several orders of magnitude higher than that with zinc phosphate. The polythiophene derivative has been found to induce the formation of a passivating and well-adhered layer between the coating and the surface, preventing the access of chloride anions and oxygen to the substrate (Marti, Fabregat, Azambulja, Aleman & Armelin, 2012).

According to Gao, Dong, Zhu, Gao C & Tu (2018), “commercially available passivation methods for white-rust protection of hot-dip galvanized steel have been applied for chromate passivation. However, hexavalent chromium (Cr-VI) is highly toxic and carcinogenic” hence the authors put forth a new means for white-rust protection of hot-dip galvanized steel based on the effects of corrosion inhibitors. In this study, the passivation solution combines the advantages of inorganic salt passivation, silane passivation and resin passivation. The corrosion resistance of the inorganic and organic composite passivation films with corrosion inhibitors was determined by a neutral salt spray test and electrochemical Tafel polarization curves. The surface chemistry of the coatings was monitored by scanning electron microscopy (SEM), X-ray Photoelectron spectroscopy (XPS) and Fourier transform infrared reflection absorption spectroscopy (FTIR). A study on the formation mechanism of the passivation film was carried out. The SEM indicated that the top surface of the passivation film was transparent, smooth, uniform and compact. The XPS and FTIR results showed that

the passivation film consisted mainly of organic functional groups including-(CH2) n-,-OH, N-H, C=O, C-Si, C-O-C, C-N, Si-O-Si, Si-O-C and so on. The corrosion resistance of passivation film with corrosion inhibitors was significantly improved than that of the passivation film without corrosion inhibitor. After 96h of the corrosion test, the corrosion area was found to be less than 5 %, which indicated that the passivation film greatly improved the corrosion resistance of the hot-dip galvanized sheet, and exhibited a very good protective effect such that it met some industrial applications conditions.

In an impedance analysis of film-forming amines for the corrosion protection of a carbon steel Octadecylamine (ODA) was used. Electrochemical impedance data analysis was performed to extract physical parameters of the ODA thin film that formed on a P275 carbon steel surface. First, surface observations and contact angle measurements showed the steel surface modification after the ODA treatment linked to the adsorption of an organic hydrophobic thin film. X-ray photoelectron spectroscopy confirmed the presence of a very thin organic layer and revealed the presence of iron oxide/hydroxide underlying the ODA film. The impedance data analysis with a power-law distribution of resistivity in the organic film allowed the permittivity and thickness to be extracted. Finally, from the impedance results with and without ODA, the instantaneous corrosion inhibition efficiency was determined (Bauxet al., 2018)

In a study to improve the active corrosion protection of carbon steel by water-based epoxy coating with smart CeO_2 nanocontainers, water-based epoxy coating containing CeO_2 nanocontainers was successfully applied on carbon steel for corrosion protection. CeO_2 nanocontainers were loaded with the corrosion inhibitor benzotriazole (BTA). Polyelectrolyte multilayers were deposited on the loaded nanocontainers by layer-by-layer assembly method. Responsive release of BTA molecules were studied in water media at different pH values using UV–vis spectroscopy. The anticorrosive performance of the epoxy coatings doped with 0.5 wt% of smart nanocontainers was tested by immersion of the coated carbon steel in 0.5 M NaCl solution. Electrochemical impedance spectroscopy (EIS) was used to estimate the influence of smart nanocontainers on the passive corrosion resistance. The self-healing performance of the coating with modified CeO_2 nanocontainers was studied by scanning Kelvin probe (SKP). From results of EIS and SKP, the addition of pH-sensitive nanocontainers into the epoxy resin inhibited the corrosion activities on the metal surface, showing a promising strategy for developing water-based epoxy coatings with long term protection performance (Liu, Gu, Wen, &Hou, 2018)

This study is an evaluation of corrosion resistance and self-healing behavior of zirconium-cerium conversion coating developed on AA2024 alloy. In the investigation, a zirconium–cerium conversion coating (ZrCeCC) was developed on aerospace aluminum alloy (AA2024) by simple immersion technique. Zirconium conversion coating (ZrCC) was also prepared for comparison. Surface morphology of ZrCC and ZrCeCC specimens exhibited smooth and cracked patterns respectively. Elemental analysis showed the presence of Zr and Ce in ZrCeCC specimen. XPS results indicated the presence of multiple oxidation states of Zr and Ce in the developed coatings. Potentiodynamic polarization results revealed the corrosion current density (i_{corr}) values obtained for both coatings (between 0.6 and 0.85μA/cm^2) were lower than bare specimen (1.2μA/cm^2). However, ZrCeCC specimen exhibited the lowest i_{corr} value at about 0.46μA/cm^2, after 168 h of immersion in 0.6 M NaCl solution. EIS studies showed that higher coating resistance (R_{coat}) value was obtained for ZrCeCC even after 168 h of immersion. The results obtained from simulated scratch cell test revealed a continuous increase in charge transfer resistance (R_{ct}) value for bare specimen which was exposed along with ZrCeCC in 0.1 M NaCl solution. The self-healing behavior of ZrCeCC was confirmed from all electrochemical tests. After 168 h of neutral salt spray exposure, the surface of ZrCeCC was almost comparable with the conventional chromate conversion coating(Yoganandan, Pradeep Premkuma, Balaraju,2015).)

In this study the corrosion inhibition of stainless steel (SS) in sulfuric acid solution containing sulfide ions was carried out. The study was carried out using weight loss method, potential-time, linear polarization, potentiodynamic polarization, electrochemical impedance measurements, scanning electron microscopy, Fourier transform infrared and energy dispersive X-ray analysis. It was found that the presence of the cephalosporin compound in the corrosive medium shifted the corrosion potential of SS to much positive side, which enhances self-passivation of SS, and the shifting increased with increasing inhibitor concentration. The cephalosporin compounds worked as effective inhibitors with mainly anodic and the efficiency increased as cefotaxime <cephapirin< cefazolin. The inhibitors form a protective adsorbed layer, which enriches the surface content of Ni and Cr and thus assists the SS to be passive. The antibiotics cephalosporins could be used as effective corrosion inhibitors for SS in acidic solutions containing sulfide ions. The inhibitors enhanced the passive oxide film of SS even in presence of aggressive ions such as sulfide ions (Hermas, Elnady, & Ali, 2019)

In an experimental and computational studies on corrosion inhibitors for mild steel in acidic medium, (1-Benzyl-1H-1,2,3-triazole-4-yl)methanol (BTM) and (1-(pyridin-4-ylmethyl)-

1H-1,2,3- triazole-4-yl)methanol (PTM) were prepared and investigated as corrosion inhibitors for mild steel in 1.0 M HCl. It was found that PTM functions as more effective inhibitor than BTM in the concentration range of 0.2 −1.0 mM. Computational chemistry studies showed that the triazole derivatives can adsorb on the mild steel surface by sharing the lone pair electrons of N atoms with iron atoms or by accepting electrons from iron surfaces. Due to its strong interaction with the mild steel surface in aqueous system, the pyridine segment was thought to be responsible for the higher inhibition efficiency of PTM (Ma, Qi, He, Tang & Lu, 2017).

In a study to examine the adsorption and corrosion inhibition of mild steel in hydrochloric acid solution by S-Allyl-O, O′-Dialkyldithiophosphates, S-allyl-O,O′-diphenyldithiophosphate (SOD1), S-allyl-O,O′-dibenzyldithiophosphate (SOD2) and S-allyl-O,O′-di(2-phenylethyl)dithiophosphate(SOD3) were successfully synthesized and characterized, which acting as the novel corrosion inhibitors for mild steel in hydrochloric acid (HCl) solution were evaluated by electrochemical measurements, weight loss measurement and scanning electron microscopy. Potentiodynamic polarization measurement indicated that the synthesized inhibitors were effective mixed-type inhibitors. The inhibition efficiency increased with inhibitor concentration increasing, and decreased with HCl concentration and temperature increasing. The adsorption of SOD1, SOD2 and SOD3 on mild steel surface obeys Langmuir isotherm. The adsorption of SOD1 and SOD3 on mild steel surface is a mixed adsorption involving both physisorption and chemisorption, while the adsorption of SOD2 on mild steel surface belongs to chemical adsorption (Laiet al., 2017)

In this study, comparative inhibition evaluation of some plants leaves extract namely *Cannabis sativa* (CS), *Rauwolfia serpentina* (RS), *Cymbopogon citratus* (CC), *Annona squamosa* (AS) and *Adhatodavasica* (AV) on the corrosion of aluminum alloy (AA) in 1 M NaOH was carried out. The corrosion tests were performed by using gravimetric, electrochemical impedance spectroscopy (EIS), potentiodynamic polarization and linear polarization resistance (LPR) techniques. RS showed maximum inhibition efficiency (η%), 97% at 0.2 g L^{-1}. Potentiodynamicpolarization curves justified that all the inhibitors were mixed-type. Surface morphology of AA was done by scanning electron microscopy (SEM) and atomic force microscopy (AFM) (Chaubey, Yadav, Singh & Quraishi, 2017).

In a study to design polymeric core-shell nanocontainers impregnated with benzotriazole for active corrosion protection of galvanized steel, polymeric nanocontainers (NCs) impregnated with corrosion inhibitor benzotriazole were formed using layer-by-layer deposition of

poly(acrylic acid) and poly(diallyldimethylammonium chloride) onto hematite particles in the presence of 0.1 M NaCl. Electric light scattering and electrophoresis were employed to control the formation and the size of NCs, as well as the stability of their suspensions. The inhibitor-loaded NCs were incorporated into the volume of the galvanized coating during the electrodeposition of zinc on the steel substrate to ensure additional self-healing effect in the case of corrosion attack. The surface morphology and the uniformity of this composite coating as well as the lack of aggregation of the nanocontainers were demonstrated by scanning electron microscopy. The influence of NCs present in the zinc electrolyte on the cathodic and anodic processes was investigated by cyclic voltammetry. The corrosion behavior of the composite coatings at conditions of external cathodic and anodic polarization was tested with potentiodynamic measurements and the results were compared to pure zinc coatings. The composite coatings with embedded NCs revealed enhanced corrosion protection of low carbon steel in comparison with the pure zinc coatings in neutral corrosion medium (Kamburova, Boshkova, Boshkov, Atanassova, &Radeva, 2018)

A comparative study of corrosion protection of the AA2024 aluminum alloy in 0.01 M NaCl solutions of Ce(III) and Ce(IV) ammonium nitrates was studied. The inhibition efficiency was evaluated applying linear sweep voltammetry (LSV) and electrochemical impedance spectroscopy (EIS). Superficial analytical techniques (optical microscopy, SEM, EDS and XPS) were applied for elucidation of the inhibition mechanism. The results showed that both cerium salts could behave either as inhibitors or activators of the corrosion process depending on the experimental conditions. The solutions of Ce(III) salt revealed better inhibitive ability than those of Ce(IV) in a relatively large range of conditions (Matter, Kozhukharov, Machkova, &Kozhukharov, 2012).

This is an experimental and theoretical investigation on adsorption properties of some diphenolicschiff bases as corrosion inhibitors at acidic solution/mild steel interface. The effect of three novel synthesizedschiff bases, namely, 1,3-bis[2-(2-hydroxy benzylidenamino) phenoxy] propane (P1), 1,3-bis[2-(5-chloro-2-hydroxybenzylidenamino) phenoxy] propane (P2), and 1,3-bis[2-(5-bromo-2-hydroxybenzylidenamino) phenoxy] propane (P3), on the corrosion of mild steel in 0.1 M HCl was investigated using potentiodynamic polarization and electrochemical impedance spectroscopy methods. Polarization measurements suggest that P1 acts as mixed type inhibitor while P2 and P3 behave as mainly cathodic inhibitors for acidic corrosion of steel. All electrochemical measurements show that inhibition efficiencies increased with increase in inhibitor concentration. This reveals that inhibitive actions of inhibitors were mainly due to adsorption

on steel surface. Adsorption of these inhibitors follows Temkin adsorption isotherm. The correlation between the adsorption ability of inhibitors and their molecular structures was investigated using quantum chemical parameters obtained by MNDO semi-empirical method. Calculated quantum chemical parameters indicate that Schiff bases adsorbed on steel surface by chemical mechanism (Yurt, Duran, & Dal, 2014).

This study was carried out to investigate phosphate ions as effective inhibitors for carbon steel in carbonated solutions contaminated with chloride ions. It focuses on sodium biphosphate (Na_2HPO_4) as corrosion inhibitor construction steel. All the tests were carried out in a solution that simulates the composition of the pores in chloride-contaminated carbonated concrete. The carbonated solution (CS) contained Na_2CO_3 (0.0015 mol L^{-1}), $NaHCO_3$ (0.03 mol L^{-1}) and NaCl (0.1 mol L^{-1}), resulting in $[Cl^-]/[OH^-]$=10000. Inhibited solutions (IS20, IS60 and IS100) incorporated 20, 60, and 100 mmol L^{-1} Na_2HPO_4 respectively. These were labeled IS20, IS60 and IS100 respectively and resulted in $[HPO_4^{2-}]/[Cl^-]$ = 0.2, 0.6, and 1. Cyclic voltammograms and anodic polarization curves were complemented with micro-Raman spectroscopy and XPS, to evaluate the surface film composition. The results showed that chloride contamination promotes active corrosion. When phosphate ions were incorporated, steel becomes passive with a more positive corrosion potential (Ecorr), and pitting presents as the predominant form of localized corrosion. Raman spectra showed a broad band centered in 982 cm^{-1}, suggesting that phosphates were incorporated to the passive film. Phosphates were also present in the corrosion products. The surface film became more protective to pitting for the highest biphosphate content. However, after pitting no repassivation was detected. After over one month in immersion, steel remains passive in the condition IS100, with inhibition efficiency higher than 99%. In contrast, in the case of IS60 and IS20, pitting was detected. It can be concluded that phosphate ions are good candidates to be used as corrosion inhibitors for steel in chloride-contaminated concrete (Yohai, Schreiner, Vazquez &Valcarce, 2016a)

In a research, the roles of a zinc phosphate pigment in the corrosion of scratched epoxy-coated steel were studied by means of electrochemical impedance spectroscopy, electrochemical noise measurement and scanning electrochemical microscopy. The experimental results of electrochemical noise measurement and electrochemical impedance spectroscopy revealed that zinc phosphate exhibited inhibition effect on the corrosion of the scratched epoxy-coated steel. The scanning electrochemical microscopy results implied that the scratched surface under zinc phosphate coating was re-healed by an insulating film. The mechanism of the inhibition effect of a zinc phosphate pigment was analyzed based upon the

combined stochastic theory and shot noise theory using the Weibull distribution and Gumbel distribution function (Shao, Jia, Meng, Zhang, & Wang, 2009)

In this study, synthesis and characterization of an effective corrosion inhibitive complex based on zinc acetate/UrticaDioica (ZnA-U.D) for corrosion protection of mild steel in chloride solution was investigated. The chemical structure and morphology of the complex were characterized by Fourier transform infrared spectroscopy (FT-IR), UV–vis, thermal gravimetric analysis (TGA), X-ray photoelectron spectroscopy (XPS) and scanning electron microscopy (SEM). The corrosion protection performance of the mild steel samples dipped in 3.5 wt.% NaCl solutions with and without ZnA-U. Dextract was investigated by visual observations, open circuit potential (OCP) measurements, electrochemical impedance spectroscopy (EIS) and polarization test. Results revealed that the ZnA successfully chelated with organic inhibitive compounds (i.e Quercetin, Quinic acid, Caffeic acid, Hystamine and Serotonin) present in the U.D extract. The electrochemical measurements revealed the effective inhibition action of ZnA-U. Dcomplex in the sodium chloride solution on the mild steel. The synergistic effect between Zn^{2+} and organic compounds present in the U.D extract resulted in protective film deposition on the steel surface, which was proved by SEM and XPS analyses (Salehi, Naderi, Ramezanzadeh, 2017).

In a study to examine the inhibition of aluminum alloy corrosion by cerous cations, the addition of small concentrations of cerous chloride (100-1000 ppm) to 0.1M sodium chloride solutions reduced the corrosion rate of 7075 by almost a factor of 10. Pre-exposure in distilled water also imparted corrosion resistance. Weight-loss corrosion rate tests, polarization and surface analysis experiments indicated that a cathodic inhibition mechanism, affecting the oxygen reduction reaction and the precipitation of cerium oxide, is operative. In practical terms, cerous ion inhibitors could provide an acceptable alternative to chromate inhibitors for this alloy (Hinton, Arnott, & Ryan, 1984).

This research investigated, the graphene oxide/silver nanostructure (GO-Ag) inhibitory effect on the corrosion of steel in the presence of sulfate reducing bacteria (SRB), via weight loss (WL) and Tafel polarization measurements. Moreover, molecular dynamic (MD) simulations were performed to obtain a deep understanding of the corrosion inhibition effect of GO-Ag. GO-Ag showed a significant antibacterial effect at 80 ppm. Moreover, WL and Tafel polarization measurements illustrated a great inhibition efficiency, which reached up to 84% reduction of WL and 98% reduction of corrosion current density (Icorr) after 7 days of incubation with GO-Ag. Based on MD simulations, bonding energy reached to the larger

value in the presence of GO-Ag, which indicated the ability of graphene oxide nanosheets to be adsorbed on the steel surface and prevent the access of corrosive agents to the steel surface. The radial distribution function (RDF) results implied distance between corrosive agent (water and SRB) and steel surface (Fe atoms), which indicated protection of the steel surface due to the effective adsorption of GO nanosheets through the active sites of the steel surface. The mean square displacement (MSD) result showed smaller displacement of the corrosive particles on the surface of steel, resulting that the GO-Ag molecules bonded with Fe molecules on the surface of steel (Kalajahiet al., 2022).

In this study the author investigated the types of corrosion inhibitor for managing corrosion in underground pipelines. Mass spectroscopy andhigh-pressureliquid chromatography on filed and synthetic samples was deployed to pinpoint the actual error value and compensation rate. Consequently, a reasonable degree of certainty for the amount of residual corrosion inhibitor was figured out to increase the reliability in the pipeline integrity management strategies (Sastri, 2010).

In another study to examine photo and thermally stable branched corrosion inhibitors containing two benzotriazole groups for Copper in 3.5 wt % sodium chloride solution. New branched conjugated derivatives with two benzotriazole groups as well as a linear analog containing one benzotriazole segment used as corrosion inhibitors for copper in 3.5 wt% sodium chloride solution containing 90 vol% water and 10 vol% ethanol solvents at 298 K were synthesized. It was shown that the corrosion of copper is inhibited more efficiently by the branched inhibitors. The adsorption mechanism on copper surface was analyzed by Langmuir isotherm and various spectral characterizations, and the results suggest a primary chemisorption adsorption on copper surface. Molecular modeling was performed. Photo and thermal stabilities of the studied inhibitors were investigated (Jing et al., 2018).

In localized approach to study the effect of cerium salts as cathodic inhibitor on iron/aluminum galvanic coupling. The inhibition effect of cerium salts on iron/aluminum galvanic coupling was investigated by electrochemical microcell and scanning vibrating electrochemical technique (SVET). The importance of the electrode geometry on the SVET responses was evidenced. The effect of concentration and the influence of the anionic part of cerium salts on the inhibitive efficiencies and protective mechanisms were studied. Cerium salts inhibit the corrosion of iron/aluminum galvanic coupling by reducing the cathodic activity. Microcell analysis confirmed the passivation of aluminum. (SEM + EDS)

analyses allowed for understanding how the cerium salts act to improve the corrosion behavior (Mouangaet al., 2015).

In this study, the impact of phosphate corrosion inhibitors on chloride binding and release in cement pastes was investigated. The impact of three kinds of phosphate corrosion inhibitors (MFP, DHP and TSP) on chloride binding and release in cement pastes was investigated by means of chloride binding isotherms (CBIs), X-ray diffraction (XRD) and thermogravimetric analysis (TGA). Experiments of chloride binding, chloride release in deionized water and phosphate solutions were implemented separately. The regularity and factors of CBIs were well studied and the results of CBIs showed that phosphate inhibitors reduced chloride binding chemically due to reactions between Friedel's salt and phosphate. Besides, the release of bound chloride can be well-calculated by CBIs. Furthermore, a modified CBI, taking effective phosphate concentration into account, has been established, and chloride penetration predictions have been made consequently (Chenet al., 2020).

In a research to evaluate protective coatings for offshore applications, corrosion and tribo-corrosion behavior in synthetic seawater coatings were widely used in the corrosion protection of metallic materials in marine environments. In this work, the corrosion and tribo-corrosion behavior of three potential coatings employed in offshore applications were evaluated. The coatings studied were a thermally sprayed carbide coating with an organic sealant (C1), a thermally sprayed aluminum with an organic sealant (C2), and an epoxydic organic coating reinforced with ceramic platelets (C3). Electrochemical impedance spectroscopy and potentiodynamic polarization techniques were employed to assess the corrosion performance of the coatings in synthetic seawater. Furthermore, unidirectional ball-on-disc tribocorrosion tests were performed to study the response of the coatings subjected to simultaneous action of wear and corrosion. The coatings were found to provide the steel substrate with enhanced corrosion resistance, both in absence and during wear process, and to improve in the tribological properties with lower coefficients of friction in seawater. The coating less affected by sliding in terms of corrosion resistance was C2 coating, which also showed the lowest coefficient of friction (Lopez-Ortega, Bayon, & Arana, 2018).

This study evaluated the performance of steel samples immersed in 3.5% NaCl aqueous solution-containing zinc aluminum polyphosphate (ZAPP) pigment extract compared to those involving conventional zinc phosphate (ZP) pigment extract and also no pigment (blank) using electrochemical tests such as electrochemical impedance spectroscopy (EIS)

and linear polarization (LP) as well as surface analysis. Impedance spectra and polarization curves revealed two different trends, showing the superiority of ZAPP pigment. Based on the results of scanning electron microscopy (SEM) and energy dispersive X-ray analysis (EDX), presence of a precipitated layer on the surface was confirmed when steel sample was immersed into the solution-containing ZAPP (Naderi & Attar, 2008).

In a particular research, the corrosion response of mild steel in 0.5 M H_2SO_4 acid solution in the presence of Moringeroliefera (MO) leaf extract was investigated using gravimetric, electrochemical, and DFT techniques. Gravimetric results indicated that MO exhibits a high inhibition value up to 93.0% when the concentration was 1.5 g/L. Inhibition value in general increased with an increase in concentration of the extracts but decreased with prolonged exposure time and temperature. Analysis of polarization curves indicated that MO extract acted as mixed-type inhibitors. The adsorption process of MO on a mild steel surface in the acid solution fitted the Langmuir isotherm. GC/MS analysis of MO extract revealed the presence of more than 29 active constituents including 9,12-Octadecadienoic acid (Z, Z) methyl ester (28.55%); n-Hexadecanoic acid (11.24%); 9,12,15-Octadecatrienoic acid methyl ester (9.31%), Benzeneacetonitrile, 4-hydroxy-(6.32%), 2-Furancarboxaldehyde,5-(hydroxymethyl)-(5.6%), Heptadecane (4.85%). Quantum chemical calculations were applied on some of the identified constituents to assess their adsorbent ability on the mild steel surface and the result revealed remarkable high interaction energies (Akalezi, Maduabuchi, Enenebaku, & Oguzie, 2020).

In a similar research to evaluate the inhibition efficiency of chrysophyllumalbidum extract in controlling corrosion of mild steel in 1 M HCl by weight loss, potentiodynamic polarization and electrochemical impedance techniques at 303 K. The effect of immersion time and temperature on inhibition efficiency of the extract was also studied. Result of inhibition was found to increase with increasing concentration of the extract but decrease with increasing time and temperature. Data from electrochemical measurements suggest that the extract functioned by adsorption of the organic matter on the metal/corrodent interface, inhibiting both the anodic and cathodic half reactions of the corrosion process. The increase in concentration of the inhibitor causes an increase in the activation energy and a decrease in the exponential factor k. The plant extracts followed Langmuir adsorption isotherm. Moreover, the process of adsorption was spontaneous, stable and considered to be physical adsorption. The thermodynamic properties recorded suggested that the process of film formation was higher than the destruction of the metal surface and that the adsorption process was exothermic (Akalezi & Oguzie, 2015).

In another research, accelerated cut-edge corrosion performance of commercialized full waterborne coating systems containing enviro-friendly corrosion inhibitors was studied on 55 wt% Al, 44 wt% Zn and 1 wt% Si galvanized steel in 5 wt% NaCl solution at ambient temperature via the Scanning Vibrating Electrode Technique (SVET). At the same volume content (7–11 wt.%), benzotriazole pigments had a better overall cut-edge corrosion performance than calcium ion exchanged silica pigments. It was due to benzotriazole's superior cathodic protection of the cut-edge in comparison with calcium silicate. Furthermore, although both enviro-friendly inhibitors did not exhibit the same performance level as the conventional Cr(VI)-containing system, they exhibited promising results in inhibiting cut-edge corrosion in a fully commercialized waterborne coating system (Sheikholeslamiet al., 2021).

Also, in a certain study, the corrosion inhibition of X70 steel in 1 M HCl by *Ginkgo* leaf extract (GLE) was investigated by conducting electrochemical measurements. The inhibition efficiency exceeded 90% in the presence of 200 mg/L GLE at all of the tested temperatures. The excellent inhibition capacity, which was attributed to the formation of inhibitor–adsorption films on the surface of the X70 steel, was confirmed by field emission scanning electron microscopy and atomic force microscopy. The adsorption of GLE on steel surface followed the Langmuir adsorption model. Potential of zero charge measurement and quantum chemical calculation were adopted to elucidate the inhibition mechanism (Qiang, Zhang, Tan, & Chen, 2018).

In a research, the assessment of inhibition efficiency of 3,4-diaminobenzonitrile was studied against steel corrosion, using electrochemical impedance spectroscopy, potentiodynamic measurements and solution assay analysis. The corrosion rate was determined with different routes; apparent Stern–Geary coefficient (*B*) derived from solution assay analysis and compared with coefficient value obtained from Tafel slopes. For blank solution, the corrosion current values were quite different when comparing results from Tafel slopes and AAS. With the presence of inhibitor, the difference became negligible. Once anodic dissolution kinetics was governed by strongly adsorbed inhibitor, resistance against charge transfer process became more important and corrosion rate results obtained from different routes came closer (Si & Erbil, 2016).

In an experiment to examine the corrosion of Al alloy 6061 in borated solutions simulating the water chemistry of post-LOCA sump water, hydrogen evolution (HE) rates were evaluated by analyzing the potentiodynamic cathodic polarization curves from rotating

cylinder electrodes, and an empirical formula predicting the HE rates as a function of solution pH was proposed based on the evaluation results. At pH 7, the dominant cathodic reaction during free corrosion was found to be the oxygen reduction reaction and the HE rate was slow; however, the HE reaction became increasingly significant as the solution pH progressively increased to 11. The HE sources on the alloy surface were inferred to be mainly the bulk matrix, which was covered with a less protective hydroxide film in more alkaline solution, as well as the trenches formed by the intense anodic dissolution of the matrix around electrochemically more noble Fe-bearing intermetallic particles. Local alkalization due to preferential oxygen reduction on these intermetallic particles may also contribute to the formation of such trenches and HE; however, this mechanism should have been mostly suppressed by the buffering capacity of the borated solutions (Huang, Lister & Uchida, 2020)

In a study, corrosion inhibition effect of 2-mercaptobenzothiazole (MBT) and 2-aminobenzothiazole (ABT) compounds on ST-37 carbon steel in 1 M hydrochloric acid solution was investigated by electrochemical impedance spectroscopy (EIS), and it was observed that both of these compounds have corrosion inhibition effect on carbon steel. Evaluation of electrochemical behavior in test solutions showed that by increasing the immersion time from 15 to 300 min, corrosion resistance of samples is increased and at the same immersion time MBT has a better corrosion inhibition in comparison to ABT. AFM technique was performed for MBT and ABT. The results of calculations showed superior inhibition efficiency of MBT in comparison to ABT. This can cause easier protonation and consequently adsorption on the metal surface occurs (Jafar, Akbarzade, &Danaee, 2019)

In one research work, the inhibitive performance of chitosan and silver nanoparticles – chitosan (AgNPs-Chi) composite towards St37 steel corrosion in 15% H_2SO_4 solution was studied using weight loss and electrochemical techniques in addition to surface morphological examination. Results obtained showed that chitosan could fairly protect St37 steel surface by 45%. Inhibition efficiency above 94% was achieved with AgNPs-Chi composite. AgNPs-Chi composite performed better at longer immersion time and elevated temperature. AgNPs-Chi retarded both anodic and cathodic redox reactions. The mode of adsorption of AgNPs-Chi onto St37 surface was described using Langmuir adsorption isotherm. Surface screening results ascertained the adsorption of AgNPs-Chi molecules on St37 surface (Solomon, Gerengi & Umoren, 2017).

In a particular study, computational modelling methods were used to investigate the properties of a range of small organic, potentially safer inhibitors and their interactions with

technologically relevant alloy surfaces. Robust and predictive computational models of corrosion inhibition for a structurally related data set of organic compounds from the literature were generated. The studies have correlated molecular features of the inhibitor molecules with inhibition and identified those features that have the greatest impact on experimentally determined corrosion inhibition. This information can be used to drive guided decision making for in silico or experimental screening of molecules for their corrosion inhibition efficiency, while considering more carefully their environmental consequences (Winkleret al., 2014).

In yet another work, a new approach of classical electrochemical analyses to investigate green synthesis of 1-Benzyl-4-Phenyl-1 H -1, 2, 3-Triazole, its application as corrosion inhibitor for mild steel in acidic medium. 1-benzyl-4-phenyl-1H-1,2,3-triazole was prepared using anenvironment friendly and facile synthetic procedure and its performance as an organic corrosion inhibitor for mild steel in $1.0\,\mathrm{mol\,L^{-1}}$ HCl was investigated using four different methods. An average efficiency of 81.7% was obtained with $2.13\,\mathrm{mmol\,L^{-1}}$ solutions of the organic compound. A new approach to classical electrochemical analyses confirmed the inhibitor adsorption on the metal surface. Temperature effect studies in the oxidation inhibition behavior as well as calculated thermodynamic parameters were consistent with a chemisorption process and atomic force microscopy showed the formation of a protective film (Machado, Alvarez, Escarpini, Maldonado, & Ariel, 2019).

Sill in a study, the authors examined the synergistic corrosion inhibition effect between calcium lignosulfonate (CLS) and three kinds of inorganic inhibitors (Na_2MoO_4, Na_2SnO_3, and $NaWO_4$) with various molar ratios on Q235 carbon steel in alkaline solution (pH 11.5) with 0.02 mol/L NaCl by cyclic potentiodynamic polarization, electrochemical impedance spectroscopy, linear polarization, scanning electron microscopy, and X-ray photoelectron spectroscopy. Molybdate and stannate in hybrid inhibitor could promote the passivation of steel and form a complex film, which could suppress the corrosion effectively. Moreover, the insoluble metal oxides in the complex film formed by three kinds of inorganic inhibitor could help the adsorption of CLS onto the steel surface. The CLS molecules could adsorb onto the steel surface and metal oxides to form an adsorption film to protect the steel from corrosion. A three-layer protection film formed by a hybrid inhibitor, including passivation film, deposition film, and adsorption film, would effectively inhibit the corrosion reactions on the steel surface. The CLS compound with molybdate with the ratio of 2:3 showed the

best inhibition effect on both general corrosion and localized corrosion (Lin, Tang, Wang, Y., Wang & Zuo, 2020).

In a study to examine the effect of surface mild steel preparation on its electrochemical behavior in neutral chloride solution without and with an inorganic inhibitor, various surface preparations were examined: alkaline degreasing, acid pickling and polishing. Open circuit potential measurements and potentiodynamic polarizations were used as corrosion monitoring techniques. The effect of chloride concentration was evaluated. The ability of inorganic inhibitors (Na_2MoO_4, $NaNO_2$, Na_2WO_4 and Na_2VO_3) to stabilize the passive state of steel in chloride containing solutions was assessed by electrochemical and surface analysis techniques. The results revealed that, among the four inhibitors studied, the sodium molybdate is the best environmentally friendly corrosion inorganic inhibitor for steel (Atmani, Lahem, Poelman, Buess-Herman & Olivier, 2013).

In a certain paper, sodium silicate as a corrosion inhibitor was studied on the inhibition effect of AZ91D magnesium alloy. From the results of the corrosion tests, sodium silicate could effectively improve the corrosion resistance of the alloy at the optimum concentration 10 mmol/L, while the pH value range from 10.5 to 12.5 is preferable. These results can provide a guide for the protection of magnesium alloy in the cooling water systems, etc (Gaoet al., 2011).

In an experimental and theoretical study of benzoxazines corrosion inhibitors, in this study, 2-Methyl-4H-benzo[*d*][1,3]oxazin-4-one (BZ1) and 3-amino-2-methylquinazolin-4(3H)-one (BZ2) were evaluated for their corrosion inhibition properties on mild steel (MS) in hydrochloric acid solution by weight loss technique and scanning electron microscopy. Results showed the inhibition efficiency values depend on the amount of nitrogen in the inhibitor, the inhibitor concentration and the inhibitor molecular weight with maximum inhibition efficiency of 89% and 65% for BZ2 and BZ1 at highest concentration of the compounds (Kadhim et al., 2017).

In a study on optimization, using potentiodynamic polarization and EIS in a combinatorial matrix of four rare earth chlorides the authors evaluated for the corrosion inhibition of aluminum alloy AA2024-T3 in aqueous solution. Two electrochemical techniques, potentiodynamic polarization (PP) and electrochemical impedance spectroscopy (EIS), were used to evaluate AA2024-T3 corrosion in 0.1 M NaCl with the addition of 10^{-3} M of rare earth chloride mixtures at time periods up to 18 h.PP experiments showed rare earth

inhibition of up to 98% within the first hour and thereafter corrosion rates were steadily decreased, the open-circuit potential (OCP) of AA2024-T3 decreased as a function of time for all the solutions indicating predominantly cathodic protection. However, differing trends in the OCP were observed during PP and EIS experiments were discussed in terms of likely time-dependent mechanisms.A comparative study of optimization models indicated the best mixture at 10^{-3} M total inhibitor concentration was predicted to be 72% cerium (Ce) and 28% (praseodymium (Pr)/lanthanum (La)) ions. As the amount of Ce was decreased from this level the corrosion inhibition was predicted to decrease also, regardless of what other rare earths (La, Pr and Nd) were added alone or in combination. Individually, La, Pr and Nd showed varying levels of corrosion inhibition activity, all of which were inferior to that of Ce. If Ce was absent entirely, then a mixture of approximately 50% Pr and 50% Nd was predicted to be preferred. This was one of the first applications of combinatorial design for the optimization of corrosion inhibitor mixtures (Musteret al., 2012).

Solomon, Gerengi, Kaya, &Umoren (2017b)used transmissions electron microscope(TEM), fourier transform infrared (FTIR) spectroscopy, ultraviolet - visible spectroscopy (UV-vis), scanning electron microscope (SEM), and energy dispersive x-ray spectroscopy (EDS) for characterization of carboxymethyl cellulose incorporated in AgNPs nanoparticles. The weight loss, electrochemical techniques such as; dynamic - electrochemical impedance spectroscopy, electrochemical impedance spectroscopy, and potentiodynamic polarization supported by surface assessment such; as SEM, atomic force microscope, and FTIR were employed for the anticorrosion study of CMC / Ag NPs on st 37 Specmen in 15% H_2SO_4 medium and they concluded that AFM and SEM graphics revealed smoother surface for st 37 specimen in the acid solution containing inhibitor than in the solution without the inhibiting agent. FTIR and EDS results showed that CMC/ AgNPs molecules were adsorbed on the metal surface.

Ramezanzadehet al (2019), used electrochemical analyses to study the theoretical molecular dynamics (MD), simulation and density functional theory (DFT) of inhibitors. The results showed that all considered organic - inorganic inhibitors adhered to steel surface when evaluated for adsorptive properties, reflecting their corrosion inhibition effect.

Martien et al, (2018) used electrochemical impedance spectroscopy, weight loss coupons and Surface analysis to study the corrosion of iron when exposed to saturated H_2S at a pH of 4. The results showed very good correlation between corrosion current and hydrogen permeation current density. The authors confirmed the validity of impedance) analysis as the

permeation efficiency was close to 100%. This revealed that the corrosion rate of 490 mm/year was measured by weight loss specimens and found to result in a calculated corrosion rate of 530 ¥/year.

Alibakhshi et al. (2014) used scanning electron microscope, energy dispersive x-ray and infrared spectroscopies to - study a synthesized sodium zinc phosphate pigment. The results indicated that the corrosion inhibitive performance of the synthesized pigment was higher than on that of the commercial zinc phosphate.

Guo et al. (2017) used density functional based tight binding (DFTB) method to investigate the adsorption properties of inhibitors. They also used frontier molecular theory to study the molecular activity of free chalcone derivatives. The study helped to understand the anticorrosive mechanism of similar Organic inhibitors and provides a feasible way to develop novel corrosion inhibitors.

Othmanet al (2018), used electrochemical impedance spectroscopy (EIS), and electrochemical frequency modulation (EFM), measurement techniques to investigate the characterization and Synthesis of a novel organic. Corrosion inhibitor for mild steel in 1M hydrochloric acid (HCI) changed the impedance parameters and suggested an adsorption of the inhibitor onto the mild steel surface, leading to the formation of protective films. The results showed that the inhibition efficiencies increased with increasing the concentrations of the inhibitors and decreased with increasing temperature.

Li et al (2011), on their part used potentiodynamic polarization and electrochemical impedance spectroscopy (EIS) methods to study the inhibition effect of Sodium molybdate (Na_2MoO_4) on the corrosion of aluminum in 1.0 M H_3PO_4 solution. The results showed that Na_2MoO_4 is a good inhibitor, and the inhibition efficiency obtained by three methods is higher than 84% at 20 mM. The adsorption of Na_2Mo0_4 was found to obey Freundlich isotherm at lower concentrations and Langmuir isotherm at higher concentration: The polarization curves indicated that Na_2Mo0_4 acts as an anodic inhibitor. The EIS Spectra exhibited three loops (two capacitive loops and one inductive loop.

Chaubeyet al (2017), used gravimetric electrochemical impedance Spectroscopy (ELS), potentiodynamic polarization and linear polarization resistance (LPR) techniques

Lunaet al (2019), used gravimetrical, electrochemical, spectroscopic and simulation methods to study the inhibition effect of ionic liquid (IL) represented by 1-ethyl-3-methylimidazolium thiocyanate (EMIM)+ (SCN)- on the corrosion of API 5L X52 Steel in 0.5M H_2S0_4 Solution at different temperatures. The scanning electron microscopy characterization revealed less surface damage in the corroded sample confirming the effectiveness of the IL, while x-ray

photoelectron spectroscopy evidenced the formation of an interfacial protective layer, composed by the inhibitor molecules and corrosion products.

Gao et al (2018), used scanning electron microscopy (SEM), X-ray photoelectron spectroscropy (XPS) and Fourier transform infrared reflection absorption spectroscopy (FTIR) to monitor the surface chemistry of coatings in a salt spray test and electrochemical Tafel polarization curves determine the corrosion resistance of inorganic and organic composite passivation films with Corrosion inhibitors.

Delaunay et al (2018) used electrochemical impedance spectroscopy to analyze film-forming amines for the corrosion protection of carbon steel in which Octadecylamine (ODA) was employed. Electrochemical impedance data analysis was performed to extract physical parameters of the ODA thin film that formed on a P275 carbon steel surface. From the impedance results with and without ODA, the instantaneous corrosion inhibition efficiency was determined.

Liuet al (2018), used Ultraviolet Visible Spectroscopy (UV-vis), electrochemical impedance Spectiooscopy (EIS) and Scanning Kelvin Probe (SKP) in a study to improve the active corrosion protection of carbon steel by water-based epoxy coatings with smart CeO_2 nanocontainers. From the results of the EIS and SKP, the addition of pH-sensitive nanocontainers into the epoxy resin inhibited the corrosion activities on the metal surface, showing a promising strategy for developing water-based epoxy coatings with long term protection performance.

Yoganandanet al (2015), used potentiodynamic polarization, electrochemical impedance spectroscopy and x-ray photo electron spectroscopy to evaluate the corrosion resistance and self-healing behavior of Zirconium-Grium Conversion Coating developed on AA 2024 ralloy by simple immersion technique. The XPS results indicated the presence of multiple oxidation states of Zr and Ce in the developed Coatings. Potentiodynamic polarization results revealed the corrosion current density (Icorr) values obtained for both coatings were lower than bare specimen. EIS results showed that a highercoatings resistance (Rcoat) value was obtained for ZrCeCC even after 168hours immersion.

Hermas et al (2019) used weight loss method, potential-time, linear polarization, potentiodynamic polarization, electrochemical impedance measurements, scanning electron microscopy, fourier transform infrared and energy dispersive x-ray analysis to study the corrosion inhibition of stainless steel (SS) in sulfuric acid solution containing sulfide ions. It was found that the presence of the cephalosporin compound in the corrosive medium shifted the corrosion potential of SS to much positive side, which in turn enhanced self-passivation of SS, and the shifting increased with increasing inhibitor concentration.

Laiet al (2017), used electrochemical measurements, weight loss measurements, scanning electron microscopy and potentiodynamic polarization measurements to evaluate the adsorption and corrosion inhibition of mild steel in hydrochloric acid solution by S-Allyl-0, O'-Dialkyldithiophosphates. Potentiodynamic results indicated that the synthesized inhibitors were effective mixed -type inhibitors. The inhibition efficiency increased with inhibitor concentration increasing and decreased with HCL concentration and temperature increasing.

Chaubey et al (2017) used gravimetric, electrochemical impedance spectroscopy (EIS), potentiodynamic polarization and linear polarization resistance (LPR) techniques to evaluate and compare the inhibition properties of some plant leaves extract namely Cannabis Sativa (CS), RauwolfaSerpentina (RS), CumbopogonCitratus (CC), Annona Squamosa (AS) and AdhatodaVasica (AV) on the corrosion of aluminum alloy (AA) in 1M NaOH. It was found that potentiodynamic polarization curves justified that all the inhibitors were mixed-type. Surface morphology of AA was done by scanning electron microscopy (SEM) and Atomic force microscopy (AFM).

In another study, Matter et al (2012), used linear sweep voltammetry (LSV) and electrochemical impedance spectroscopy (EIS), superficial analytical techniques (optical microscopy, SEM, EDS, XPS to compare the corrosion protection of the AA 2024 aluminum alloy in 0.01M NaCl Solutions of Ce (111) and Ce (IV) ammonium nitrates. The results showed that both cerium salts could behave either as inhibitors or activators of the corrosion depending on the experimental conditions.

Yurt et al (2014), investigated the adsorption properties of some diphenolic schiff labeled as P1, P2 and P3 bases as corrosion inhibitors at acidic solution / mild steel interface using potentiodynamic polarization and electrochemical impedance spectroscopy methods. The polarization measurements suggested that P1 acts as mixed type inhibitor while P2 and P3 behaved as mainly cathodic inhibitors for acidic corrosion of steel. All electrochemical measurements showed that inhibition efficiencies increased with an increase in inhibitor concentration.

Akalezi et al (2020), investigated the corrosion response of mild Steel in 0.5M H_2S0_4 acid solution in the presence of moringer oleifera (MO) leaf extract using gravimetric, electrochemical, and DFT techniques. Gravimetric results showed that MO exhibited high inhibition efficiency up to 93.0% at a concentration of 1.5g/L. Polarization results indicated that MO extract acted as a mixed-type inhibitor.

In another study, Akalezi& Oguzie (2015), used weight loss, potentiodynamic polarization gravimetric and electrochemical techniques, whereas the agar disc diffusion method and electrochemical impedance spectroscopy to evaluate the inhibition efficiency of Chrysophyllumalbidum extract in controlling corrosion of mild steel in 1M HCL. They also studied the effect of immersion time and temperature on the inhibition efficiency of the extract. Results from electrochemical measurements suggested that the extract functioned by adsorption of the organic matter on the metal /corrodent interface, inhibiting both the anodic and cathodic sites.

Yohaiet al (2016), investigated phosphate ions as effective inhibitors for carbon steel in carbonated solutions contaminated with chloride ions using cyclic voltammograms, anodic polarization, micro-Raman spectroscopy and XPS. The results showed that chloride contamination promotes active corrosion. They concluded that phosphate ions are good candidates to be used as corrosion inhibitors for steel in chloride contaminated environment.

Yaoet al (2009) evaluated the role n of a zinc phosphate pigment in the corrosion of scratched epoxy-coated steel using electrochemical impedance spectroscopy, electrochemical noise measurement and scanning electrochemical microscopy. The experimental results of electrochemical noise measurement and electrochemical impedance spectroscopy showed that zinc phosphate exhibited inhibition effect on the corrosion of the scratched epoxy-coated steel.

Salehi et al (2017) used fourier transform infrared spectroscopy (FT-IR), UV-vis, thermal gravimetric analysis (TGA), x-ray photoelectron spectroscopy (XPS), and scanning electron microscopy (SEM) to examine the synthesis and characterization of an effective corrosion inhibitive complex based on zinc acetate/UrticaDioica (ZnA-U.D) for corrosion protection of mild steel in chloride solution. Results revealed that the ZnA successfully chelated with organic inhibitive compounds present in the U.D extract. The electrochemical measurements revealed the effective inhibition action of ZnA-UD complex in the sodium chloride solution on the mild steel. The synergistic effect between Zn^{+} and organic compounds present in the UD extract resulted in protective film deposition on the steel surface, based on the SEM and XPS.

Mouangaet al (2015) used electrochemical microcell and scanning vibrating electrode technique to analyze the effect of cerium salts as cathodic inhibitors on iron / aluminum galvanic coupling. The results showed that carium salts inhibit the corrosion of Iron/aluminum galvanic coupling by reducing the cathodic activity. Microcell analysis confirmed the passivation of aluminum.

Sheikholeslami et al (2021) used scanning vibrating electrode technique (SVET) to evaluate the corrosion performance of commercialized full waterborne coating systems containing enviro-friendly corrosion inhibitors in 55 wt% Al, 44 wt% Zn, and 1wt% Si galvanized steel in 5wt%

NaCl solution at ambient temperature. The results showed promising outcome in inhibiting cut-edge corrosion in a fully commercialized waterborne coating system.

Lin et al (2020) used dynamic polarization, electrochemical, spectroscopy, linear polarization, scanning electron microscopy and x-ray photoelectron spectroscopy to examine the synergistic corrosion inhibition effect between calcium lignosulfonate (CLS) and three kinds of inorganic inhibitors (Na_2 MoO_4, Na_2SnO_3, and $NaWO_4$) with various molar ratios an Q235 carbon steel in alkaline solution (pH 11.5) with 0.02 mol/L NaCl. From the results of the examination, it was observed that the CLS compound with molybdate of the ratio 2:3 showed the best inhibition effect on both general and localized corrosion.

2.7 Summary of Literature Review

Generally speaking, several works have been reported in the literature, as noted. There is a huge economic cost associated with corrosion running into trillions of dollars annually including human lives. Corrosion failure is perhaps one of the most insidious ways an engineering system can fail catastrophically. As clearly stated in section 2.4 of this literature review, most corrosion failures occur unexpectedly. Subsequently, what is of paramount interest to the corrosion engineer is to ensure that corrosion failures are minimized to save the huge cost associated with it, through corrosion prevention, mitigation, control and management. To achieve this, researchers have been up and working in an effort to creating effective and efficient solutions in order to maintain and sustain the integrity of infrastructures by adopting appropriate methodologies. Currently, organic compounds are established as one of the most effective and profitable methods of corrosion inhibition, as such, research is oriented towards organic compounds such as plant extracts because of their association with E4 (efficiency, economy, ecology and environmental friendliness) policy and are used for different industrial applications. To confirm this, many studies from the literature have indeed reported such and the convergence is indeed unambiguous. However, there are numerous challenges of using these compounds. One of the biggest challenges of using organic corrosion inhibitors is their limited solubility, especially in polar electrolytes. It is curious to note that out of the enormous literature reported in this study, only few considered the evaluation of solubility in their reported findings. It seems that despite the enormous research on the subject area of organic corrosion inhibition no serious attention is given to one of the major challenges militating against its development and design. For instance, the insolubility of an inhibitor in crude oil drilling and recovery can lead to emulsion formation which will jeopardize the entire drilling process, sometimes leading to complete loss of the oil well. Because of this, when evaluating compatibility issues of corrosion inhibitors for oil and gas operations, the effect that an inhibitor has on the emulsion forming tendency of well fluids is critical in the selection of the proper inhibitor. Likewise, almost all the

reported studies have demonstrated wonderful outcomes in terms of inhibition performance, consistently maintaining that inhibitor concentration has a direct relationship with inhibition efficiency. Be that as it may, recently, adequate efficiency at lower inhibitor dosages or concentration and cost effectiveness are also important requirements for a substance or molecule to be utilized as corrosion inhibitor. Consequently, these reports have only demonstrated the huge gap between what is obtainable in the field and research findings.

2.7.1 Literature gap

All reported studies have the problem of methodological gap such that coupon tests performed in almost all the experiments were carried out on stationary electrolyte. However, for inhibitor's qualification for industrial applications, coupon tests in the presence of fluid flow, shear stress and motion are often recommended. The tests include: burble test, rotating cage autoclave test, jet impingement, high temperature and pressure, and rotating cylinder electrode tests. Although in the absence of these tests, using a variation of methodologies is often recommended to close the gap (Jacobs, 2011; Muller-Bloch & Kranz, 2014; Miles, 2017).

CHAPTER THREE

MATERIALS AND METHODS

3.1 Materials

The materials and chemicals/reagents used in this project work and their suppliers are presented in tables 3.1a and 3.1b respectively.

Table 3.1a: List of materials and suppliers

S/N	**MATERIAL**	**NAME OF SUPPLIER**
1	Carbon Steel (test coupons)	Leoco & Co. Ltd, PH
2	Emery Carbide Abrasive with Mohs hardness = 9.5	GZ Ind. Supplies Ltd, PH.
3	Biovia Materials Studio Software Version 8.	BIOVIA (provided by ACEFUELS general purpose lab.
4	Origin Software	OriginLab Corporation (provided by ACEFUELS general purpose lab.
5	*Musa paradisiacal* Leaf	From Omukoro farms, PH.

Table 3.1b: List of chemicals/reagent and suppliers

S/N	CHEMICAL/REAGENT	NAME OF SUPPLIER
1	De-ionized water = 18MΩ*.cm*	GZ Ind. Supplies, PH.
2	Acetone $\geq$ 99.5%	labstore.ng
3	Ethanol (70%)	Barivan Chemicals, PH.
4	NaCl $\geq$ 99.5%	Barivan Chemicals, PH.
5	Silica gel $\geq$ 99%	Jopec business concept Ltd, PH.

3.2 Equipment

The equipment used for this project work and their manufacturers are listed in table 3.2

Table 3.2: List of Equipment and name of manufacturer

S/N	EQUIPMENT/MODEL	MANUFACTURER (S)
1	Metallographic Lapping and Polishing Machine (UNIPOL-820)	Zhengzhou CY Scientific Instrument Co. Ltd.
2	Hot Air Oven Dryer	Zhengzou Wollen Instrument EquipmentCo. Ltd.
3	Beaker (s)	Runlab
4	Nima Industrial Electric Grinder	DMSALES
5	FA2104 Electric Weighing Balance	Changzhou Xingyun Electrionic Equipment
6	PerkinElmer Spectrum IR 10.7	PerkinElmer Inc.
7	Potentiostatic/Galvanostat	Biologic
8	Magnetic Stirrer	Biobase Group
9	Gas Chromatography Mass Spectroscopy (GC-MS)	Agilent
10	Atomic Force Microscope (AFM) 5500M II	Hitachi High-Tech
11	Optical Tensiometer	Biolin Scientific

3.3 Methods

3.3.1 Experimental Work Flow and Procedures

The experimental work flow involves five major steps which are crucial for the project implementation and completion as follows:

1. Sourcing, selection and collection of materials needed for the project work.
2. Preparation of specomen from the sourced materials for experimental purposes
3. Following established harzard and operability guidelines/standards to carry out all experimental procedures in the laboratory
4. Evaluation and analyses of data generated in course of the experimentation
5. Presentation and reporting of findings, and results of evaluation and analyses

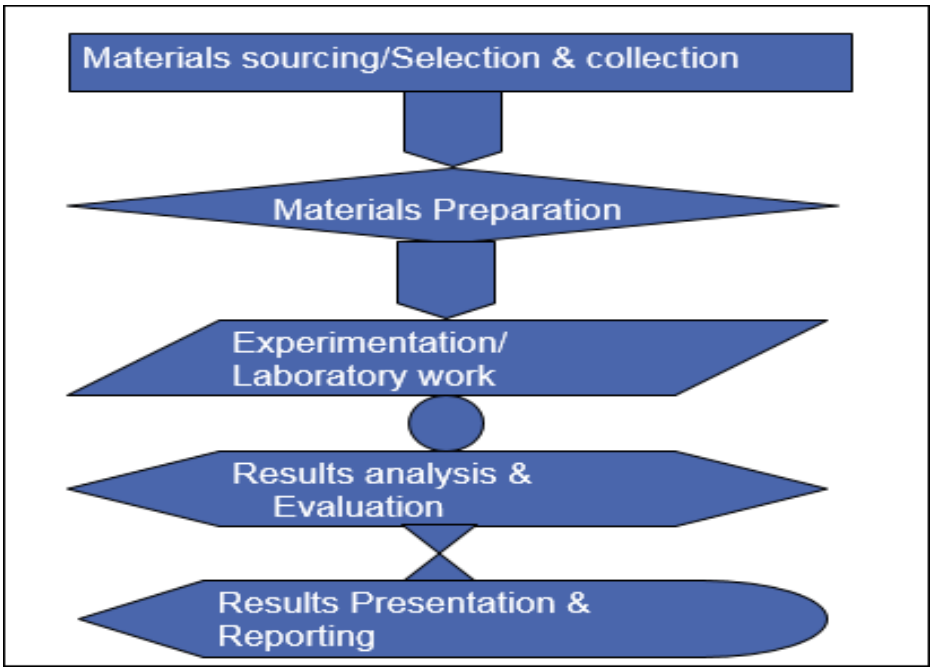

Figure 3.1: Experiment Design/work flow (Drawn by PhD student)

The following sub-sections describe the experimrntal procedures

3.3.2 Preparation of MPL Extract

The MPL was collected at Port Harcourt, Rivers State, Nigeria. And was then transported in a clean sack bag to the Africa Centre of Excellence in Future Energies and Electrochemical Systems' General Purposes Research Laboratory at Federal University of Technology, Owerri, where the leaves were oven dried before crushing into powdered form. Thereafter, it was weighed, dissolved into 70% ethanol and then allowed to stay for 48 hours before it was extracted and concentrations of 10g/L, 20g/L, 40g/L, 60g/L, 80g/L and 100g/L prepared from it for use. Figure 3.14 shows the MPL extraction process according to Verma et al.

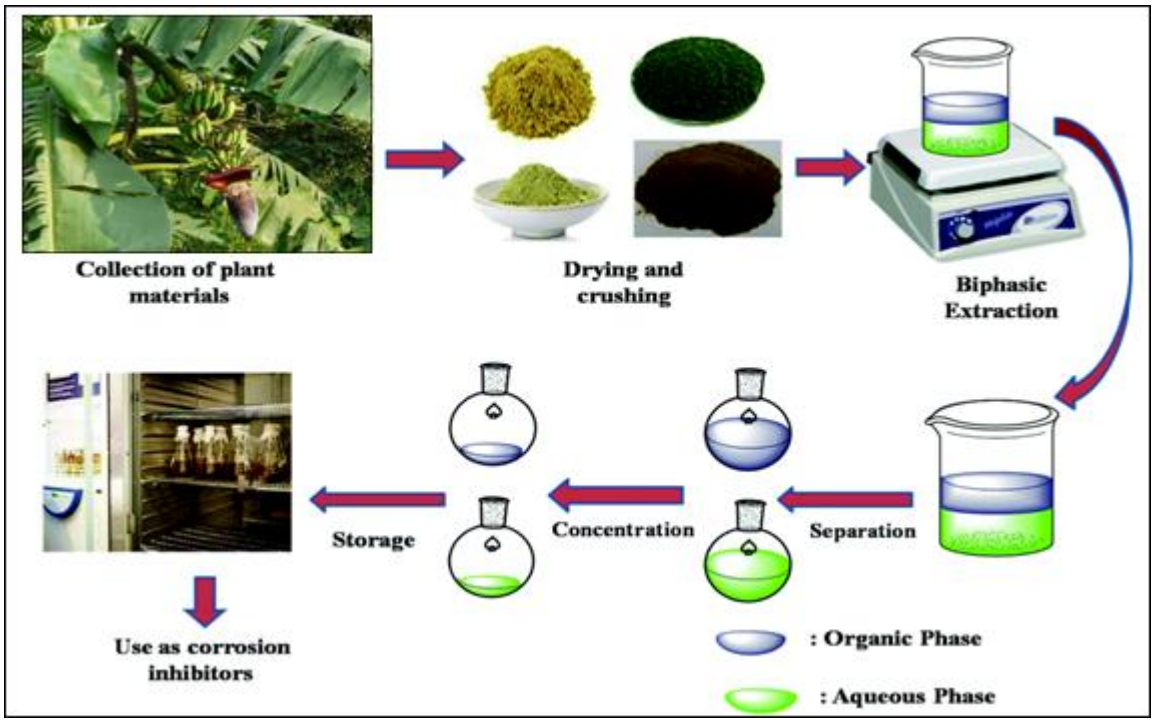

Figure 3.2**:** Inhibitor extraction process (Adapted form Verma et al., 2021)

3.3.3 GC-MS Structural Analysis of MPL

The gas chromatography mass spectroscopy (GC-MS) was used to investigate the compounds in the MPL in which scanned results obtained were compared with spectral data with the NIST 14 mass spectral Standard library.

The Gas Chromatography Mass Spectroscopy (GC-MS) series 7820A gas chromatograph coupled to 5975C inert mass spectrometer produced by Agilent Technologies was used to investigate the potential compounds in the MPL extract in which scanned results obtained were compared with spectral data with the NIST 14 mass spectral Standard library [16]. Firstly, the MPL extract sample was prepared using ethanol as organic solvent. Then 10µg/mL of the sample was injected into the compartment tray of the GC. In order not to block the syringe, care was taken to avoid particles or precipitates. The sample was then passed through the column and the stationary phase was attained. And the resultant peaks were then analyzed considering the retention time and the intensity count and the details of analysis were recorded.

3.3.4 Fourier Transform Infrared Spectroscopy (FT-IR) Analysis of Functional Groups and substituents Present in the MPL Extract.

Perkin Elmer spectrum 2 (UATR) FT-IR, IR 10.7.2 produced by PerkinElmer Inc. was used to carry out the FT-IR analysis on the MPL extract to evaluate the types of functional groups present.

A liquid sample of the MPL extract was used. Firstly, the liquid cell of the FT-IR was assembled with the IR transparent window. And then, a few drops of the liquid sample was introduced into the cell and carefully sealed. Secondly, the sample was placed in the FT-IR spectrometer and scanned. The spectrometer directs infrared beams at the sample and the absorbance is measured taking the frequency into consideration. Finally, the spectrum is then analyzed and the results recorded.

3.3.5 Simulation of Marine Environment/Preparation of Corrodent (3.5wt % NaCl) Solution

According to the National Oceanic and Atmospheric Administration, (NOAA, 2023), the standard sodium chloride concentration of seawater is approximately 3.5% by weight, which is equivalent to 35 parts per thousand (ppt). This means that for every litre of seawater, there are about 35 grams of dissolved salts, with sodium chloride being the most abundant (NOAA, 2023). So, in order to simulate the seawater environment, a test solution was prepared by measuring 35g of NaCl and dissolving it into 1Litre of de-ionized water. After then, the various MPL inhibitor concentrations were measured and mixed with the test solution in different beakers for immersion.

3.3.6 Gravimetric or Weight Loss Measurement

The preparation of test specimen followed ISO 11845 standard procedure. The original material was a pipe but it was cut into test coupon sizes of 2.0 cm x 2.0 cm x 0.6 cm dimensions, a wire brush was used to de-scale it. Thereafter, the coupons were placed on the metallographic lapping and polishing machine (UNIPOL-820) manufactured by Zhengzhou CY Scientific Instrument Co., Ltd, where they were neatly polished using abrasive emery paper of grit sizes of between150 and 1000 micron of various grades. This was done to obtain a very smooth surface for the weight loss measurements. In course of the machining, attention was given to the edges for proper polishing. Furthermore, the coupons were washed with distilled water, degreased in ethanol, dry cleaned and dipped into acetone. Then, they were dried with dry air and stored under a desiccator containing silica gel until when they were used.

The polished coupons were weighed using FA2104 electronic weighing balance and then were completely immersed in the prepared test solution (corrodent) in the absence and

presence of the MPL inhibitor at various concentrations in different beakers. A blank specimen was immersed in the test solution in the absence of the MPL inhibitor. Each specimen was exposed for 1 hour, 6 hours, 24 hours, 48 hours, 72 hours, 96 hours and 120 hours at room temperature (25^{0}C) while the pressure remained atmospheric. They were then removed at the expiration of the allotted time, thoroughly cleansed with acetone and then reweighed to measure the weight loss by subtracting the final weight after immersion from the initial weight before immersion according to Equation.(3.1);

$$\text{Weight Loss}, \Delta W = Wi - Wf \qquad 3.1$$

Where, ΔW is weight loss, Wi is the initial weight before immersion, Wf is the final weight after immersion. After the weight loss was determined, the corrosion rate was calculated using Equation 3.2:

$$\text{Corrosion Rate}, CR\ (mm/y) = [\Delta W \times \kappa]/\ \rho\ AT \qquad 3.2$$

Where, K is a constant that defines the units for the corrosion rate in mm/y; K = 87600, ΔW is weight loss (g), ρ is density (g/cm^3), A is the surface area of the specimen (cm^2) and T is the exposure time in hours. The inhibition efficiency (%IE) was calculated using the Equation 3.3

$$\%IE = [(CRa - CRp\ )\ /\ CRa] \text{ x } 100 \qquad 3.3$$

The corrosion rates in the absence and presence of the inhibitor are CR_a and CR_P respectively.

Also, the maximum saturation surface occupied by the inhibitor on a given available adsorption surface known as the surface coverage was determined using Equation 3.4

$$\text{Surface Coverage } (\theta) = Inhibition\ Efficiency,\ IE \div 100 \qquad 3.4$$

3.3.7 Surface Morphology of carbon steel in the sea water environments.

The atomic force microscopy (AFM) was used to study the surface morphology of the submerged carbon steel sample in 3.5wt% NaCl solution in the presence and absence of

100g/L MPL by recording AFM images of the samples after an immersion time analysis of 48h.

The test specimen or coupons were thoroughly cleansed and the mounted onto the AFM's test specimen holder using tape to ensure stability during the scan. The probe is then installed…it is a sharp tip on the cantilever. Thereafter, the laser optics is properly aligned to be able totrack the deflection of the cantilever as it interacts with the test specimen. This was done by bringing the probe close to the surface until a weak force of causes a slight deflection in the cantilever. The lasers's feedback system is then used to maintain a constant force between the tip of the probe and the metal surface. After that, the scan speed and the size of the area to be imaged are optimized in conformity with the experimental requirements. The probe is then scanned across the test specimen's surface line by line and as the tip encounters peaks and valleys on the surface, as the cantilever deflects. The feedback system adjusts the vertical position of the specimen to keep the cantilever in a steady state of constant deflection. Furthermore, the software records the 3D position of the tip at each point, creating high resolution topographic image of the metal surface and the results compared with the specimen in the presence and absence of the MPL corrosion inhibitor.

3.3.8 Contact Angle Measurements

The contact angle measurement seeks to quantify the wettability of the polished carbon steel substrate, the carbon steel in 3.5wt%NaCl solution in the presence and absence of the MPL inhibitor.

The sessile drop method was used to measure the contact angles for carbon steel (a) dry polished carbon steel, (b) immersed in 3.5wt% NaCl without MPL inhibitor, (c) immersed in 3.5wt% NaCl containing 100g/L MPL inhibitor by depositing water on the solid surfaces of these specimens after immersion. The droplet is placed on the solid specimens and the image of the drop is taken by a high-resolution camera. The contact angle of each of the specimen is then automatically determined by the software and recorded.

3.3.9 Electrchemical Investigation

The Electrochemical investigations were carried out using a Radiometer analytical PGZ100 potentiostat device, controlled by a computer equipped with Volta master 4 software, which allows data acquisition and processing. For electrochemical tests, a conventional three electrode cell: a saturated calomel electrode (SCE) reference electrode, a platinum counter electrode, and a carbon steel working electrode were used. Before each experiment, the working electrode was kept immersed for 30 minutes at the open circuit potential (OCP). This appropriate time was necessary to obtain the stabilization of the free potential (EOCP). Electrochemical impedance spectroscopy measurements were carried out at the open circuit

potential with an applied frequency starting from 100 kHz at 0.01 Hz using sinusoidal potential perturbation. The Nyquist representations of the impedance were analyzed and simulated by EC-Lab software, and then the EIS parameters were determined. The polarization curves were obtained with a scan rate of $1mV.s^{-1}$ and in the potential range −1800 to −600 mV vs SCE in the presence of 100g/L MPL at different concentrations after EIS measurements. The inhibition efficiency IE_{EIS} (%) and IE_I (%) was calculated using equations 3.5 and 3.6:

$$IE_{EIS}\ (\%) = (1 - R_P/R_{PO}) \times 100 \qquad 3.5$$

Where, IE_{EIS} (%) is the inhibition efficiency of the electrochemical impedance spectroscopy,
R_{PO} is polarization resistance of carbon steel without MPL and
R_P is the polarization resistance in the presence of MPL

$$IE_I\ (\%) = (1 - i_{corr'} / i_{corr}) \times 100 \qquad 3.6$$

Where, IE_I (%) is inhibition efficiency of the potentiodynamic polarization.
$i_{corr'}$ and i_{corr} are the corrosion current density values without and with MPL respectively,

3.3.10 Density Functional Theory (DFT) Analysis of MPL Inhibitory Properties

Material studio (version 8.0, BIOVIA) was used to perform Density Functional Theory (DFT) calculations of isolated MPL inhibitor molecules using the DMol3 module, quantum chemical parameters such as; E_{LUMO}, E_{HOMO}, energy band gap (ΔE), chemical hardness (η), electronegativity (χ), dipole moment (μ), global Softness (σ), fraction of electron transfer (ΔN) and other important parameters were computed considering equations (3.7-3.18).
E_{HOMO}: Energy of highest occupied molecular orbital
E_{LUMO}: Energy of the lowest unoccupied molecular orbital

IE: Ionization potential or Energy (eV), $IE = - E_{HOMO}$ 3.7

EA: Electron affinity (eV), $EA = -E_{LUMO}$ 3.8

ΔE: Energy band gap (eV), $\Delta E = E_{LUMO} - E_{HOMO}$ 3.9

χ: Electronegativity (eV), $\chi = (IE + EA)/2 = -(E_{HOMO} + E_{LUMO})/2$ 3.10

η: Global hardness (eV), $\eta = (IE - EA)/2 = (E_{LUMO} - E_{HOMO})/2$ 3.11

σ: Global softness $(eV)^{-1}$, $\sigma = 1/\eta = -2/(E_{HOMO} - E_{LUMO})$ 3.12

ω: electrophilicity index (eV), $\omega = \chi^2/2\eta$ 3.13

μ: chemical potential (Debye), $\mu \approx = 12(E_{LUMO} + E_{HOMO})$ 3.14

ε: nucleophilicity $(eV)^{-1}$, $\varepsilon = 1/\omega$ 3.15

ω^-: electron donating power (eV), $\omega^- = (3IE + EA)^2 \div 16(IE - EA)$ 3.16

ω^+: electron accepting power (eV), $\omega^+ = (IE + 3EA)^2 \div 16(IE - EA)$ 3.17

ΔN: Fraction of electron(s) transfer, $\Delta N = \chi Fe - \chi Inh \div 2(\eta Fe + \eta Inh)$ 3.18

Where, χFe and χinh are the absolute electronegativities of the iron atom (Fe) and the MPL inhibitor molecule respectively.

Consequently, DFT simulations represent the most powerful computational tool in terms of which the adsorption ability and corrosion inhibition effectiveness of a compound can be described. Therefore, DFT studies are mostly used to correlate the relative inhibition effect of a series of compounds having similar molecular structures. In general, higher E_{HOMO}, global softness (σ), dipole moment (μ) and lower E_{LUMO}, ΔE, electronegativity (χ) and chemical hardness (η) values are associated with high inhibition efficiency. Also, the Fukui indices are determined with the help of equation 3.19.

$F^2(r) \approx F^+(r) - F^-(r)$ 3.19

The isolated MPL inhibitor molecules studied were; 6-Amino-1,3,5-triazine-2,4(1H,3H)-dione (ATD); 2,3-Dihydrothiaphene(DDT); 2-Deoxyhexopyranose (DP); Octamethylcyclotetrasilozane (OMTS); 2,6,10-Dodecatrien-1-ol,3,7,11-trimethyl-(2Z,6Z)-(DT); 9-Octadecenamide (ODA).

However, in this study, molecular density was used to determine the orientation of the MPL inhibitor molecules on the carbon steel surface.

3.3.11 Molecular Dynamics (MD) Simulation of MPL in 3.5 wt. % NaCl

To effectively elucidate and analyze the effect of substituent groups on the orientation of corrosion inhibitors over the metal surface, MD or MC (Monte Carlo) simulations are often utilized. However, in this study, molecular dynamics simulation was used to determine the orientation of the MPL inhibitor molecules on the carbon steel surface.

In order to carry-out the simulation process a high stability quench adsorption approach on a surface of densely packed iron, Fe (110) atoms was adopted (Verma, Obot, Bahadur, Sherif & Ebenso, 2018a; Spangberg, 2003 ; Verma, Lgaz, Verma, Ebenso, Bahadur, & Quraishi., 2018d). The studied isolated MPL molecules were then simulated. The Fe crystal was cleaved across by the Fe (110) plane at a fractional depth of 3.0 Å. The bottom layers' form was constrained before the surfaces were optimized to avoid edge effects caused by the sizes of the molecules. The temperature was fixed at 298 K and Nose-Hoover (NH) method was adopted for temperature control along with geometry optimization.

Firstly, amorphous cell calculation was performed to simulate seawater (3.5 wt% NaCl solution) by packing 450 molecules of water and 18 molecules of sodium chloride ion in a cell. Pure iron (Fe) framework was imported from materials studio database, and carbon steel surface was built using the 'build' tool in the software. The whole system was assembled using the build layer tool.

The MD simulation was conducted in a simulation box of 35Å x 35Å x 48. 26Å, considering some periodic boundary conditions. Carbon steel surface was built via Fe (110) surface configuration, since it is the most stable surface configuration of carbon steel.

Secondly, adsorption of MPL inhibitor onto the carbon steel surface already immersed in 3.5 wt.% NaCl solution was simulated using the Forcite module to determine the interaction of MPL inhibitor materials with the metal surface. The Forcite quench simulation was performed under constant temperature (at 298 K) as earlier stated. Also, the Andersen Thermostat, NVT (number of particls, N; volume of the simulation box, V; temperature of the system, T) were all held constant) ensemble with a time step of 1.0 fs and simulation time of 5 ps was employed. Further, the COMPASSII (Condensed-Phase Optimized Molecular Potentials for Atomic Simulation Studies II) force field was used (Sun, Jin, Yang, Akkermans, Robertson, Spenley, Miller &Todd., 2016; Yuhuan &Wenxiang,2020), while non-bond interactions and van der Waals electrostatic were set as atom-based and Ewald summation method, respectively. Additionally, the radial distribution function (RDF) was

adopted in the evaluation of bond lengths of the interacting molecules while also utilizing the Forcite module to perform these calculations (Verma, Obot, Bahadur, Sherif & Ebenso, 2018a; Spangberg, 2003; Verma et al., 2018d).

3.3.12 Adsorption Isotherm and Mechanism

In order to gain insights of the nature and behavior of adsorption between the MPL and the carbon steel like a monolayer formation or surface heterogeneity, the test of isotherms was carried out on three models namely; Langmuir, Temkin and Frumkin using equation 3.20 to determine the adsorption parameters

$$\Delta G^{\circ}_{ads} = -RTln55.5K_{ads} \qquad 3.20$$

Where; concentration of H_2O = 55.5 mol/L in the solution; R is the universal gas constant in $Jmol^{-1}$ K^{-1} and T is the temperature in K. The values of linear coefficients of determination (R^2) and the equation of expression for the Langmuir isotherm are presented in Table 4.10.

3.3.13 Analysis of results

The experimental results were presented, analyzed and reported using Origin software that was provided by the ACE-FUELS Laboratory in the ACE-FULS general purpose laboratory, FUTO.

CHAPTER FOUR

RESULTS AND DISCUSSION

4.1 Results

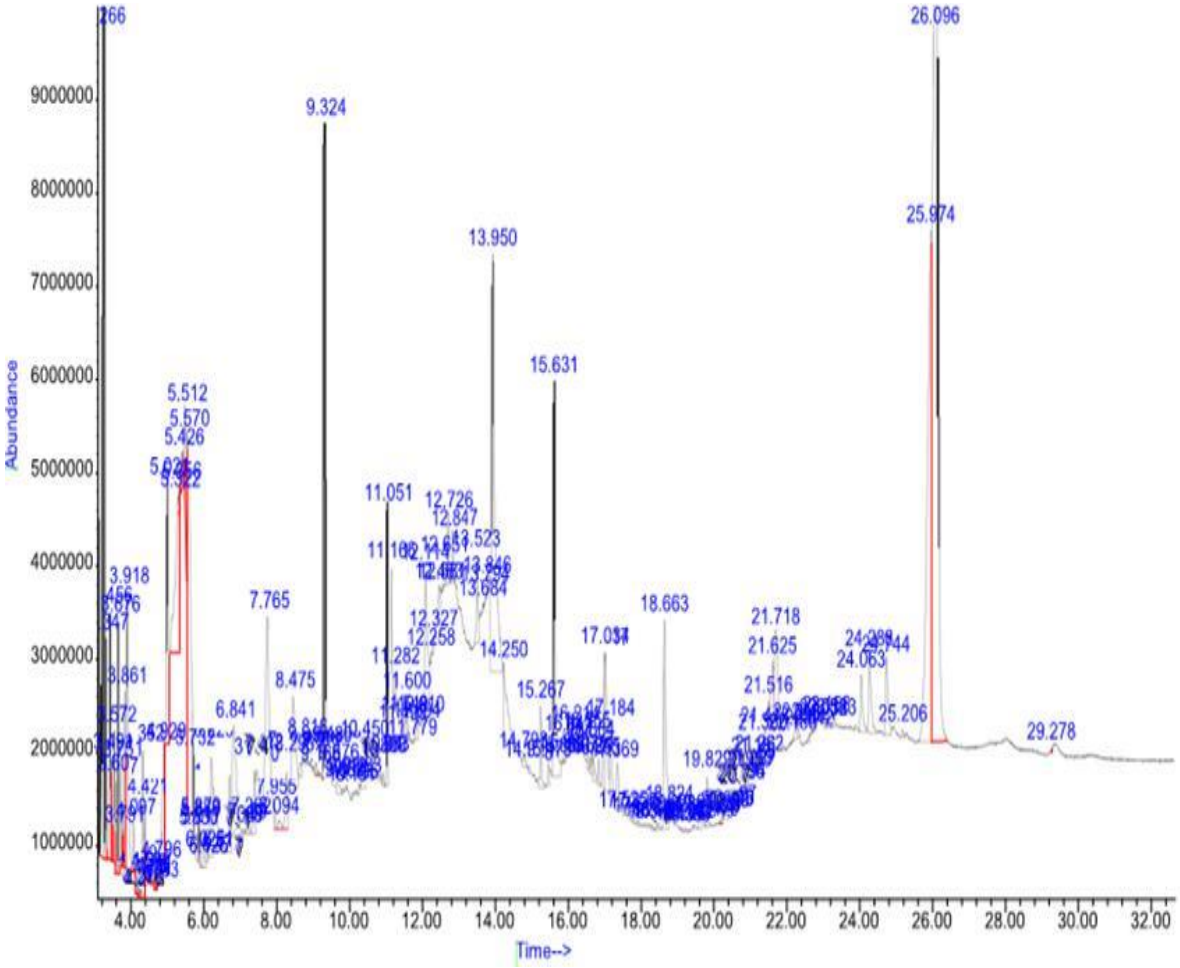

Figure 4.1: GC-MS result of MPL extract

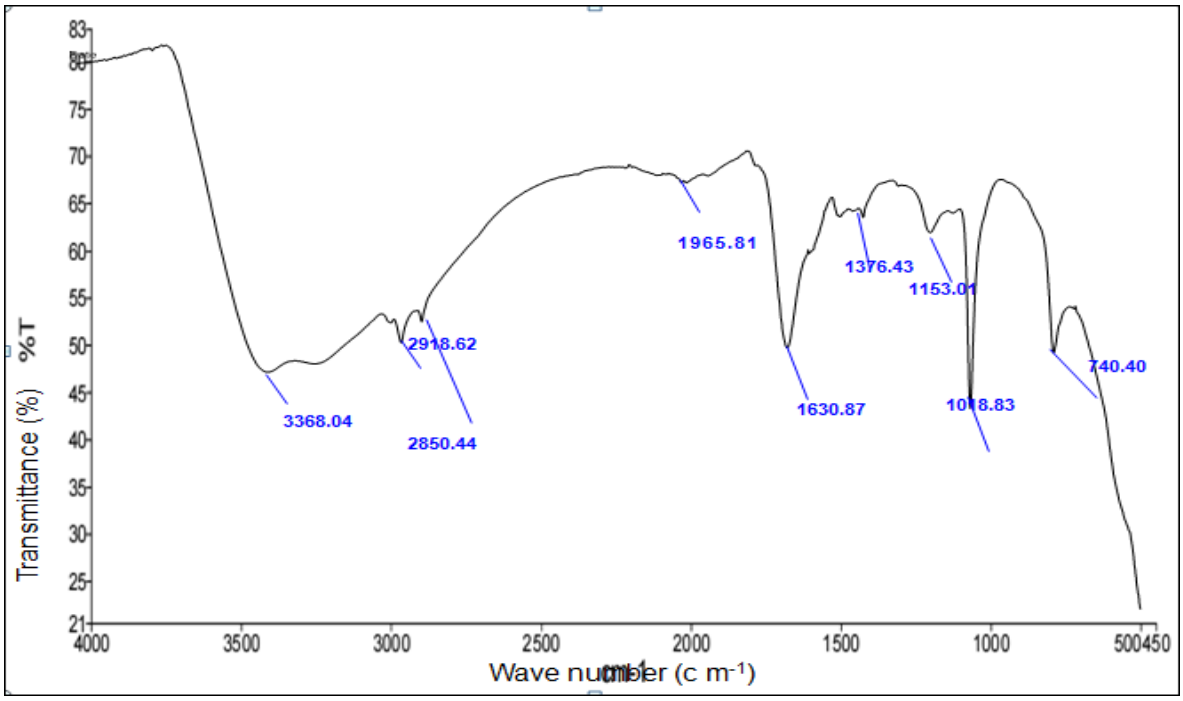

(a)

Figure 4.2a: FT-IR spectrum of MPL substituents

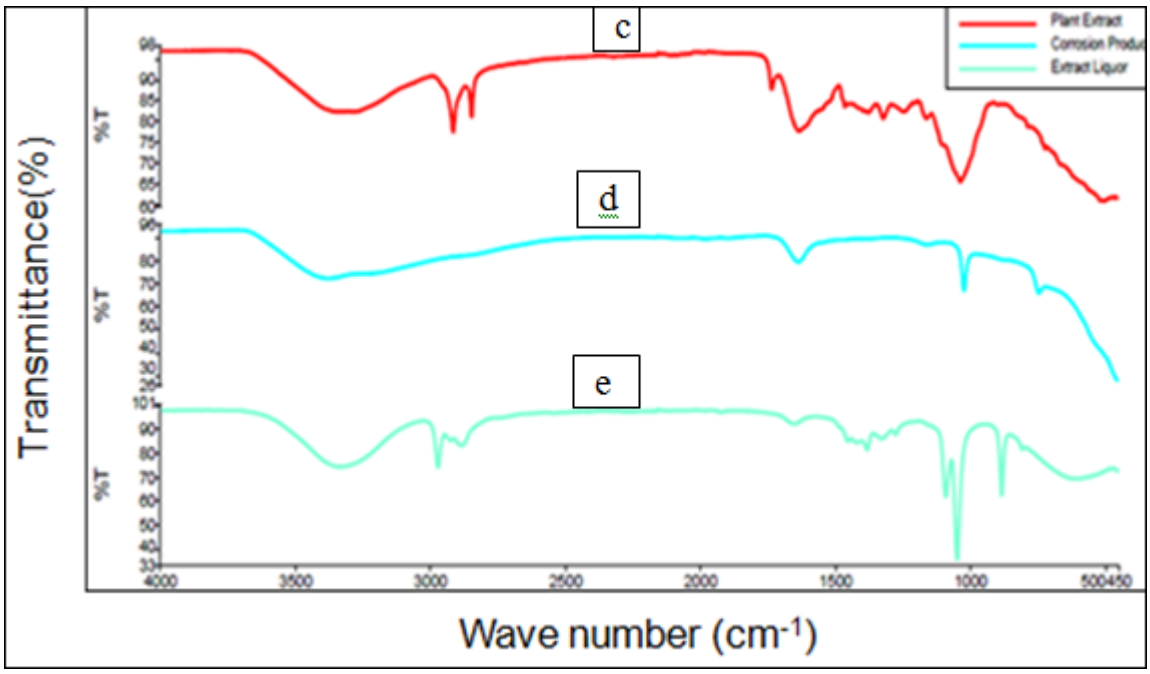

(b)

Figure 4.2b: FT-IR spectrum of MPL substituents for (c) extract powder, (d) corrosion product and (e) liquor

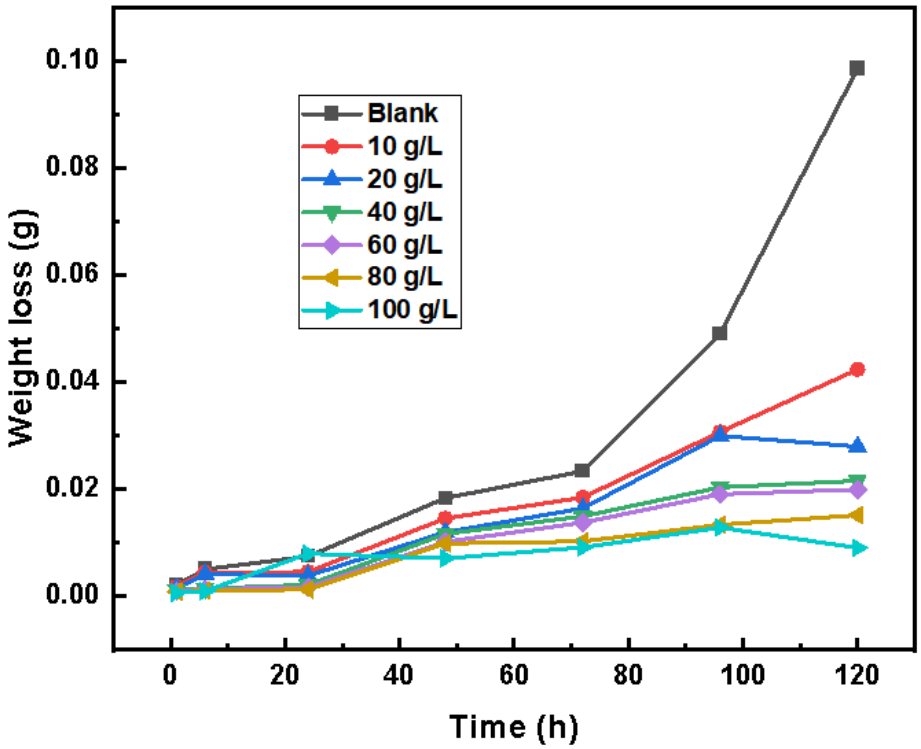

Figure 4.3(a): Effect of time on the weight loss of carbon steel immersed in 3.5 wt% NaCl solutions in the presence and absence of different concentrations of MPL inhibitor at 25^{o}C

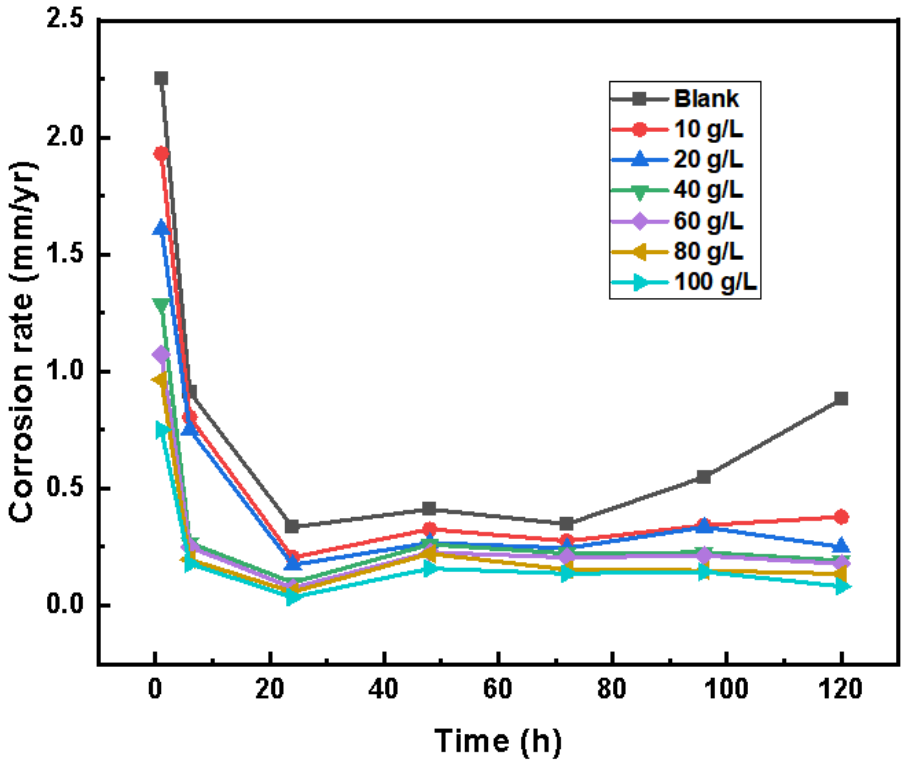

Figure 4.3(b): Effect of time on corrosion rates of carbon steel immersed in 3.5 wt% NaCl solution in the presence and absence of different concentrations of MPL inhibitor at 25^{o}C

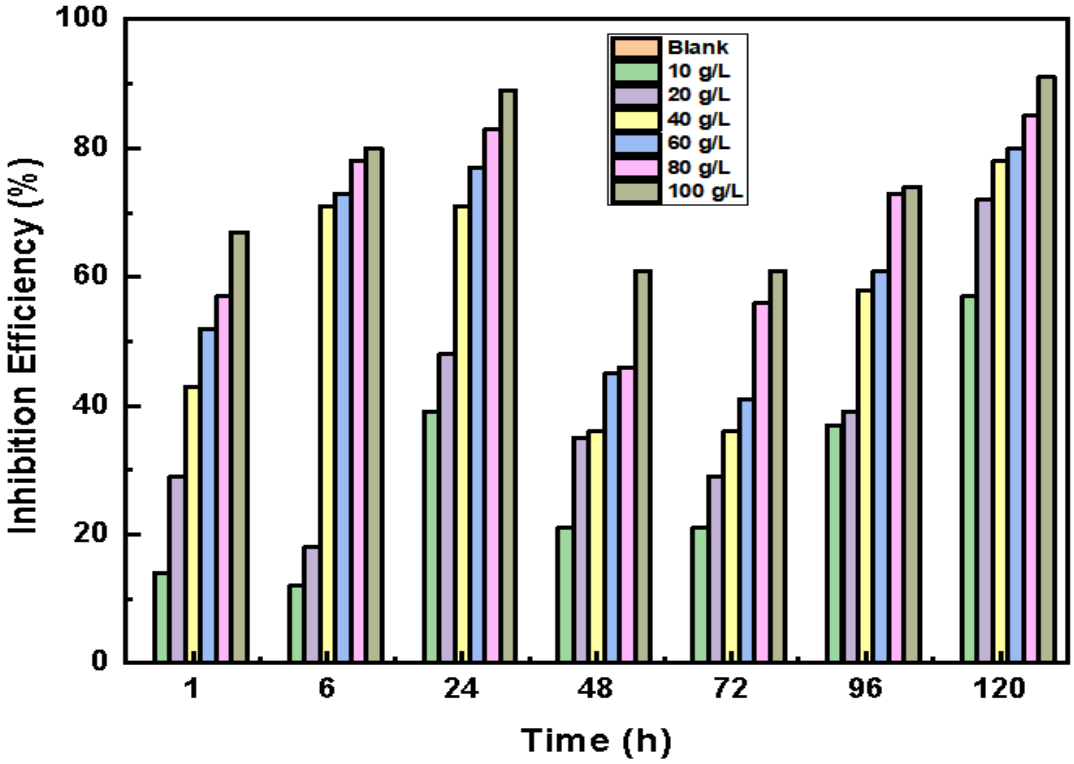

Figure 4.3(c): Effect of time on inhibition efficiency of MPL on carbon steel immersed in 3.5 wt% NaCl solution in the presence and absence of different concentrations of MPL inhibitor at 25^{o}C

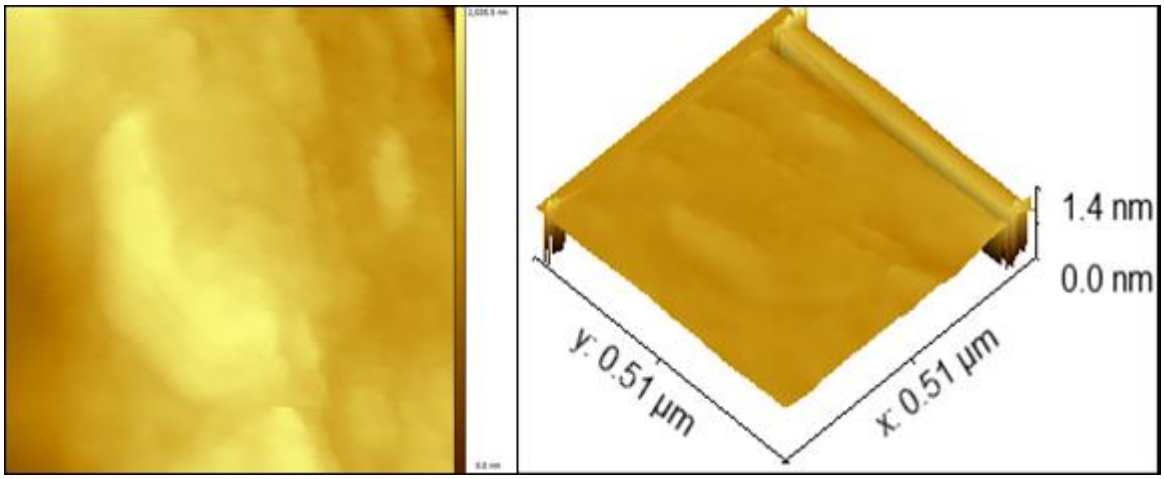

(a)

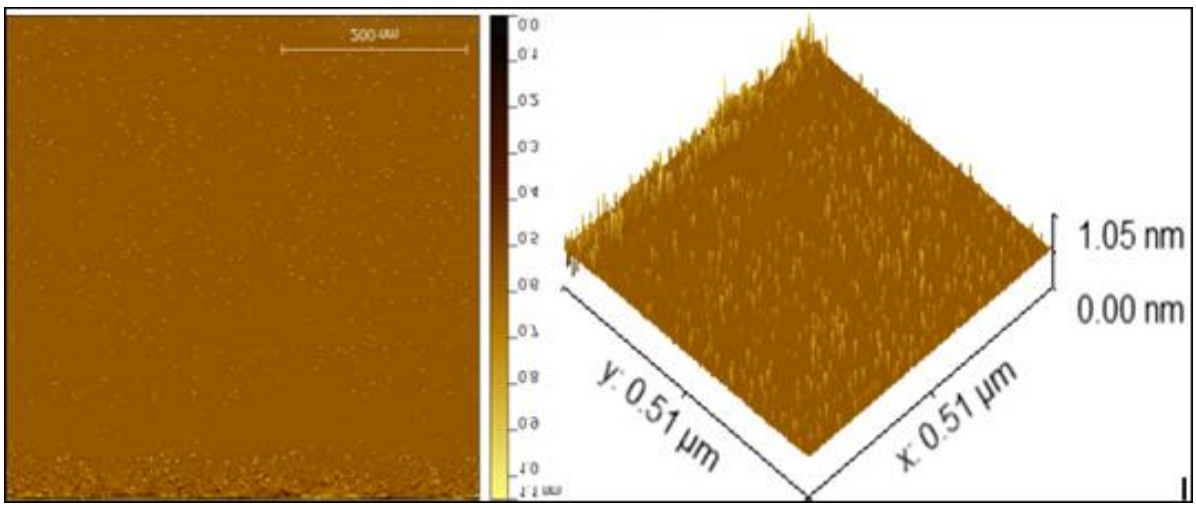

(b)

Figure 4.4: 2D views and 3D surface topographies of carbon steel (a) in 3.5wt%NaCl (Blank), (b) in 3.5wt%NaCl + 100g/L MPL respectively

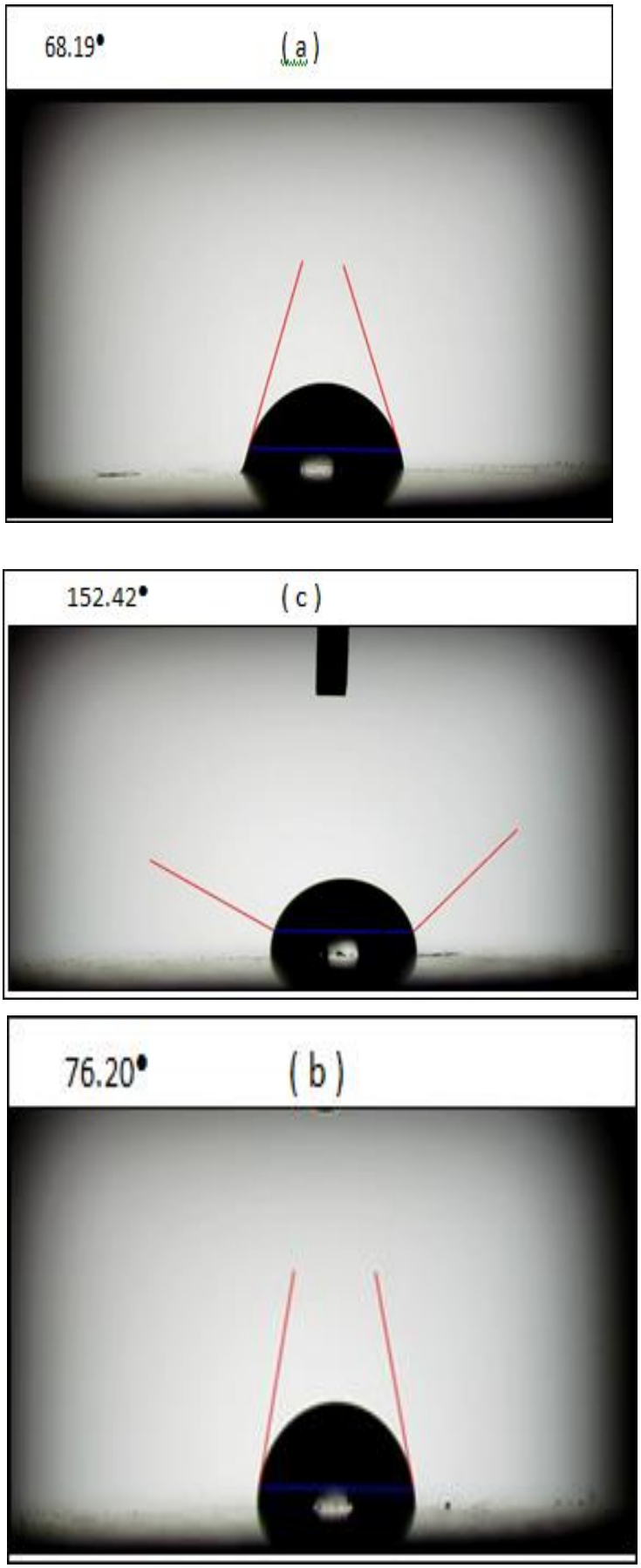

Figure 4.5: Contact angle measurements for carbon steel (a) dry polished carbon steel, (b) immersed in 3.5wt% NaCl without MPL inhibitor, (c) immersed in 3.5wt% NaCl containing 100g/L MPL inhibitor

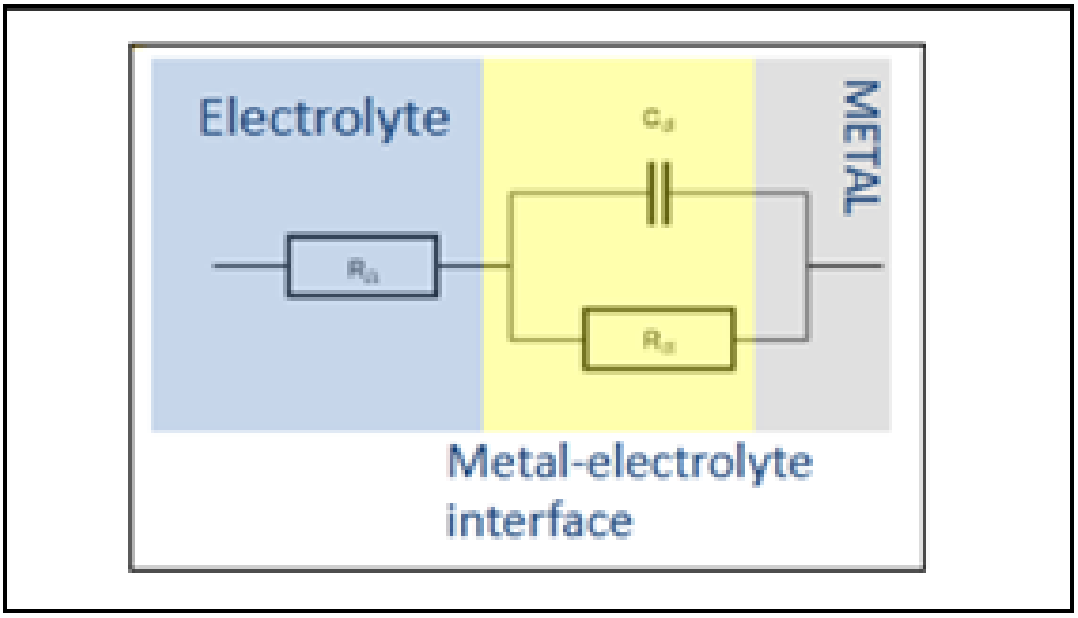

(a)

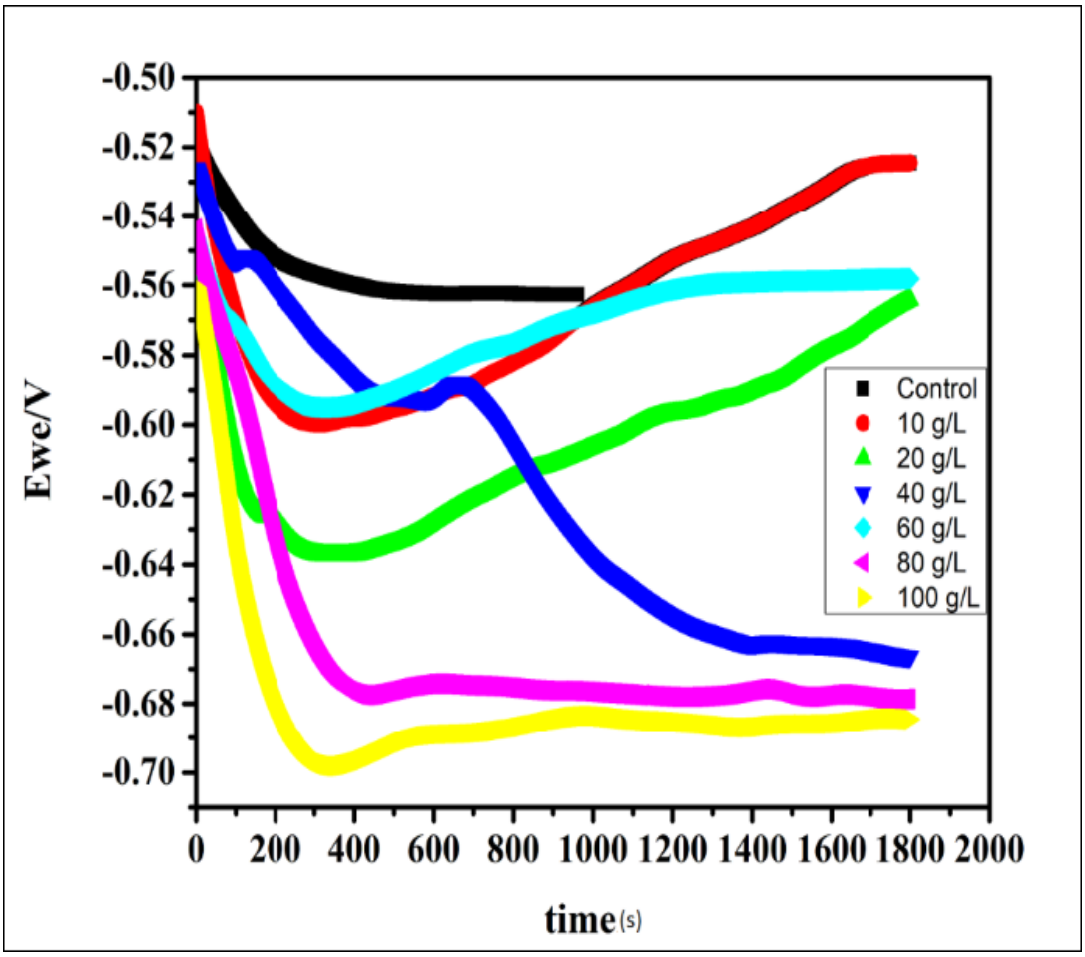

(b)

Ewe/V= working electrode potential relative to a reference electrode

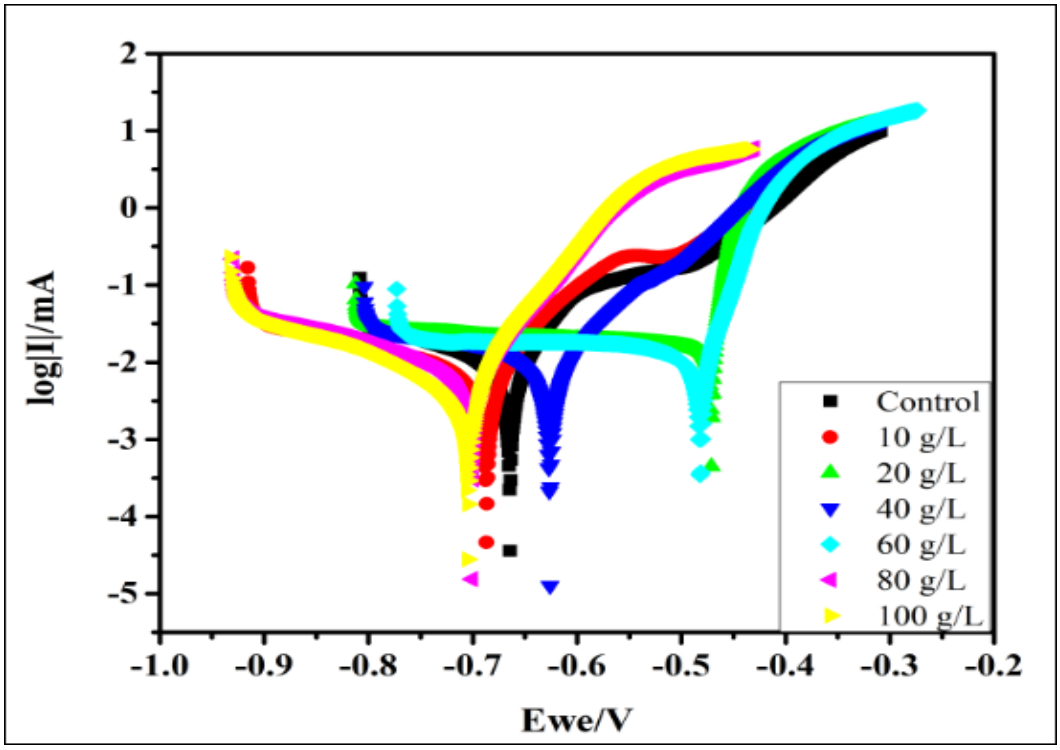
log|I|/mA
Ewe/V
Control
10 g/L
20 g/L
40 g/L
60 g/L
80 g/L
100 g/L

(c)

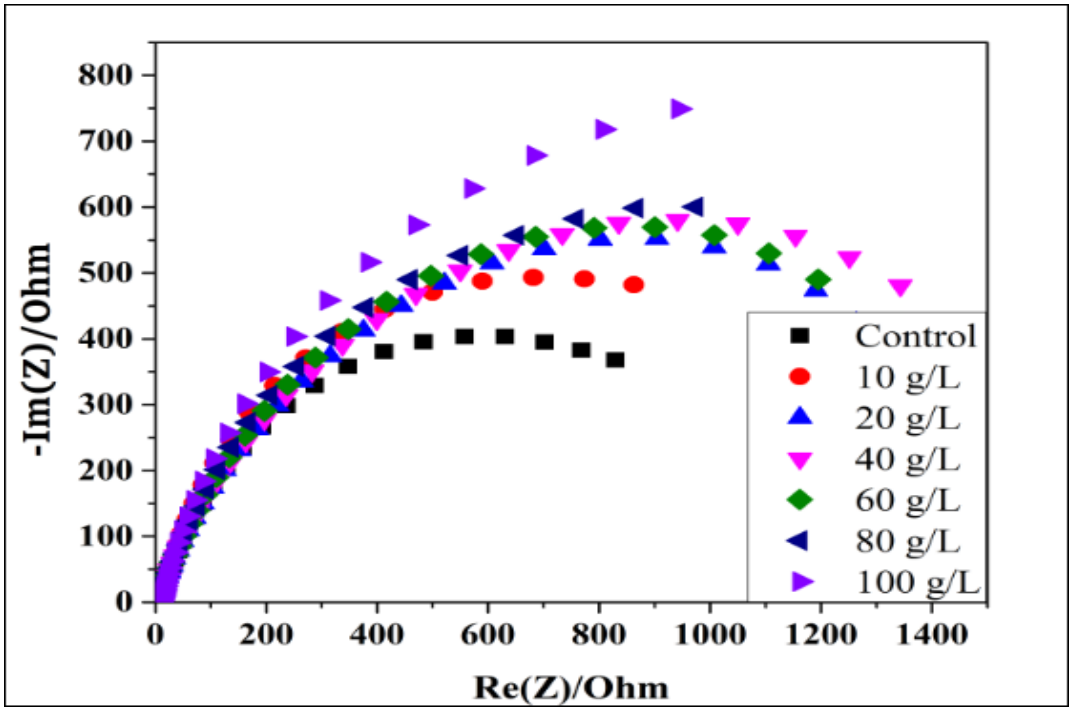
-Im(Z)/Ohm
Re(Z)/Ohm
Control
10 g/L
20 g/L
40 g/L
60 g/L
80 g/L
100 g/L

(d)

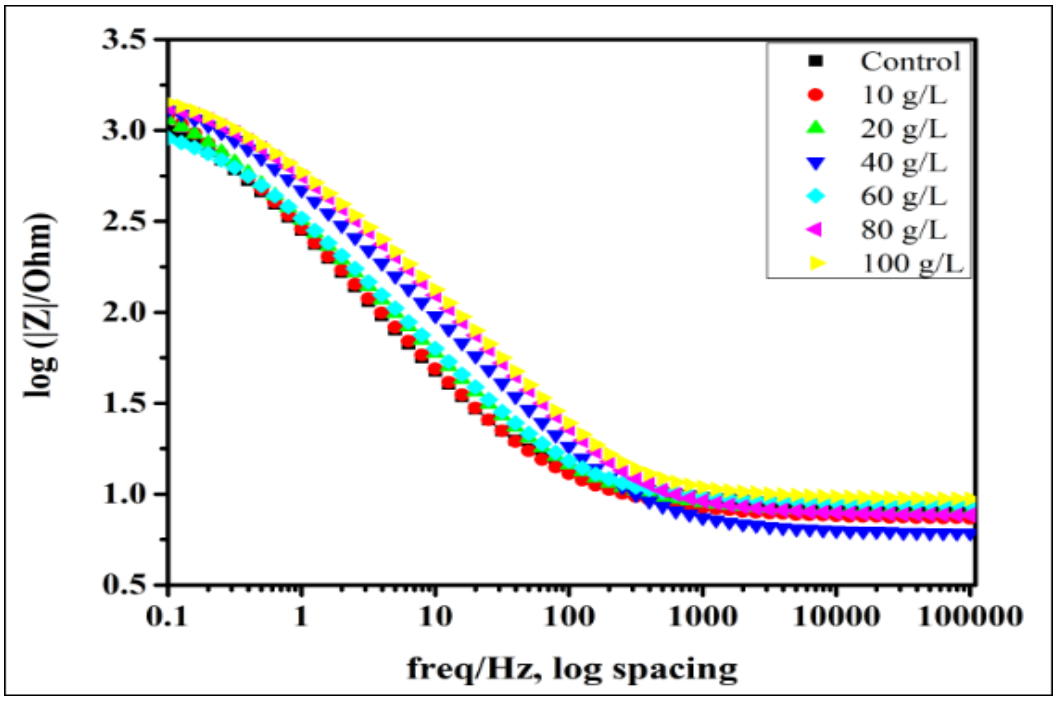

(e)

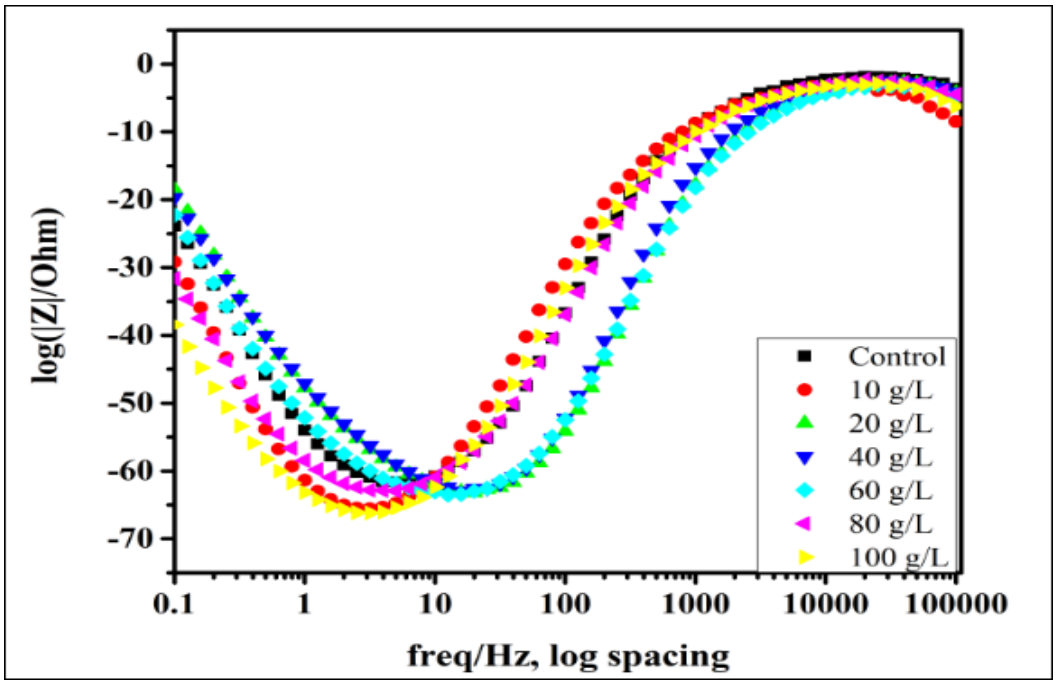

(f)

Figure 4.6: (a) Equivalent circuit model (b) OCP (c) Tafel, (d) Nyquist ,(e) Bode and (f) Phase angle, plots of carbon steel in 3.5wt% NaCl with and without various concentrations of MPL at Ecorr after 30 mins immersion

Isolated Compound(s)	Optimized Structure	HOMO orbitals	LUMO orbitals
1(ATD)	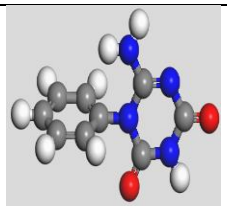	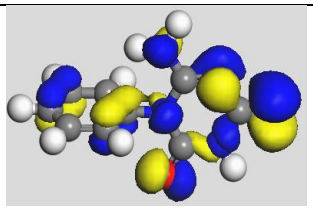	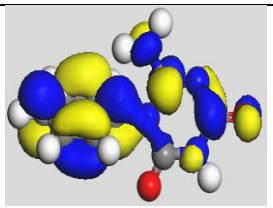
2(DDT)	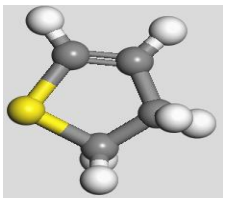	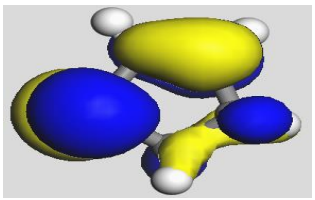	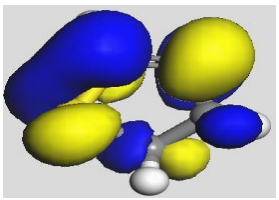
3(DP)	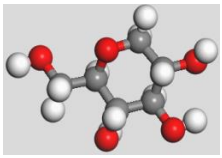	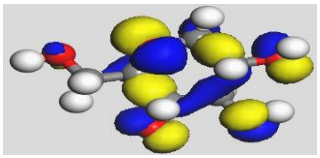	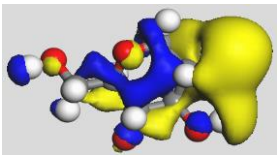
4(OMTS)	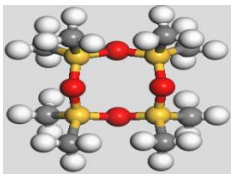	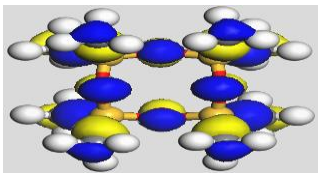	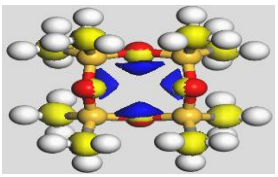
5(DT)	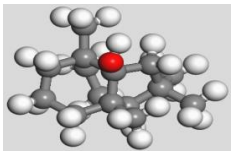	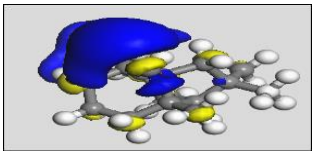	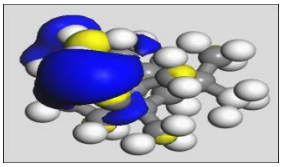
6(ODA)	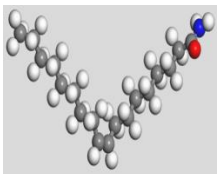	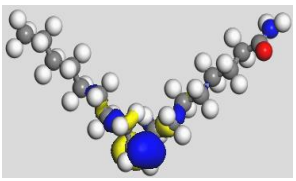	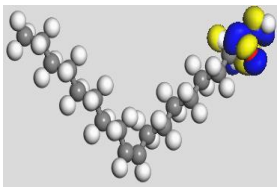

LEGEND: ●red = Oxygen (O), ●gray = Carbon (C), ●yellow = Sulphur (S), ●blue = Nitrogen (N), ●white = Hydroge (H)

Figure 4.7a: HOMO and LUMO densities of the isolated compounds present in the MPLExtract

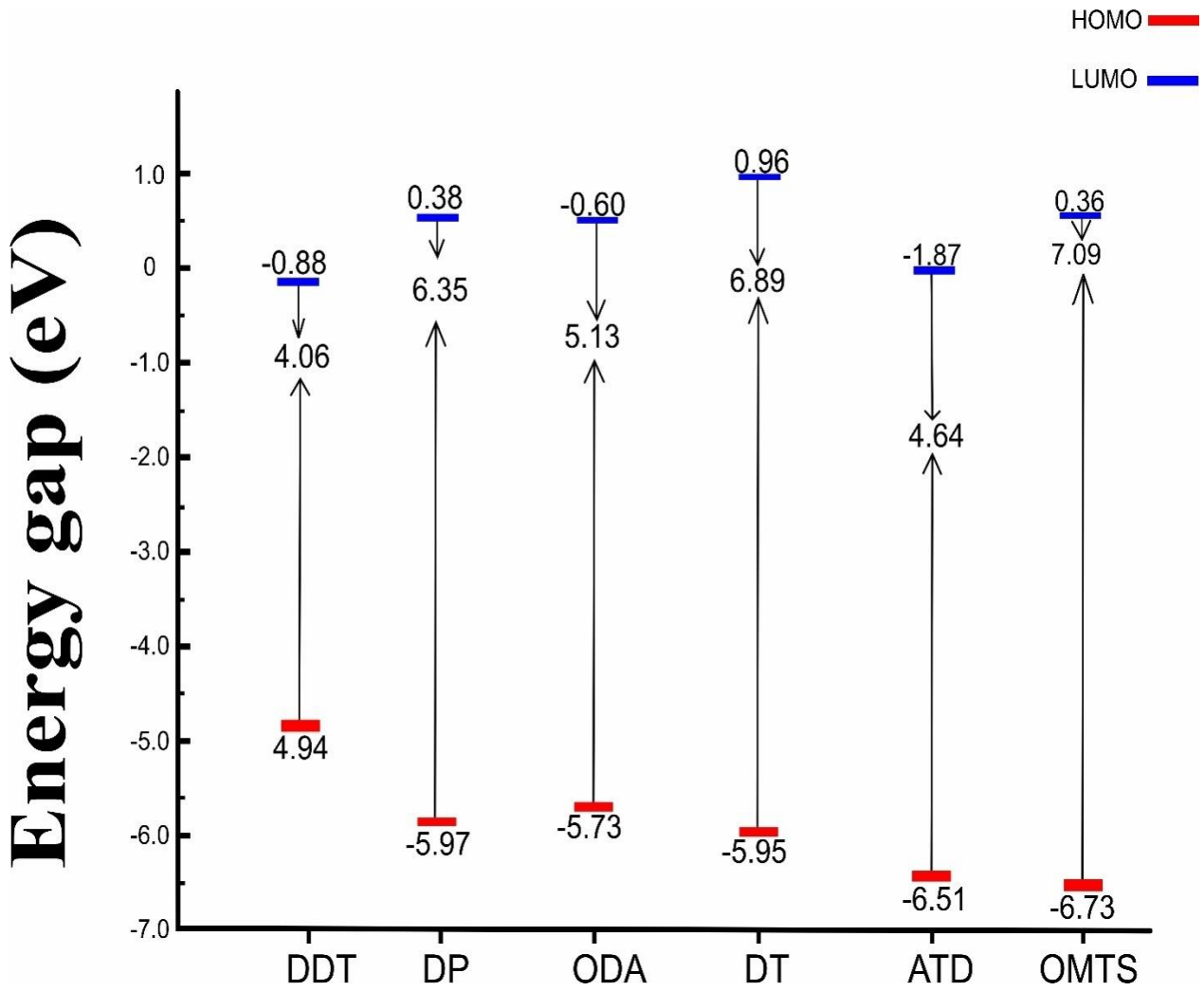

Figure 4.7b: A graphical representation of HOMO and LUMO energy levels of the compounds present in the MPL and their corresponding band gaps.

S/N	Isolated Compounds	Fukui Numbering
1	(ATD)	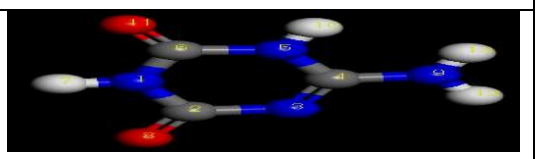
2	(DDT)	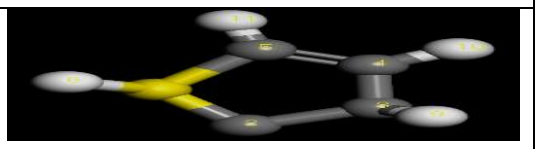
3	(DP)	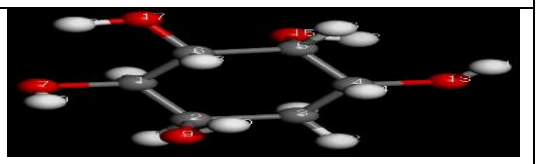
4	(OMTS)	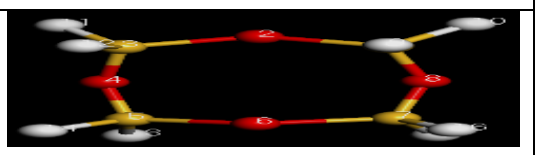
5	(DT)	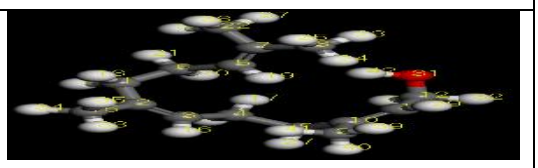
6	6(ODA)	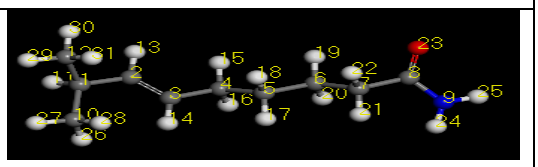

LEGEND: ●red = Oxygen (O), ●gray = Carbon (C), ●yellow = Sulphur (S), ●blue = Nitrogen (N), ●white = Hydroge (H)

Figure 4.8: Fukui functions for electrophilic and nucleophilicmaps showingnumbering of atoms of isolated compounds of the MPL inhibitor molecule.

Isolated compounds	Side View	Top View	Adsorption Energy (Kcal/mol)
1(ATD)	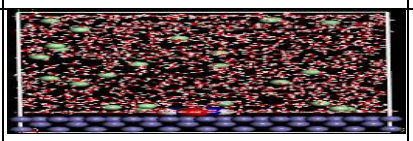	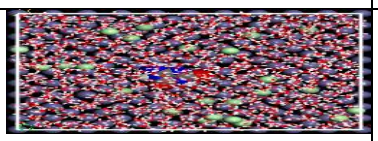	-60.77
2(DDT)	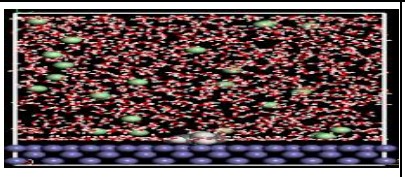	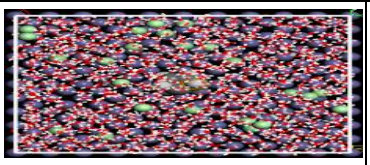	-35.928
3(DP)	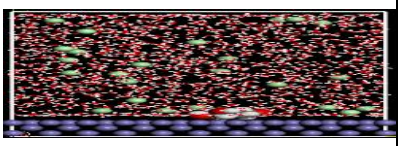	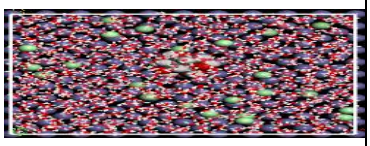	-54.044
4(OMTS)	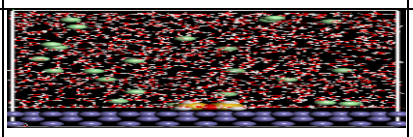	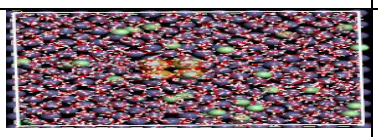	-61.399
5(DT)	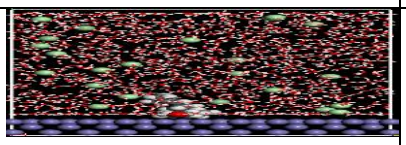	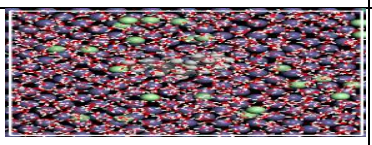	-76.883
6(ODA)	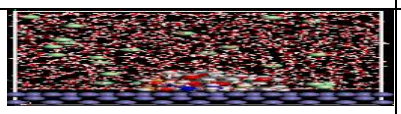	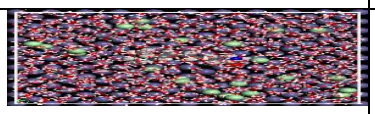	-89.019
MPL (final superstructure molecules)	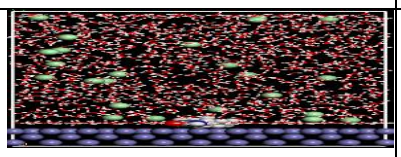	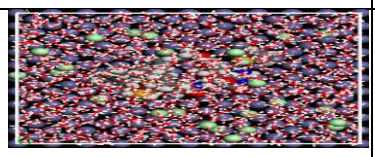	-184.954

LEGEND: 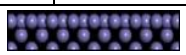 **= Metal surface;**  **= MPL inhibitor molecule**

Na^+ = ● Cl $^-$ =●

Figure 4.9(a)**:** The equilibrium adsorption mode of MPL molecules onto Fe (110) surface in top and side views

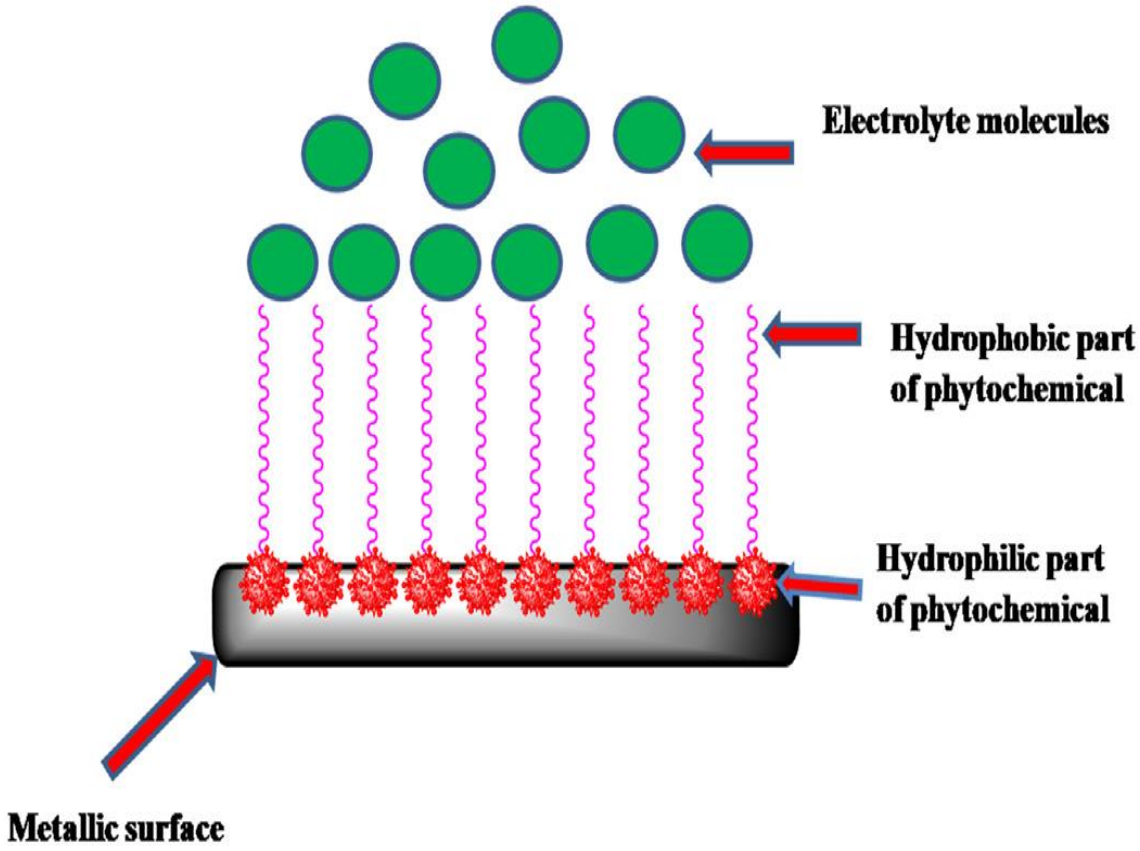

Figure 4.9(b): The reaction mechanism of inhibitor molecules on metal surface

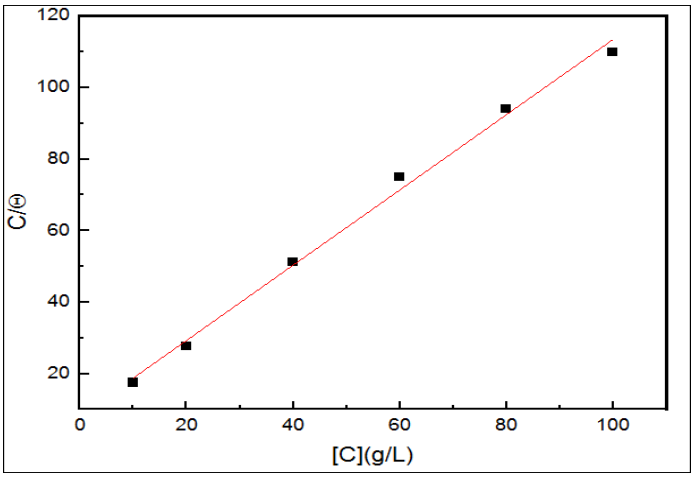

(a)

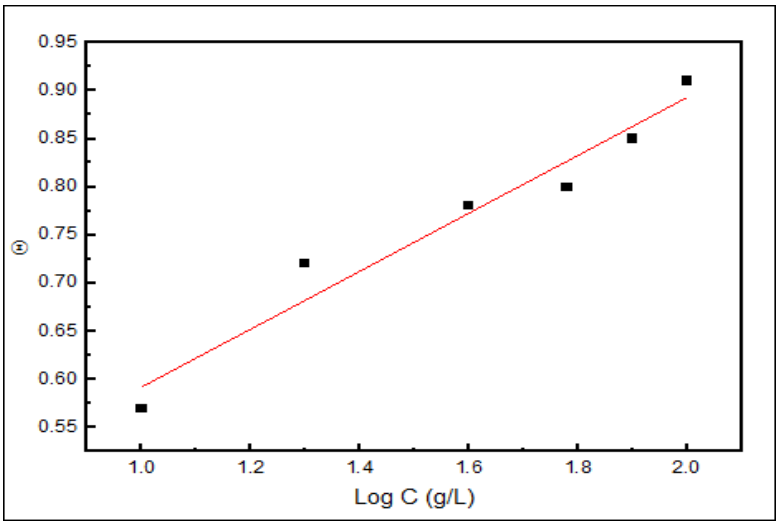

(b)

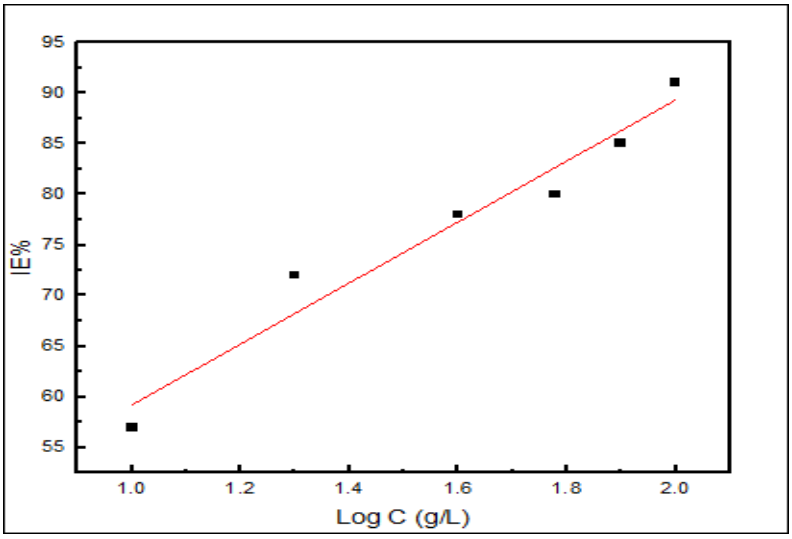

(c)

On the isotherms: C= concentration; Θ = degree of surface coverage

Figure 4.10: Adsorption isotherms (a) Langmuir isotherm (b) Temkin isotherm (c) Frumkin isotherm

Table 4.1: Names of Compounds with their chemical formulae, structures and molecular weight(s) present in MPL extract

Name of Compound	Chemical Formula	Chemical Structure	Molecular Weight (g/mol)
6-Amino-1,3,5-triazine-2,4(1H,3H)-dione	$C_3H_4N_4O_2$	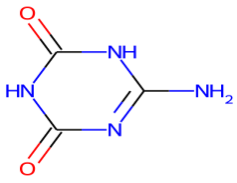	**128.09**
2,3-Dihydrothiophene	C_4H_6S	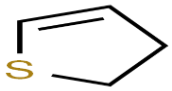	**86.16**
2-Deoxyhexopyranose	$C_6H_{12}O_5$	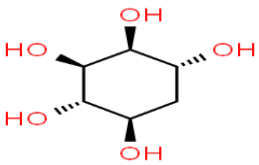	**164.16**
Octamethylcyclotetrasilozane	$C_8H_{24}O_4Si_4$	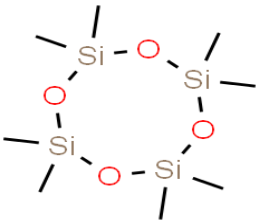	**296.616**
2,6,10-Dodecatrien-1-ol,3,7,11-trimethyl-(2Z,6Z)-	$C_{15}H_{26}O$	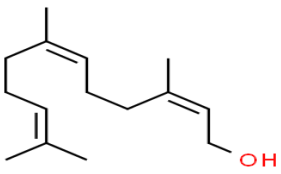	**222.37**
9-Octadecenamide	$C_{18}H_{35}NO$	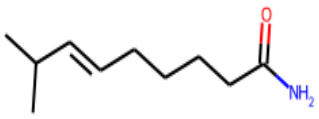	**281.477**

Table 4.2 FT-IR of MPL-extract showing functional groups present

S/N	Functional Group	Characteristic Absorption wavenumber (cm^{-1})
1	N-H and O-H	3368.04 (3500-3200)
2	C-H	2918.62 (2950-2850)
3	C-H	2850.44 (2950-2850)
4	C□C	1630.87 (1680-1640)
5	Methyl, C-H	1370.43 (1370-1350)
6	C-O	1153.01 (1260-1050)
7	Aromatic, C-H	740.40 (860-680)

Table 4.3: Weight loss (g), corrosion rate (mm/y) of carbon steel and IE (%) of MPL extract (inhibitor) in 3.5wt% NaCl solution at various concentrations (g/L) and exposure time (h)

Conc.	1 hr			6 h			24 h			48 h		
(g/L) MPL	ΔW(g)	CR (mm/y)	IE(%)	ΔW(g)	CR (mm/y)	IE(%)	ΔW(g)	CR (mm/y)	IE(%)	ΔW(g)	CR (mm/y)	IE(%)
Blank	0.0021	2.2533		0.0051	0.9121		0.0075	0.3353		0.0184	0.4113	
10	0.0018	1.9314	14	0.0045	0.8048	12	0.0046	0.2057	39	0.0146	0.3264	21
20	0.0015	1.6095	29	0.0042	0.7511	18	0.0039	0.1744	48	0.0120	0.2683	35
40	0.0012	1.2876	43	0.0015	0.2683	71	0.0022	0.0984	71	0.0117	0.2615	36
60	0.0010	1.0730	52	0.0014	0.2504	73	0.0017	0.0760	77	0.0102	0.2280	45
80	0.0009	0.9657	57	0.0011	0.1967	78	0.0013	0.0581	83	0.0099	0.2213	46
100	0.0007	0.7511	67	0.0010	0.1788	80	0.0008	0.0358	89	0.0071	0.1587	61

Table 4.3: continues

Conc.	72 h			96 h			120 h		
(g/L) MPL	ΔW(g)	CR (mm/y)	IE(%)	ΔW(g)	CR (mm/y)	IE(%)	ΔW(g)	CR (mm/y)	IE(%)
Blank	0 .0234	0.3487		0.0491	0.5488		0.0986	0.8817	
10	0.0185	0.2757	21	0.0307	0.3431	37	0.0424	0.3791	57
20	0.0165	0.2459	29	0.0300	0.3353	39	0.0280	0.2504	72
40	0.0150	0.2235	36	0.0204	0.2280	58	0.0216	0.1931	78
60	0.0138	0.2057	41	0.0191	0.2135	61	0.0200	0.1788	80
80	0.0103	0.1535	56	0.0134	0.1498	73	0.0152	0.1359	85
100	0.0092	0.1371	61	0.0129	0.1442	74	0.0091	0.0823	91

Table 4.4: Surface roughness values such as average mean roughness Ra and root mean square roughness Rq of carbon steel without and with 100g/L MPL after 48 hrs of immersion time

Inhibitor	Ra(nm)	Rq (nm)
Test Sample + 3.5wt% NaCl(Blank)	28	71
Test Sample + 3.5wt%NaCl + 100g/L MPL	9	34

Table 4.5: Contact angle measurements/properties of dry polished carbon steel, and carbon steel immersed in 3.5wt%NaCl with and without MPL inhibitor.

Property	**Dry polished Carbon Steel**	**Carbon steel immersed in 3.5wt% NaCl**	**Carbon steel immersed in 3.5wt%NaCl + 100g/L MPL**
Contact angle value (Ɵ) in degrees	68.19	76.20	152.42
Nature of wettness	Hydrophilic	Hydrophilic	Superhydrophobic
Wettability	Good	Good	Poor
Solid surface free energy	High	High	Low

Table: 4.6a: Potentiodynamic polarization parameters of carbon steel with various MPL extract concentrations in seawater environment at 298K

	Ecorr (mV)	Icorr (µA)	β c (mV)	βa (mV)	corrosion rate (mm/y)	IE (%)
Blank	-694.347	87.403	20264870.0	208.5	0.440 422	
10g/L	- 686.940	22.108	9 701 369.0	155.2	0.260 322	74.71
20g/L	-471.103	21.679	962361664.0	52.8	0.255 271	75.20
40g/L	-626.121	20.991	50 723840.0	110.0	0.247 17	75.98
60g/L	-481.808	19.979	21903806.0	63.7	0.237 335	77.14
80g/L	-700.390	16.342	15 049968.0	82.9	0.192 428	81.30
100g/L	-705.223	8.615	17521452.0	77.1	0.136 767	90.14

Ecorr: Corrosion Potential; Icorr: Corrosion Current; βc: Cathodic slope; βa: Anodic slope

Table: 4.6b: Electrochemical impedance spectroscopy parameters of carbon steel with various MPL extract concentrations in seawater environment at 298K

	R1 (Ohm)	Q2 (F.s^(a - 1))	a2	R2 (Ohm)	IE%
Control	8.9458	0.0006	0.7870	1140	
10 g/L	8.8653	0.0008	0.8041	5403	79.0
20 g/L	7.5921	0.0003	0.7792	5516	79.3
40 g/L	9.3170	0.0003	0.7805	5586	79.6
60 g/L	6.1062	0.0004	0.7764	5593	79.6
80 g/L	8.0875	0.0007	0.7759	6694	83.0
100 g/L	7.6941	0.0008	0.7914	7112	84.0

R1=Ohmic drop or Solution resistance; Q2=Double layer capacitance; R2=Charge transfer resistance; a2=CPE (constant-phase element)

Table 4.7: Quantum Chemical Descriptors/Parameters in theisolatedMPLCompounds

Descriptor	**DDT**	**DP**	**ODA**	**DT**	**ATD**	**OMTS**
$\mathbf{E}_{HOMO}$	-4.939	-5.973	-5.73	-5.952	-6.505	-6.727
$\mathbf{E}_{LUMO}$	-0.879	0.38	-0.601	0.958	-1.871	0.362
$\Delta\mathbf{E}$	4.06	6.353	5.129	6.91	4.634	7.089
χ	2.909	2.7965	3.1655	2.497	4.188	3.1825
μ	-2.909	-2.7965	-3.1655	-2.497	-4.188	-3.1825
H	2.03	3.1765	2.5645	3.455	2.317	3.5445
Σ	0.492611	0.314812	0.38994	0.289436	0.431593	0.282127
Ω	2.084306	1.230979	1.953673	0.902317	3.784925	1.428736
ϵ	0.479776	0.812361	0.511856	1.108258	0.264206	0.69992
$\omega+$	0.883556	0.229792	0.691486	0.085692	1.98055	0.280548
$\omega-$	3.792556	3.026292	3.856986	2.582692	6.16855	3.463048
ΔN	0.716502	0.440186	0.617177	0.36136	0.903755	0.448935

Table 4.8: Fukui electrophilic $F^{+}(r)$, nucleophilic $F^{-}(r)$, and dual Fukui descriptor $F^{2}(r)$ for ATD isolated MPL molecule

Atom	**F^{+} (r)**	**F^{-} (r)**	**F^{2} (r)**	**Atom**	**F^{+} (r)**	**F^{-} (r)**	**F^{2} (r)**
N (1)	0.042	0.021	0.021	O (8)	0.132	0.264	- 0.132
C (2)	0.125	0.085	0.040	N (9)	0.106	0.106	0.000
N (3)	0.076	0.143	- 0.067	H (10)	0.042	0.032	0.010
C (4)	0.174	0.052	0.122	O (11)	0.076	0.106	- 0.030
N (5)	0.035	0.027	0.008	H (12)	0.047	0.039	0.008
C (6)	0.057	0.047	0.010	H (13)	0.043	0.035	0.008
H (7)	0.044	0.043	0.001				

Table 4.9: Fukui electrophilic $F^{+}(r)$, nucleophilic $F^{-}(r)$, and dual Fukui descriptor $F^{2}(r)$ for DDT isolated MPL molecule

Atom	**F^{+} (r)**	**F^{-} (r)**	**F^{2} (r)**	**Atom**	**F^{+} (r)**	**F^{-} (r)**	**F^{2} (r)**
S (1)	0.055	0.152	-0.097	H (7)	0.094	0.152	-0.058
C (2)	0.104	0.273	-0.169	H (8)	0.078	0.070	0.008
C (3)	-0.033	-0.028	-0.005	H (9)	0.078	0.070	0.008
C (4)	0.208	0.037	0.171	H (10)	0.088	0.041	0.047
C (5)	0.158	0.043	0.115	H (11)	0.077	0.037	0.04
H (6)	0.094	0.152	-0.058				

Table 4.10: Fukui electrophilic $F^{+}(r)$, nucleophilic $F^{-}(r)$, and dual Fukui descriptor $F^{2}(r)$ for DP isolated MPL molecule

Atom	**F^{+} (r)**	**F^{-} (r)**	**F^{2} (r)**	**Atom**	**F^{+} (r)**	**F^{-} (r)**	**F^{2} (r)**
C (1)	-0.017	-0.013	-0.004	O (13)	-0.013	0.042	-0.055
C (2)	-0.004	-0.007	0.003	H (14)	0.184	0.039	0.145
C (3)	-0.023	-0.008	-0.015	O (15)	0.000	0.110	-0.110
C (4)	-0.062	-0.010	-0.052	H (16)	0.066	0.085	-0.019
C (5)	-0.019	-0.016	-0.003	O (17)	0.012	0.169	-0.157
C (6)	-0.057	-0.017	-0.04	H (18)	0.149	0.077	0.072
O (7)	-0.002	0.145	-0.147	H (19)	0.096	0.036	0.06
H (8)	0.027	0.067	-0.04	H (20)	0.387	0.018	0.369
O (9)	-0.075	0.066	-0.141	H (21)	0.131	0.016	0.115
H (10)	0.046	0.058	-0.012	H (22)	0.060	0.031	0.029
H (11)	0.031	0.030	0.001	H (23)	0.034	0.044	-0.01
H (12)	0.048	0.040	0.008				

Table 4.11: Fukui electrophilic $F^{+}(r)$, nucleophilic $F^{-}(r)$, and dual Fukui descriptor $F^{2}(r)$ for OMTS isolated MPL molecule

Atom	$F^{+}(r)$	$F^{-}(r)$	$F^{2}(r)$	Atom	$F^{+}(r)$	$F^{-}(r)$	$F^{2}(r)$
Si (1)	0.197	0.008	0.189	H (9)	0.042	0.114	- 0.072
O (2)	-0.032	0.058	-0.09	H (10)	0.036	0.077	-0.041
Si (3)	0.197	0.008	0.189	H (11)	0.036	0.077	-0.041
O (4)	-0.041	0.056	-0.097	H (12)	0.042	0.114	-0.072
Si (5)	0.219	0.011	0.208	H (13)	0.041	0.090	-0.049
O (6)	-0.039	0.052	-0.091	H (14)	0.042	0.088	-0.046
Si (7)	0.219	0.011	0.208	H (15)	0.041	0.090	-0.049
O (8)	-0.041	0.056	-0.015	H (16)	0.042	0.088	-0.046

Table 4.12: Fukui electrophilic F+(r), nucleophilic F−(r), and dual Fukui descriptor F2(r) for DT isolated MPL molecule

Atom	$F^{+}(r)$	$F^{-}(r)$	$F^{2}(r)$	Atom	$F^{+}(r)$	$F^{-}(r)$	$F^{2}(r)$
C (1)	-0.007	-0.011	0.004	C (22)	-0.004	-0.002	-0.002
C (2)	0.018	0.077	-0.059	H (23)	0.021	0.023	-0.002
C (3)	-0.009	0.081	-0.090	H (24)	0.013	0.014	-0.001
C (4)	-0.012	-0.016	0.004	H (25)	0.016	0.024	-0.008
C (5)	0.024	0.035	-0.011	H (26)	0.064	0.031	0.033
C (6)	-0.009	-0.016	0.007	H (27)	0.053	0.029	0.024
C (7)	0.031	0.043	-0.012	C (28)	-0.011	0.001	-0.012
C (8)	-0.009	-0.006	-0.003	H (29)	0.080	0.033	0.047
C (9)	-0.024	-0.008	-0.016	H (30)	0.040	0.015	0.025
C (10)	0.093	0.010	0.083	O (31)	0.018	0.028	-0.01
C (11)	0.122	0.040	0.082	H (32)	0.059	0.023	0.036
C (12)	0.013	-0.005	0.018	H (33)	0.007	0.029	-0.022
H (13)	0.014	0.040	-0.026	H (34)	0.011	0.044	-0.033
H (14)	0.021	0.057	-0.036	H (35)	0.010	0.043	-0.034
C (15)	-0.002	-0.007	0.005	H (36)	0.009	0.013	-0.004
H (16)	0.022	0.066	-0.044	H (37)	0.018	0.022	-0.004
H (17)	0.005	0.020	-0.015	H (38)	0.016	0.022	-0.006
H (18)	0.050	0.066	-0.016	H (39)	0.038	0.019	0.019
H (19)	0.000	0.021	-0.021	H (40)	0.059	0.024	0.035
H (20)	0.015	0.032	-0.017	H (41)	0.042	0.013	0.029
H (21)	0.015	0.030	-0.015	H (42)	0.072	0.004	0.068

Table 4.13: Fukui electrophilic $F^{+}(r)$, nucleophilic $F^{-}(r)$, and dual Fukui descriptor $F^{2}(r)$ for ODA isolated MPL molecule

Atom	F^{+} (r)	F^{-} (r)	F^{2} (r)	Atom	F^{+} (r)	F^{-} (r)	F^{2} (r)
C (1)	-0.013	-0.027	0.014	H (17)	0.020	0.027	-0.007
C (2)	0.053	0.130	- 0.077	H (18)	0.021	0.033	-0.012
C (3)	0.046	0.128	- 0.082	H (19)	0.032	0.020	0.012
C (4)	-0.013	-0.020	0.007	H (20)	0.033	0.019	0.014
C (5)	-0.009	-0.010	0.001	H (21)	0.052	0.025	0.027
C (6)	-0.020	-0.008	-0.012	H (22)	0.090	0.023	0.067
C (7)	-0.027	-0.002	-0.025	O (23)	0.174	0.128	0.046
C (8)	0.200	0.022	0.178	H (24)	0.049	0.017	0.032
N (9)	0.098	0.023	0.075	H (25)	0.055	0.021	0.034
C (10)	-0.004	-0.014	0.010	H (26)	0.006	0.019	- 0.013
H (11)	0.020	0.063	-0.043	H (27)	0.008	0.022	-0.014
C (12)	-0.005	-0.004	-0.001	H (28)	0.006	0.022	- 0.016
H (13)	0.028	0.082	-0.054	H (29)	0.015	0.028	-0.013
H (14)	0.027	0.079	-0.052	H (30)	0.007	0.021	-0.014
H (15)	0.018	0.042	-0.024	H (31)	0.009	0.027	- 0.018
H (16)	0.024	0.062	-0.038				

Table 4.14: Bond length analysis in NaCl medium via RDF

Interaction	Bond length (Å)
Fe (110)-N	2.970
Fe (110)-O	3.49
Fe (110)-S	3.27
Fe (110)-Si	3.19
Fe (110)-C	2.97

Table 4.15: Parameters of the Langmuir adsorption isotherm

Adsorption Isotherm	Equation	R^{2}	K_{ads}	ΔG^{0}_{ads} (KJ.mol^{-1})
Langmuir	$C/\Theta = C + 1/K_{ads}$	0.998	8.31748	-15.199

4.2 Discussion

4.2.1 GC-MS

The result of GC-MS investigation as shown on the chromatogram in Figure 4.1, revealed the presence of various compounds consisting heteroatoms such as N, O, S or Pi-electrons in their molecular structures as presented in Table 4.1. The presence of heteroatoms in MPL extract makes it a viable inhibitor. It has been widely reported that plant extracts are rich in polar molecules with oxygen and nitrogen as well as nonpolar compounds with aromatic rings, aliphatic chains, heterocyclic rings and functional moieties (Verma et al., 2024). These are thought to promote the adsorption of inhibitors on the surfaces of metals and form a protective film on metallic surface without affecting the surrounding and hence decreases corrosion rate (Verma et al., 2024). From Figure 4.1, a number of base peaks that are the highest are observed and they represent compounds found in the MPL molecule, these compounds are presented in table 4.1, when compared with the NIST 14 mass spectral standard library (Altameme, Hameed and Kareem, 2015; Ouandaogo et al., 2023). The table shows the names of compounds with their chemical structures, molecular formulae and molecular weights (g/mol) containihg heteroatoms. From the GC-MS investigation, the inhibition of the rate of corrosion by MPL extract could be attributed to the presence of the aforementioned phytochemicals which are made up of S, N,O, pi-bonds and other heteroatoms in the structures which are also responsible for donating electrons thereby acting as strong Lewis bases as such increasing electron density at the adsorption centers on the surface of the metal substrate which in like manner acts as strong Lewis acids. Also, the electronegativities that exist within these heteroatoms create a dipole-dipole moment which forms localized regions for electrons in the direction of the most electronegative atoms as such a donor-acceptor interaction between the MPL extract (inhibitor) and the metal surface is formed.

4.2.2 FT-IR

FT-IR investigation of the functional groups and substituents present in the MPL extract as shown in Figure 4.2a are identified absorption bands associated with (N-H) and (O-H) hydrophilic polar functional groups which falls between 3500-3200 cm^{-1}, while the (C-H) stretching vibration was noted in the range 2950-2850cm^{-1}. The vibration of (C=C) stretching was observed at around 1680-1640cm^{-1}, while that corresponding to (methyl C-H) vibration stretching was observed at between 1370-1350 cm^{-1}. The absorption vibration in the range 1260-1050$cm^{-1}$was due to C-O functional group.Also the vibration between 860-680cm^{-1} was identified as (Aromatic C-H). All the functional groups identified are electron-donating groups (EDGs) or substituents. EDGs help to increase electron density at the adsorption sites

thereby facilitating electron transfer that will enable inhibitor-metal surface interaction. Figure 4.2b show FT-IR spectrum for (c) the MPL extract powder, (d) the corrosion product and (e) extract liquor. Available literature has shown that the adsorption efficiency of inhibitor molecules on the metal surface can be significantly influenced by the ability of the functional groups to increase electron density at the inhibitor/metal interface (adsorption site) (Verma et al, 2021). Table 4.2 shows the functional groups and substituents identified in the MPL extract.

4.2.3 Gravimetric/Weight Loss

The effect of the MPL inhibitor on carbon steel in 3.5wt% NaCl solution is shown in figure 4.3(a,b&c). The parameters such as weight loss, corrosion rate and inhibition efficiency in the absence and presence of the various concentrations of the MPL inhibitor in 3.5wt% NaCl solution over the immersion time 1hr, 6hr, 24hr, 48hr, 72hr, 96hr and 120hr can also be seen on table 4.3. Figure 4.3a show weight loss against time, it is observed that as the MPL inhibitor concentration increases,the weight loss decreases with time. Looking at figure 4.3b, it is observed that as the MPL inhibitor concentration was increased, thecorrosion rate decreased with time. Figure 4.3c also shows that as the MPL inhibitor concentration is increased, the inhibitor efficiency increased with time. Looking at the concentration of 100g/L of MPL inhibitor, the inhibition efficiency was observed to be 91% at an immersion time of 120 hours. This high efficiency can be attributed to the corrosion inhibition effectiveness of the MPL corrosion inhibitor. As expected, this led to a decrease in corrosion rate from 0.8817 mm/y to 0.0823 mm/y over an exposure time of 120 hours as shown in figure 4.3d and table 4.3. Likewise, the weight loss experienced by the test specimen decreased from 0.0986g to 0.0091g. Overall, looking at table 4.3and figure 4.3(a, b &c), it is observed that as the MPL extract concentration was increased, there was a corresponding increase in the inhibition efficiency confirming the effectiveness of the MPL extract in reducing carbon steel corrosion in 3.5 wt% NaCl solution. This can be attributed to the fact that the substituent groups in the MPL inhibitor molecules contain polar functional groups that are electron donating and have high bonding energy that are not easily overcome by some external energy.

4.2.4 Surface Morphology

Atomic force microscopy (AFM) gives microscopic images for carbon steel surface topography perfectly, which assesses the roughness of the examined metal. The 2D and 3D AFM morphologies of the surface of carbon steel in 3.5wt% NaCl solution in the absence and presence of 100g/L MPL are shown in figure 4.4 (a) and (b) respectively. The image of the surface of carbon steel in 3.5wt% NaCl without 100g/L MPL as shown in figure 4.4a and

table 4.4 have a larger mean roughness value approximately (Ra = 28nm) and root mean square roughness value is approximately (Rq = 71nm) than that in the presence of 100g/L MPL which has lower mean roughness value approximately (Ra = 9nm) and root mean square roughness value approximately (Rq = 34nm) as shown in figure 4.4(b). These results show that carbon steel in 3.5wt%NaCl solution is severely corroded because of the presence of corrosive chloride ions. The obtained roughness of inhibited carbon steel as shown in figure 4.4 (b) shows the presence of Langmuir films on the surface of the sample because of the effectiveness of the adsorbed layer of MPL on the surface, hence effectively impeding the corrosion of carbon steel.

4.2.5 Contact Angle Measurements

From figure 4.5a and table 4.5 it is observed that the dry polished carbon steel surface has a low contact angle of approximately 68.19• indicating that the surface is favourable to wetting, hence hydrophilic, therefore, exposing the surface to corrosive ions from moisture. Likewise, from figure 4.5b and table 4.5 it is observed that the surface of carbon steel immersed in 3.5wt%NaCl in the absence of the MPL inhibitor also has a low contact angle of approximately 76.20• also indicating that the surface is favourable to wetting, hence hydrophilic as well, therefore prone to corrosive chloride ions in the solution. However, looking at figure 4.5c and table 4.5 it is observed that the surface of carbon steel immersed in 3.5wt%NaCl in the presence of 100g/L MPL has a high contact angle of approximately 152.42•indicating that the surface is not favourable to wetting, hence hydrophobic. This can be attributed to the thin film (Langmuir films) from the MPL inhibitor which adsorbed on the surface of the metal effectively shielding the surface from corrosive chloride ions and enhancing its water repellant properties. From these observations it is evident that the MPL inhibitor contributes to modifying the surface characteristics of carbon steel in seawater environment, making it less prone to water and more resistant corrosive chloride ion's induced degradation. The MPL has indeed functioned as a good corrosion inhibitor for carbon steel in seawater by causing a surface-active action wherby the hydrophilic head of the MPL molecule adher strongly on the metal/inhibitor interface while the hydrophobic tail of the MPL inbibitor spreads out causing a repellant action on the surface thereby preventing water to get in contact with the metal surface hence restricting corrosive chloride ions from reaching the surface.

4.2.6 Electrochemical Investigation

The open circuit potential of carbon steel in 3.5wt% NaCl solution in the absence and presence of various concentrations of MPL is as shown in figure 4.6b, it can be observed that the open circuit potentials cross one another indicating a change in the dorminant corrosion

mechanism occurring on the carbon steel surface. In this case a change from uniform to pitting corrosion due to variations in chloride ion concentration causing the corrosion potential to shift in a more negative direction as a result of passivity breakdown.

The corrosion parameters obtained from potentiodynamic polarization (PDP) are presented in table 4.6a while figure 4.6c shows the Tafel plots which is related to the activation energy of the reaction, thereby indicating the reaction rate. By observing the Tafel plots, a significant shift towards the cathodic branch is observed with corrosion potentials moving towards positive direction meaning higher tendency to resist corrosion rate. Considering table 4.6a, the concentration of MPL extract at 100g/L showed the lowest corrosion rate of about 0.1mm/y with inhibition efficiency of 90.1%. Also it is observed that the corrosion current values significantly reduced from approximately 87μA for the blank to approximately 9μA for 100g/L MPL, indicating reduced corrosion rate. This result is in line with the shifting of the polarization curves which indicate that as the MPL concentration increased from 10g/L to 100g/L there was a reduction of current density. The cathodic branch of the Tafel plot as in figure 6c clearly shows the transition from activation-controlled reaction which limiting step is the transfer of electrons (oxidation) to the surface of the metal, to diffusion-controlled reaction which limiting step is the transport of chemical species such as diffusion (reduction) of oxygen to water. This is in line with the reactions that govern carbon steel when immersed in NaCl solution whereby the oxidation of iron and reduction of oxygen occurs. It is also observed from the Tafel plots that the polarization curve of the 100g/l MPL shows limiting current density. Again, looking at the polarization slopes of all the MPL concentrations of the Tafel plots, it is observed that the slopes shift towards more positive current densities with the 100g/L shifting to the most positive value indicating reduction in corrosion rate. The ability of MPL inhibitor to control the activation reaction (oxidation) and the diffusion reaction (oxygen reduction) makes it a mixed-type corrosion inhibitor. A close observation showed hydrogen evolution due to limited oxygen to get to the surface of the metal thereby limiting current density and hence corrosion rate.

The electrochemical impedance spectroscopy (EIS) of carbon steel in 3.5wt% NaCl solution in the absence and presence of MPL extract (inhibitor at various concentrations was also investigated and the parameters are presented in table 4.6b. The Nyquist plot, Bode plot and Phase angle are shown in figure 4.6d, 4.6e and 4.6f respectively. The Nyquist plot is explained using an equivalent circuit model as shown in figure 4.6a. The semicircular shape of the Nyquist plot demonstrates the charge transfer resistance at the metal/electrolyte interface, with the semicircle diameter of each concentration corresponding to the extent of corrosion resistance. As the concentration of the MPL was increased from 10g/L to 100g/L,

the diameters of the semicircles also increased, indicating better corrosion resistance. The largest semicircle is observed at 100g/L of MPL concentration showing the highest corrosion protection which is in line with the inhibition efficiency of 84% as shown in table 4.6b. It is also observed that the transfer charge resistance $R_2 \equiv Rct$ is highest at 100g/L of MPL inhibitor. Also, the polarization resistance, Rp is highest at 100g/L of MPL concentration indicating lower corrosion current, hence slower corrosion rate. There is absence of pure capacitance response but broadened peak heights at higher MPL concentrations indicating a clear charge transfer resistance between the corrosion media and the metal surface. From figure 4.6d, it was observed that as the MPL concentration increased, the Nyquist plot showed a widened diameter and increased peak heights indicating a higher charge transfer resistance (R_{ct}). A one-time constant was detected in Bode diagrams see figure 4.6(e, f) with a characteristic increase in absolute impedance values and decrease in phase angle confirming the prevalence of charge transfer mechanism over the electrolyte/substrate interface.

4.2.7 DFT

All quantum chemical properties were obtained after geometric optimization with respect to the DMol3 model at the DFT level. The optimized molecular structures of the studied MPL isolated molecules compounds are as shown in figure 4.7a while the HOMO and LUMO energy levels of the compounds present in the MPL and their corresponding band gaps are shown in figure 4.7b. The computed values of the quantum chemical parameters for the isolated molecules present in the MPL extract are stated in table 4.7. Generally, the global reactivity of molecules can be estimated from the energies of the frontier molecular orbitals (Zarrouk et al., 2014; Cao et al., 2014) such as: HOMO orbital which represents the ability of a molecule to lose electrons, and LUMO orbital which indicates the ability of a molecule to accept electrons. Therefore, the high inhibition performance of an inhibitor could be attributed mostly to the molecule with the highest HOMO and the lowest LUMO energies at the same time.

The results from table 4.7 and figure 4.7 show that the E_{HOMO} values did increase (less negative; destabilized) in the following order: DDT > ODA > DT > DP > ATD > OMTS. Therefore, the ability to contribute to electron donation to the vacant d-orbital of the carbon steel surface is expected to follow the same order. Increasing values of E_{HOMO} facilitate adsorption and therefore enhance the inhibition efficiency, by influencing the transport process through the adsorbed layer. Hence, higher values of E_{HOMO} indicate better tendency towards the donation of electron, enhancing the adsorption of the MPL inhibitor on carbon steel and therefore better inhibition efficiency.

On the other hand, the E_{LUMO} values did decrease (more negative; stabilized) in the following order: ATD < DDT< ODA <OMTS > DP < DT, and thus the ability to accept electrons would be expected to follow the same order. It has also been found that an inhibitor does not only donate an electron to the unoccupied d-orbital of the metal ion but can also accept electrons from the d-orbital of the metal leading to the formation of a feedback bond hence forming strong covalent bond. Therefore, the tendency for the formation of a feedback bond would depend on the values of E_{LUMO}. The lower the E_{LUMO}, the easier is the acceptance of electrons from the d-orbital of the carbon steel to the MPL inhibitor.

The energy band gap, ΔE represents the difference between the energies of HOMO and LUMO orbitals. The ΔE values of the studied compounds decreased in the following order: OMTS > DT > DP > ODA > ATD > DDT, and thus the contribution to the inhibitor performance is predicted to follow the same order. As ΔE decreased, the reactivity of the molecules increased, leading to an increase in the inhibition efficiency of the MPL inhibitor (Verma, Ebenso, Quraishi & Hussain., 2021). This was in line with the result of the gravimetric method where the inhibition efficiency of the MPL inhibitor was found to be 91%. The electronegativity (χ) values for the isolated molecules decreased in the following order: DT < DP < DDT < ODA < OMTS < ATD and their individual contribution to the inhibition efficiency of 91% for the MPL inhibitor follow the same order. In the same vein, the chemical hardness (η) decreased in the following order: DDT < ATD < ODA < DP < DT < OMTS making the metal act like a Lewis acid and hence as an electron acceptor, and the positive contribution to the inhibition efficiency of 91% for the MPL inhibitor followed the same order.

On the other hand, the values of global softness (σ) and dipole moment (μ) increased in the following order: DDT > ATD > ODA > DP > DT > OMTS and DT > DP > DDT > ODA > OMTS > ATD respectively, making the MPL inhibitor act as a Lewis base and hence an electron donor to the d-orbital of the metal, while the increased dipole moment showed the tendency of the MPL inhibitor to adsorb on the carbon steel metal surface. Also, the positive contribution of these values to the high inhibition of 91% for MPL is expected to follow the same order.

Considering the electrophilic (ω) and nucleophilic (ϵ) descriptors, it is theorized that lower electrophilicity value and higher nucleophilicity value suggest the ability of an inhibitor molecule to transfer electrons to the unoccupied d-orbital of the metallic surface (Lukovits et al., 2001). As presented in table 4.7, it is observed that the values for (ω) decreased in the following order; DT< DP < OMTS < ODA < DDT < ATD while the values (ϵ) increased in the following order; DT > DP > OMTS > ODA > DDT > ATD respectively, thereby making

all the MPL isolated inhibitor molecules contribute positively to electron transfer to the carbon steel d-orbitals, hence enhancing the MPL/carbon steel interface interaction and eventually translating to the impressive inhibition effectiveness of the MPL inhibitor.

Likewise, considering the electron donating (ω-) and the electron accepting (ω+) powers descriptors, it is again theorized that systems with small electron donating powers (ω-) have good electron donating ability. That is, the lower the electron donating power of an inhibitor molecule, the better its electron donating capabilities will be. Again, from table 4.7, it can be observed that all the values of (ω+) for the isolated molecules of the MPL are less than the values of (ω-) showing their better proclivity to give electrons than accepting.

Subsequently, the ΔNdescriptor which is the fraction of electrons transferred gives an indication of the capacity to transfer electrons to the metal surface. According to Lukovits et al, if $\Delta N<3.6$ then the inhibition efficiency of the inhibitor molecules is increasing with electron affinity on the metal surface (Lukovits et al., 2001). Hence improved electron releasing power was replaced by electron-donating group by altering a hydrogen atom of the aromatic ring. Consequently, in this study, all the isolated MPL inhibitor molecules studied have shown that ΔNvalues are less than 3.6 which indicate that the inhibitor's molecules are electron donors and the metal surface is an acceptor. Therefore, these descriptors show ample correlation with the high corrosion inhibition effectiveness of MPL on carbon steel corrosion in 3.5wt % NaCl solution.

The HOMO and LUMO densities of the isolated compounds are represented in figure 4.7.

From the figure the various electron densities and the active sites for preferred adsorption of inhibitor/metal interaction can be visualized. Firstly, considering the DDT molecule in figure 4.7 it can be seen that the presence of heteroatoms such as, N and S has created electron-rich centers at these regions thereby increasing electron density for interaction at the MPL/carbon steel adsorption site. Also, the presence of the carbon -carbon double bonds and carbon bonded to sulfur (heteroatom) created electron centers making the region an electron density site. Thismakes the MPL inhibitor a strong electron donor and the carbon steel an electron acceptor at the adsorption site. Secondly, the presence of hydroxyl polar functional groups along the ring of the DP molecule as shown in figure 4.7makes the surrounding region a localized region for electron density thereby favoring MPL inhibitor and carbon steel interaction at the adsorption site. Thirdly, considering figure 4.7, it is observed that the presence of four methyl functional groups within the OMTS molecule makes the surrounding region attractive for electrons to spend more time, hence, favoring localization of electrons. This contributes to the ability of the MPL to function as electron donor to the carbon steel since this is a donor/acceptor phenomenon. Fourthly, the ODA molecule in figure 4.7 shows

the presence of carbon-carbon double bond and amide functional groups. These functional groups promote electron density. Also, the presence of lone pair electrons from the nitrogen atom makes these sites suitable for electron density as such contributing to the electron donating ability of the MPL inhibitor. Furthermore, the presence of dimethyl-amino substituents in the 1,3,5 triazine of the ATD molecule significantly increases localization on the nitrogen atom, thereby promoting electron density at the sites. This contributes to the electron donating power of the MPL inhibitor. In addition, the presence of hydroxyl and carbon-carbon double bonds on the DT molecule makes these regions suitable for electron density. It is important to note that, from the above information, the MPL has shown the presence of electron-rich centers, heteroatoms and polar regions which most often are responsible for both chemical and physical adsorption, suggestive of a mixed-type inhibitor. According to Miralrio and Espinoza-Vazquez; electron-rich sites and heteroatoms have been found to be responsible for chemisorptions, whereas physisorption is due to the presence of polar groups (Miralrio and Espinoza-Vazquez, 2020). Hence, the high corrosion inhibition efficiency of 91% for the MPL inhibitor can be attributed to the individual contributions of the electron donating ability of each of these isolated molecules.

4.2.8 Fukui Indices of Isolated MPL Inhibitor Molecule

Further analysis of the active sites of the inhibitor molecule is carried out through condensed Fukui functions, which often gives additional information that throws more light to the reactivity and inhibitory properties of potential inhibitor molecules which the E_{HOMO} and E_{LUMO} have earlier provided. As such, figure 4.8, is the Fukui electrophilic and nucleophilic maps of the isolated compounds of the MPL inhibitor molecule showing numbering of atoms. The sites for nucleophilic ($F^{+}(r)$) and electrophilic ($F^{-}(r)$ reactions could be determined in terms of the electronic populations as reported in the literature (Dagdag et al., 2020a; Dagdag et al., 2020b; Dagdag et al., 2019). The value of dual descriptor ($F^{2}(r)$) which is estimated using Eq. (3.19) is intented to provide information for chemical reaction.

Fukui indices ($F^{+}(r)$ and $F^{-}(r)$), and the dual descriptor ($F^{2}(r)$) for the isolated compounds in the MPL inhibitor molecule under investigation were calculated and presented in Tables4.8 to 4.13. The atoms with the high values of $F^{+}(r)$ form the chemical species of the aromatic benzene amine ring which are located at each end of the molecule. These sites are considered as charge acceptors during MPL/metal (carbon steel) interactions, if $F^{2}(r) > 0$. On the other hand, atoms with high values of $F^{-}(r)$ represent sites for electron donation. Therefore, considering table 4.8-4.13, atoms with the highest electron-donating regions are ATD[N(3), O(8), N(9),O(11)]; DDT[S(1), C(2), H(6), H(7)]; DP[O(7), O(15), O(17)]; OMTS[H(9), H(12)]; DT[null]; ODA[C(2),C(3),O(23)]. However, chemical species with charge acceptors

are ATD[C(2), C(4)]; DDT[C(4),C(5)]; DP[H(4), H(18), H(20), H(21)]; OMTS[Si(1), Si(3), Si(5), Si(7)]; DT[C(11)]; ODA[C(8), O(23)]. It is an established fact that carbon steel has coordination affinity towards N-, O- and S- bearing ligands and can be seen on the electron-donating regions of the compounds of the MPL molecule. Hence adsorption on the carbon steel can be attributed to coordination through hetero-atoms and pi electrons of the aromatic rings. Futher, the double bonds seen on the charge acceptors of the compounds of the MPL molecule allow for back donation of the metal d-orbitals to the MPL molecule thereby encouraging strong coordination bonding. Interestingly, these results are quite in agreementwith the electron distribution over the HOMO and LUMO surfaces.

4.2.9 MD Simulation

From figure 4.9a, it is observed that the orientation of the MPL inhibitor molecules on the metal surface is planaras such it covers a larger part of the metallic surface contributing to large surface coverage and acts as a superior corrosion inhibitor. When an inhibitor approaches the metallic surface, due to the effect of different attractive and repulsive forces it gets polarized and acquires a specific orientation depending upon the nature of the electronic structure of the inhibitor molecules (Verma et al., 2021). The mechanism of the interaction is shown in figure 4.9b. Generally, electron donating substituents force the inhibitor molecules to obtain either a vertical orientation or planar orientation (Toghan et al., 2023). In this case, the presence of heterocycles and electron donating substituents forced the MPL inhibitor to attain a planar orientation on the carbon steel surface as such improving inhibition efficiency. The MD simulations generated a final super-structure model of MPL onto the carbon steel surface which is presented in figure 4.9(a). To evaluate the adsorption capacity of the MPL compound on the carbon steel surface, the adsorption energy which reflects the strength of the inhibitor molecule's binding to the metal surface was measured. The results showed a high adsorption energy value -184.954 kJ/mol, indicating that the studied molecules adsorb easily onto the metal surface and exhibit strong intermolecular interactions. This is possible due to the functional groups and aromatic ring's inductive effects, which interact with the metal surface in a planar orientation. These findings provide solid indication that the MPL molecule has a robust interaction with the carbon steel (Fe) surface and suggest that it could be a promising candidate for application as a corrosion inhibitor.

4.2.10 Bond Lengths

The radial distribution function which helps to determine the bond lengths of interacting molecules can be calculated using MD simulation. This parameter gives an insight into the type of interaction between molecules. The interactionbetween two or more molecules can

be a chemical adsorption (chemisorption) or a physical adsorption (physisorption). Chemical adsorption is associated with shorterbond length between 1.0 and 3.5 Å and gives high bond strength, while physical adsorption is marked by bond length greater than 3.5 Å and correspondingly indicates lower bond strength (Dagdag et al., 2020a; Dandag et al., 2020b). Thus, if the interaction between an inhibitor molecule and metal substrate is a chemical interaction, high bond strength is expected and consequently the molecule is expected to perform as a good corrosion inhibitor.

However, if it is a physical interaction, the bond length is lower in strength and the molecule might not perform well in corrosion protection of the metal. As a result, in our case, the bond lengths of the atoms of the MPL isolated molecules with respect to the carbon steel were analyzed using the radial distribution function. The values of the bond lengths determined by the RDF analysis are stated in Table 4.14. Based on the correlation of bond lengths of interacting atoms to chemical and physical adsorptions, it could be seen that all the atoms of the MPL molecules were chemically adsorbed on the steel surface. These results are quiteinagreement with the obtained adsorption energies.

4.2.11 Adsorption Isotherms

To understand the mechanism of interactions between the MPL molecules and the carbon steel in 3.5wt. % NaCl) at 298K, three models of adsorption isotherms were tested. Firstly, the Langmuir Isotherm was tested. Followed by the Temkin Isotherm and thirdly, the Frumkin Isotherm was tested as shown in figure; 4.10 (a, b and c) respectively. From the fittings of the three isotherms, the Langmuir isotherm showed a regression coefficient R^2 = 0.998 and a slope of 1.02 ≈ 1. However, the Temkin and Frumkin showed regression coefficients of 0.977 and 0.977, and slopes of 0.30 and 30.10 respectively. Therefore, the experimental data for the MPL extract obeyed the Langmuir adsorption isotherm better than the other two isotherms that were tested. So, considering the Langmuir Isotherm, the values of the equilibrium constant K_{ads} can be determined from the values of the standard free adsorption energies ΔG°_{ads} using Eq. (3.20) (ELouadi et al., 2015; Ben Hmamou et al., 2012**)**: The value of the coefficient of correlation shows that the adsorption of MPL on the carbon steel surface followed the Langmuir model. It is reported that the value of ΔG^0_{ads} around -20 $kJmol^{-1}$or less corresponds to the electrostatic interaction (Kokalj, 2023). In this case, ΔG^0_{ads} is -15.199$KJmol^{-1}$ and the interaction between the charged inhibitor molecules and the charged carbon steel surface is indeed electrostatic (Murulana et al., 2016). According to the results obtained in figure 4.10 (a, b & c) the adsorption mode of MPL molecules on the carbon steel surface is a physical adsorption. The parameters of the Langmuir adsorption isotherm considered after the testis presented in table 4.15.

CHAPTER FIVE

CONCLUSION AND RECOMMENDATIONS

5.1 Conclusion

In conclusion, the overall results have shown that substituents play a significant role in determining the corrosion inhibition effect of organic corrosion inhibitors. Obviously, because of their electron donating or electron withdrawing nature, these substituents affect the overall electron density at the donor site(s) of the inhibitor molecules. As such they have clearly demonstrated that the interaction of organic corrosion inhibitors with the metallic surface involves a donor–acceptor (charge sharing) phenomenon. Consequently, the high inhibition properties of the MPL can be attributed to the hydrophilic polar functional head which interacts strongly with aqueous environments in which case it is solvated through a dipole-dipole interaction and its hydrophobic tail that acts as a passivating film barrier protecting the substrate from corrosive species. The presence of Langmuir films on the MPL/carbon steel adsorption site is an indication that the MPL inhibitor can function as a biosurfactant and this was due to the presence of saponins in its molecules. Further, the methodologies adopted in the study corroborated one another making a strong case for the validation of the findings.

5.2 Recommendations

From the findings of this study it is interesting to note that *Musa paradisiacal* leaf extract-based inhibitor has been found to be a surfactant and can effectively protect carbon steel from corrosion in seawater environment. However, as a surfactant, its industrial applications are enormous, as such, the following recommendations may be necessary as they serve as contribution to the field and also as value for purposes of sustainability:

1. Continous research and development of this biosurfactant should be intensified as it promises to be a sustainable option in corrosion protection and also has the potential to be used for cleaning of oil spillage which has been a very worrisome issue in the oil producing communities in Nigeria in particular and Africa in general.
2. *Musa paradisiacal* leaf is abundant in Africa as waste material. Therefore, harnessing its application in the important areas of corrosion protection and cleaning of oilspillage will mean creating a material for global consumption and sustainability.
3. Future studies should seek to evaluate the corrosion inhibition effectiveness of MPL inhibitor in acidic media using a variation of methodologies to see if the efficiency will improve further or otherwise. If otherwise, then synergism with zinc phosphate,

an industry standard corrosion inhibitor in the oil and gas industry which has the challenge of insolubility, should be tested to see if the synergized alternative can perform better than the individual inhibitors.

4. Likewise, the MPL inhibitor should be tested for the inhibition of scale in acidic media during oil recovery operations in oil and gas drilling.

5.3 Contribution to Knowledge

A novel and sustainable corrosion inhibitor has been designed for industrial applications.

REFERENCES

Abd El Al, E. E., Abd El Wanees, S., Farouk, A., & Abd El Haleem, S. M. (2013). Factors Affecting the Corrosion Behaviour of aluminum in Acid SolutionsII. Inorganic Additives as Corrosion Inhibitors for Al in HCl Solutions. *Corros. Sci.*, *68*.

Ahmad, S., Basavaraja, L. R., & Bhattacharjee, B. (2000). Design procedures for cathodic protection systems for RC members. *Indian Concrete Journal*, *74*(4), 208-216.

Ahmad, Z. (2006). *Principles of corrosion engineering and corrosion control*. Elsevier.

Ahmed, S. K., Ali, W. B., &Khadom, A. A. (2019). Synthesis and investigations of heterocyclic compounds as corrosion inhibitors for mild steel in hydrochloric acid. *International Journal of Industrial Chemistry*, *10*(2), 159-173.

Akalezi, C. O., &Oguzie, E. E. (2016). Evaluation of anticorrosion properties of Chrysophyllumalbidum leaves extract for mild steel protection in acidic media. *International Journal of Industrial Chemistry*, *7*(1), 81–92.

Akalezi, C. O., Enenebaku, C. K., &Oguzie, E. E. (2013). Inhibition of acid corrosion of mild steel by biomass extract from the Petersianthusmacrocarpus plant. *J. Mater. Environ. Sci*, *4*(2), 217-226.

Akalezi, C., Maduabuchi, A., Enenebaku, C., &Oguzie, E. (2020). Experimental and DFT evaluation of adsorption and inhibitive properties of Moringa oliefera extract on mild steel corrosion in acidic media. Arabian Journal of Chemistry. 13. 9270-9282.

Al, U., Station, N., & Dhabi, A. (1996). Mechanism of Corrosion Inhibition by Sodium Molybdate. *Desalination*, *107*.

Alhaffar, M, T., Umoren, S, A., Obot, I, B and Ali, S, A. (2018). Isoxazolidine Derivatives as Corrosion Inhibitors for Low Carbon Steel in HCl Solution: Experimental, Theoretical and Effect of KI Studies, *RSC Adv.*, *8* (4), 1764–1777. https://doi.org/10.1039/C7RA11549K

Ali, N., &Fulazzaky, M. A. (2020). The empirical prediction of weight change and corrosion rate of low-carbon steel. *Heliyon*, *6*(9), e05050. https://doi.org/10.1016/j.heliyon.2020.e05050

Alibakhshi, E., Ghasemi, E., &Mahdavian, M. (2014). Sodium zinc phosphate as a corrosion inhibitive pigment. *Progress in Organic Coatings*, *77*(7), 1155-1162.

Alibakhshi, E., Ramezanzadeh, M., Haddadi, S. A., Bahlakeh, G., &Ramezanzadeh, B. (2019). Persian Liquorice Extract as a Highly Efficient Sustainable Corrosion Inhibitor for Mild Steel in Sodium Chloride Solution. *J. Clean. Prod.*, *210*.

Alibakhshi, Eiman&Ghasemi, Ebrahim &Mahdavian, Mohammad. (2013). Corrosion inhibition by lithium zinc phosphate pigment. Corrosion Science. 77. 222-229. 10.1016/j.corsci.2013.08.005.

Alrashed, M. M., Jana, S., &Soucek, M. D. (2019). Corrosion Performance of Polyurethane Hybrid Coatings with Encapsulated Inhibitor. *Prog. Org. Coat., 130*.

Al-Sabagh, A. M., Migahed, M. A., Sadeek, S. A., &Basiony, N. M. (2018). Inhibition of Mild Steel Corrosion and Calcium Sulfate Formation in Highly Saline Synthetic Water by a Newly Synthesized Anionic Carboxylated Surfactant. *Egypt. J. Pet., 27*.

Alvarez, P. E., Fiori-bimbi, M. v, Neske, A., Brandán, S. A., &Gervasi, C. A. (2018). RolliniaOccidentalis Extract as Green Corrosion Inhibitor for Carbon Steel in HCl Solution. *J. Ind. Eng. Chem., 58*.

Ammar, S., Iling, A. W. M., Ramesh, K., & Ramesh, S. (2020). Development of Fully Organic Coating System Modified with Epoxidized Soybean Oil with Superior Corrosion Protection Performance. *Prog. Org. Coat., 140*.

Anwo, A. B., Ajanaku, K. O., Fayomi, O. S. I., & Olanrewaju, A. (2019). Efficacy of Corrosion phenomena, challenges and control in steel industry: An overview. In *Journal of Physics: Conference Series* (Vol. 1378, No. 3, p. 032055). IOP Publishing.

Ardakani, E, K., Kowsari, E and Ehsani, A. (2020). Imidazolium-Derived Polymeric Ionic Liquid as a Green Inhibitor for Corrosion Inhibition of Mild Steel in 1.0 M HCl: Experimental and Computational Study, *Colloids and Surfaces A: Physicochemical and Engineering Aspects*, *586*, 124195. https://doi.org/10.1016/j.colsurfa.2019.12 4195.

Arrhenius, G., Caldwell, K., &Wold, S. (2008). A tribute to the memory of Svante Arrhenius (1859-1927): A scientist ahead of his time. IVA.

Arukalam, I. O., Madu, I. O., &Ishidi, E. Y. (2021). High performance characteristics of Lupinusarboreus gum extract as self-healing and corrosion inhibition agent in epoxy-based coating. *Progress in Organic Coatings*, *151*, 106095.

Arukalam, I. O., Oguzie, E. E., & Li, Y. (2018). Nanostructured superhydrophobic polysiloxane coating for high barrier and anticorrosion applications in marine environment. *Journal of colloid and interface science*, *512*, 674-685.

Arzola, S., Palomar-Pardavé, M. E., &Genesca, J. (2003). Effect of resistivity on the corrosion mechanism of mild steel in sodium sulfate solutions. *Journal of applied electrochemistry*, *33*(12), 1233-1237.

Ashassi-sorkhabi, H., &Kazempour, A. (2020). Incorporation of Organic/Inorganic Materials into Polypyrrole Matrix to Reinforce Its Anticorrosive Properties for the Protection of Steel Alloys: A Review. *J. Mol. Liq., 309*.

Askari, F., Ghasemi, E., Ramezanzadeh, B., &Mahdavian, M. (2015). The Corrosion Inhibitive Properties of Various Kinds of Potassium Zinc Phosphate Pigments: Solution Phase and Coating Phase Studies. *Prog. Org. Coat., 85*.

Aslam, R., Mobin, M., Shoeb, M., Murmu, M., & Banerjee, P. (2021). Proline nitrate ionic liquid as high temperature acid corrosion inhibitor for mild steel: Experimental

and molecular-level insights. *Journal of Industrial and Engineering Chemistry*, *100*, 333-350.

Atmani, F., Lahem, D., Poelman, M., Buess-Herman, C., & Olivier, M. G. (2013). Mild Steel Corrosion in Chloride Environment: Effect of Surface Preparation and Influence of Inorganic Inhibitors. *Corros. Eng. Sci. Technol.*, *48*.

Ayoub, G. M., Azar, N., Fadel, M. E., & Hamad, B. (2004). Assessment of hydrogen sulphide corrosion of cementitious sewer pipes: a case study. *Urban Water Journal*, *1*(1), 39-53.

Bagotsky, V. S. (Ed.). (2005). *Fundamentals of electrochemistry*. John Wiley & Sons.

Bahlakeh, G., Ramezanzadeh, M., &Ramezanzadeh, B. (2017). Experimental and Theoretical Studies of the Synergistic Inhibition Effects between the Plant Leaves Extract (PLE) and Zinc Salt (ZS) in Corrosion Control of Carbon Steel in Chloride Solution. *J. Mol. Liq.*, *248*.

Baldin, E. K. K., Kunst, S. R., Beltrami, L. V. R., Lemos, T. M., Quevedo, M. C., Bastos, A. C., Ferreira, M. G. S., Santos, P. R. R., &Sarmento, V. H. v. (2016). Ammonium Molybdate Added in Hybrid Films Applied on Tinplate Effect of the Concentration in the Corrosion Inhibition Action. *Thin Solid Films*, *600*.

Bancroft, W. D. (2002). Electrolytic theory of corrosion. *The Journal of Physical Chemistry*, *28*(8), 785-871.

Banerjee, S., Poria, S., Sutradhar, G, & Sahoo, P. (2021). Nano-indentation and Corrosion Characteristics of Ultrasonic Vibration Assisted Stir-Cast AZ31–WC–Graphite Nano-composites. *Inter Metalcast***15**, 1058–1072.

Baral, A., &Engelken, R. D. (2002). Chromium-based regulations and greening in metal finishing industries in the USA. *Environmental Science & Policy*, *5*(2), 121–133.

Bastidas, D. M., Criado, M., Fajardo, S., Iglesia, A. L. a., &Bastidas, J. M. (2015). Corrosion Inhibition Mechanism of Phosphates for Early-Age Reinforced Mortar in the Presence of Chlorides. *Cem. Concr. Compos.*, *61*.

Bastos, A. C., Ferreira, M. G. S., & Sim, A. M. (2005). Comparative Electrochemical Studies of Zinc Chromate and Zinc Phosphate as Corrosion Inhibitors for Zinc. *Prog. Org. Coat.*, *52*.

BAUER, O., KRÖHNKE, O. and MASING, G., 1936-1940. Die KorrosionmetallischerWerkstoffe (3 volumes). Hirzel, Leipzig.

Baux, J., Caussé, N., Esvan, J., Delaunay, S., Tireau, J., Roy, M., ... &Pébère, N. (2018). Impedance analysis of film-forming amines for the corrosion protection of a carbon steel. *Electrochimica Acta*, *283*, 699-707.

Beech, I. B., &Gaylarde, C. C. (1999). Recent advances in the study of biocorrosion: an overview. *Revista de microbiologia*, *30*, 117-190.

Bhattarai, J. (2013). Study on the corrosive nature of soil towards the buried-structures. *Scientific World*, *11*(11), 43-47.

Bradford, S. A. (2000). The practical handbook of corrosion control in soils.

Brown, D., Darr, D., Morse, J & Laskowski, B. (2012). Analatom, Inc., 517Weddell Dr. Suite 4, Sunnyvale, CA, USARaimondo Betti, Columbia University, 610 SW Mudd Building, New York, NY, USA

Bundy, K. J. (2008). Biomaterials and the Chemical Environment of the Body. In *Joint replacement technology* (pp. 56-80). Woodhead Publishing.

Burstein, G. T., & Sasaki, K. (2000). Effect of impact angle on the slurry erosion–corrosionof 304L stainless steel. *Wear*, *240*(1-2), 80-94.

Busby, J. P., Entwisle, D., Hobbs, P., Jackson, P., Johnson, N., Lawley, R., ... &Zawadzka, J. (2012). A GIS for the planning of electrical earthing. *Quarterly Journal of Engineering Geology and Hydrogeology*, *45*(3), 379-390.

C…&El Harfi, A. (2020a), "Highly durable macromolecular epoxy resin as anticorrosive coating material for carbon steel in 3 % NaCl: computational supported experimental studies", Appl Polym Sci e49003:1–12. https:// doi. org/ 10. 1002/ app. 49003

Cabrera, N., & Mott, N. F. (1948). REP PROG PHYS. *Rep. Prog. Phys.*, *12*, 163-184.

Caddock, B. D., Evans, K. E., & Hull, D. (1990). Stress-corrosion failure envelopes for E-glass fibre bundles. *Journal of Materials Science*, *25*(5), 2498–2502.

Chaker, V., & Palmer, J. D. (1989). ASTM Committee G-1 on Corrosion of Metals. *Effect of Soil Characteristics on Corrosion. ASTM International*, *81*.

Chalkidis, A., Jampaiah, D., Hartley, P. G., Sabri, Y. M., & Bhargava, S. K. (2020). Mercury in natural gas streams: A review of materials and processes for abatement and remediation. *Journal of hazardous materials*, *382*, 121036

Chandler, C. J., & Richer, J. S. (2000). The structure of protostellar envelopes derived from submillimeter continuum images. *The Astrophysical Journal*, *530*(2), 851.

Chatterjee, U. K., Bose, S. K., & Roy, S. K. (2001). *Environmental degradation of metals: Corrosion technology series/14*. CRC Press.

Chaubey, N., Yadav, D. K., Singh, V. K., & Quraishi, M. A. (2017). A Comparative Study of Leaves Extracts for Corrosion Inhibition Effect on aluminum Alloy in Alkaline Medium. *Ain Shams Eng. J.*, *8*.

Chen, Y.; Jiang, L.; Yan, X.; Song, Z.; Guo, M.; Zhao, S & Gong, W. (2020). Impact of Phosphate Corrosion Inhibitors on Chloride Binding and Release in Cement Pastes. *Construction and Building Materials*, *236*, 117469.

Chezeau, N. (1857). Albert, Marcel, Germain, René Portevin (1880-1962). *Itinéraires de chimistes*, *2007*, 150.

Chigondo, M., &Chigondo, F. (2016). Recent natural corrosion inhibitors for mild steel: an overview. *Journal of Chemistry, 2016*.

Chigondo, M., &Chigondo, F. (2016). Recent Natural Corrosion Inhibitors for Mild Steel: An Overview. *J. Chem., 2016*.

Chigozie, Akoma &Osarolube, Eziaku&Nnanna, Lebe& Wisdom O., John. (2015). Corrosion Inhibition of Crown Corks of Carbonated Drinks Using ChyrsohyllymAlbidium Extract. *International journal of engineering researches and reviews*. 3. 67-74.

Chris, L.(2001). The Collapse of the Silver Bridge. *West Virginia Historical Society Quarterly* 15, No. 4. Accessed September 30, 2024. http://www.wvculture.org/history/wvhs/wvhs1504.html

Chyżewski, E., & Evans, U. R. (1939). The classification of anodic and cathodic inhibitors. *Transactions of The Electrochemical Society*, *76*(1), 215.

Cigna, R., Proverbio, E., &Rocchini, G. (1993). A study of reinforcement behaviour in concrete structures using electrochemical techniques. *Corrosion science*, *35*(5-8), 1579-1584.

Cinitha, A., Umesha, P. K., &Iyer, N. R. (2014). An overview of corrosion and experimental studies on corroded mild steel compression members. *KSCE Journal of Civil Engineering*, *18*(6), 1735-1744.

Cobb, H. M. (2010). The Life of Harry Bearley (1871-1948). *The History of Stainless Steel*.

Corrales-Luna, M., Le Manh, T., Romero-Romo, M., Palomar-Pardavé, M., & Arce-Estrada, E. M. (2019). 1-Ethyl 3-methylimidazolium thiocyanate ionic liquid as corrosion inhibitor of API 5L X52 steel in H2SO4 and HCl media. *Corrosion Science*, *153*, 85-99.

Cui, J., Shi, R., & Pei, Y. (2017). Novel Inorganic Solid Controlled-Release Inhibitor for Q235-b Anticorrosion Treatment in 1 M HCl. *Appl. Surf. Sci., 416*.

Cyster, M. J., Smith, J. S., Vogt, N., Opletal, G., Russo, S. P., & Cole, J. H. (2021). Simulating the fabrication of aluminium oxide tunnel junctions. *npj quantum information*, *7*(1), 1-12.

Dagdag, O., Berisha, A., Safi, Z., Hamed, O.,Jodeh, S., Verma, C...& El Harfi, A. (2019), "DGEBA-polyaminoamide as effective anticorrosive material for 15CDV6 steel in NaCl medium: computational and experimental studies," J Appl Polym Sci 48402:1–10. https:// doi. org/ 10. 1002/ app

Dagdag, O., Berisha, A., Safi, Z.,Dagdag, S.,Berrani, M.,Jodeh, S., Verma,

Dagdag, O., Guo, L.,SaFI, Z., Verma, C.,Ebenso, E, E.,Wazzan, N.,Masroor,

Daoud, D., Douadi, T., Issaadi, S., &Chafaa, S. (2014). Adsorption and Corrosion Inhibition of New Synthesized Thiophene Schiff Base on Mild Steel X52 in HCl and H2SO4 Solutions. *Corros. Sci., 79*.

Davis, J. R. (Ed.). (2000). *Corrosion: Understanding the basics*. Asm International.

de Damborenea, J., Conde, A., & Arenas, M. A. (2014). 3 - Corrosion inhibition with rare earth metal compounds in aqueous solutions. In M. Forsyth & B. B. T.-R. E.-B. C. I. Hinton (Eds.), *Woodhead Publishing Series in Metals and Surface Engineering* (pp. 84–116). Woodhead Publishing. https://doi.org/https://doi.org/10.1533/9780857093 585.84

Ding, R., Li, W., Wang, X., Gui, T., Li, B., Han, P., ... & Song, L. (2018). A brief review of corrosion protective films and coatings based on graphene and graphene oxide. *Journal of Alloys and Compounds*, *764*, 1039-1055.

Divine, S. (2016). Guadalajara sewer explosion. Lama University. Mexico.

Dodds, P. C., Williams, G., & Radcliffe, J. (2017). Chromate-Free Smart Release Corrosion Inhibitive Pigments Containing Cations. *Prog. Org. Coat.*, *102*.

Dou, B., Xiao, H., Lin, X., Zhang, Y., Zhao, S., Duan, S., ... & Fang, Z. (2021). Investigation of the anti-corrosion properties of fluorinated graphene-modified waterborne epoxy coatings for carbon steel. *Coatings*, *11*(2), 254.

Du Plessis, E., Granados, G. M., Barnes, I., Ho, W. H., Alexander, B. J. R., Roux, J., & McTaggart, A. R. (2019). The pandemic strain of Austropucciniapsidii causes myrtle rust in New Zealand and Singapore. *Australasian Plant Pathology*, *48*(3), 253-256.

Ebenso, E. E., Eddy, N. O., &Odiongenyi, A. O. (2008). Corrosion inhibitive properties and adsorption behaviour of ethanol extract of Piper guinensis as a green corrosion inhibitor for mild steel in H_2SO_4. *African Journal of Pure and Applied Chemistry*, *2*(11), 107-115.

Eddy, N. O. (2009). Ethanol extract of Phyllanthus amarus as a green inhibitor for the corrosion of mild steel in H2SO4. *PortugaliaeElectrochimica Acta*, *27*(5), 579-589.

Efunda engineering fundamentals (n.d). Retrieved from https//: www.efunda.com

Ekuma, C, E. &Idenyi, N, E. (2007). Statistical Analysis of the Influence of Environment on Prediction of Corrosion from its Parameters. *Research Journal of Physics, 1: 27-34.*

el Hajjaji, F, S., R, M., M, H., B, C., DS, A., & SM, Q. M. (2019). El Hajjaji, F, Salim, R, Messali, M, Hammouti, B, Chauhan, DS, Almutairi, SM, Quraishi, MA, "Electrochemical Studies on New Pyridazinium Derivatives as Corrosion Inhibitors of Carbon Steel in Acidic Medium." J. Bio- Tribo-Corrosion, 5 (1). In *Bio- Tribo - Corrosion* (Vol. 5, Issue 1).

Eliyan, F. F., &Alfantazi, A. (2013). Corrosion of the Heat-Affected Zones (HAZs) of API-X100 pipeline steel in dilute bicarbonate solutions at 90 C–An electrochemical evaluation. *Corrosion science*, *74*, 297-307.

Etteyeb, N., &Nóvoa, X. R. (2016). Inhibition Effect of Some Trees Cultivated in Arid Regions Against the Corrosion of Steel Reinforcement in Alkaline Chloride Solution. *Corros. Sci.*, *112*.

EVANS, U.R., 1948. An Introduction to Metallic Corrosion. Edward Arnold, London.

Farag, A. A., Migahed, M. A., &Badr, E. A. (2019). "Thiazole Ionic Liquid as Corrosion Inhibitor of Steel in 1 M HCl Solution: Gravimetrical, Electrochemical, and Theoretical Studies. *J. Bio- Tribo-Corrosion*, *5*.

Fateh, A., Aliofkhazraei, M., &Rezvanian, A. R. (2020). Review of Corrosive Environments for Copper and Its Corrosion Inhibitors. *Arab. J. Chem.*, *13*.

Feng, Y., & Cheng, Y. F. (2017). An Intelligent Coating Doped with Inhibitor-Encapsulated Nanocontainers for Corrosion Protection of Pipeline Steel. *Chem. Eng. J.*, *315*.

Fiedler, S., Vepraskas, M. J., & Richardson, J. L. (2007). Soil redox potential: importance, field measurements, and observations. *Advances in agronomy*, *94*, 1-54.

Findlay, S. J., & Harrison, N. D. (2002). Why aircraft fail. *Materials today*, *5*(11), 18-25.

Fonseca D., Tagliari M. R., Guaglianoni W. C., Tamborim S. M., Borges M. F. (2024). Carbon Dioxide Corrosion Mechanisms: Historical Development and Key Parameters of CO_2-H_2O Systems. *International Journal of Corrosion*. Volume 2024, Issue 1. Jan 2024. https://doi.org/10.1155/2024/5537767

Fontana, M. G & Staehle, R, W. (2013). Advances in corrosion Science and technology. Springer, New York.

Frankel, G.S. (2016). Fundamentals of Corrosion Kinetics. In: Hughes, A., Mol, J., Zheludkevich, M., Buchheit, R. (eds) Active Protective Coatings. Springer Series in Materials Science, vol 233. Springer, Dordrecht. https://doi.org/10.1007/978-94-017-7540-3_2

FRM. (1941). Robert Boyle, 1627-1691.

Fu, J., Zhang, T. F., Xia, Q., Lim, S. H., Wan, Z., Lee, T. W., & Kim, K. H. (2015). Oxidation and corrosion behavior of nanolaminated MAX-phase Ti2AlC film synthesized by high-power impulse magnetron sputtering and annealing. *Journal of Nanomaterials*, *2015*.

Gaines, R. H. (1910). Bacterial Activity as a Corrosive Influence in the Soil. *Industrial & Engineering Chemistry*, *2*(4), 128-130.

Gan, M. (2023). Corrosion Control (III): Corrosion Inhibitors. In *Corrosion in CO2 Capture, Transportation, Geological Utilization and Storage*; Zhang, L., Ed.; Engineering Materials; Springer Nature Singapore: Singapore; pp 111–130. https://doi.org/10.1007/978-981-9 9-2392-2_7

Gangopadhyay, S., &Mahanwar, P. A. (2018). Recent Developments in the Volatile Corrosion Inhibitor (VCI) Coatings for Metal: A Review. *J. Coat. Technol. Res.*, *15*.

Gao, B., Dong, L., Zhu, G., Gao, C., & Tu, G. (2018). Effect of Corrosion Inhibitors on Chromate-Free Passivation of Hot-Dip Galvanized Steel. *Medziagotyra*, *24*.

Gao, H., Li, Q., Chen, F. N., Dai, Y., Luo, F., & Li, L. Q. (2011). Study of the Corrosion Inhibition Effect of Sodium Silicate on AZ91D Magnesium Alloy. *Corros. Sci.*, *53*.

Gesmundo, F. (1992). The corrosion behavior of Ni-Mo alloys in a H sub 2/H sub 2 O/H sub 2 S gas mixture. *Oxidation of Metals;(United States)*, *37*.

Gharbi, O., Thomas, S., Smith, C., &Birbilis, N. (2018). Chromate replacement: what does the future hold? *Npj Materials Degradation*, *2*(1), 1–8.

Giridhar, G., Manepalli, R. K. N. R., & Apparao, G. Chapter 8 - Contact Angle Measurement Techniques for Nanomaterials. In *Thermal and Rheological Measurement Techniques for Nanomaterials Characterization*;

Gobara, M., Baraka, A., Akid, R., &Zorainy, M. (2020). Corrosion Protection Mechanism of Ce4+/Organic Inhibitor for AA2024 in 3.5% NaCl. *RSC Adv.*, *10*.

Goff, A., Aukarasereenont, P., Nguyen, C. K., Grant, R., Syed, N., Zavabeti, A., ... &Daeneke, T. (2021). An exploration into two-dimensional metal oxides, and other 2D materials, synthesised via liquid metal printing and transfer techniques. *Dalton Transactions*, *50*(22), 7513-7526.

Gopiraman, M., Selvakumaran, N., Kesavan, D., &Karvembu, R. (2012). Adsorption and Corrosion Inhibition Behaviour of N-(Phenylcarbamothioyl) Benzamide on Mild Steel in Acidic Medium. *Prog. Org. Coat.*, *73*.

Gorobez, J., Maack, B., &Nilius, N. (2021). Growth of Self-Passivating Oxide Layers on Aluminum—Pressure and Temperature Dependence. *physica status solidi (b)*, *258*(5), 2000559.

Gowraraju, N. D., Jagadeesan, S., Ayyasamy, K., Olasunkanmi, L. O., Ebenso, E. E., & Subramanian, C. (2017). Adsorption Characteristics of Iota-Carrageenan and Inulin Biopolymers as Potential Corrosion Inhibitors at Mild Steel/Sulphuric Acid Interface. *J. Mol. Liq.*, *232*.

Griffiths, O. (2002). Need, greed, and protest in Japan's black market, 1938-1949. *Journal of Social History*, 825-858.

GUNDRY, R., 1993 (Editor). Corrosion 93. A 50-year History of Corrosion Prevention and Control. NACE.

Guo, L., Qi, C., Zheng, X., Zhang, R., Shen, X., & Kaya, S. (2017). Toward Understanding the Adsorption Mechanism of Large Size Organic Corrosion Inhibitors on an Fe(110) Surface Using the DFTB Method. *RSC Adv.*, *7*.

Guo, L., Tan, J., Kaya, S., Leng, S., Li, Q., & Zhang, F. (2020a). Multidimensional Insights into the Corrosion Inhibition of 3,3-Dithiodipropionic Acid on Q235 Steel in H2SO4 Medium: A Combined Experimental and In Silico Investigation. *J. Colloid Interface Sci.*, *570*.

Guo, L., Zhang, R., Tan, B., Li, W., Liu, H., & Wu, S. (2020b). Locust Bean Gum as a Green and Novel Corrosion Inhibitor for Q235 Steel in 0.5 M H2SO4 Medium. *J. Mol. Liq., 310*.

Guo, S., Si, R., Dai, Q., You, Z., Ma, Y., & Wang, J. (2019). A Critical Review of Corrosion Development and Rust Removal Techniques on the Structural/Environmental Performance of Corroded Steel Bridges. *J. Clean. Prod., 233*.

Guo, Z., Xing, R., Liu, S., Zhong, Z., Ji, X., Wang, L & Li, P. (2007). Antifungal Properties of Schiff Bases of Chitosan, N-Substituted Chitosan and Quaternized Chitosan. *Carbohydrate Research***2007**, *342* (10), 1329–1332. https://doi.org/10.1016/ j.carre s.2007.04.006

HABASHI, F. (2019). History of Corrosion Research. CIM Bulletin, Quebec, Canada

Habeeb, H. J., Luaibi, H. M., Dakhil, R. M., Kadhum, A. A. H., Al-Amiery, A. A., &Gaaz, T. S. (2018). Development of New Corrosion Inhibitor Tested on Mild Steel Supported by Electrochemical Study. *Results Phys., 8*.

HACHE, A. La Corrosion des Métaux. Presses Universitaires de France

Haddadi, S. A., Ramazani, S. A. A., Mahdavian, M., Taheri, P., & Mol, J. M. C. (2018). Fabrication and Characterization of Graphene-Based Carbon Hollow Spheres for Encapsulation of Organic Corrosion Inhibitors. *Chem. Eng. J., 352*.

Hamadi, L., Mansouri, S., Oulmi, K., &Kareche, A. (2018). The Use of Amino Acids as Corrosion Inhibitors for Metals: A Review. *Egypt. J. Pet., 27*.

Han, J., Zhang, J., & Carey, J. W. (2011). Effect of bicarbonate on corrosion of carbon steel in CO2 saturated brines. *International Journal of Greenhouse Gas Control*, *5*(6), 1680-1683.

Hao, Y., Liu, F., Han, E., Anjum, S., & Xu, G. (2013). The Mechanism of Inhibition by Zinc Phosphate in an Epoxy Coating. *Corros. Sci., 69*.

Hart, E. (2016). Corrosion inhibitors: Principles, mechanisms and applications. In *Corrosion Inhibitors: Principles, Mechanisms and Applications*. Nova Science Publishers, Inc. https://doi.org/10.5772/57255

Hartley, H. B. (1960). The Wilkins Lecture-Sir Humphry Davy, Bt., PRS 1778–1829. *Proceedings of the Royal Society of London. Series A. Mathematical and Physical Sciences*, *255*(1281), 153-180.

Haruna, K., & Saleh, T. A. (2019). Cyclodextrin-Based Functionalized Graphene Oxide as an Effective Corrosion Inhibitor for Carbon Steel in Acidic Environment. *Prog. Org. Coat., 128*.

Harvey, T. J., Walsh, F. C., &Nahlé, A. H. (2018). A Review of Inhibitors for the Corrosion of Transition Metals in Aqueous Acids. *J. Mol. Liq., 266*.

Heakal, F. E. T., &Elkholy, A. E. (2017). Gemini surfactants as corrosion inhibitors for carbon steel. *Journal of Molecular Liquids*, *230*, 395-407.

Hemant, M. (2019). The fact factor, https://thefactfactor.com/#google_vignette

Hermas, A. E. A., Elnady, A. M., & Ali, R. M. (2019). Corrosion Inhibition of Stainless Steel in Sulfuric Acid Solution Containing Sulfide Ions. *Anti-Corrosion Methods Mater.*, *66*.

Hihara, L. (2015). Hihara, LH, "Electrochemical Aspects of Corrosion-Control Coatings." In: Intelligent Coatings for Corrosion Control, pp. 1–15. Elsevier Inc., 2015. In *"Electrochemical Aspects of Corrosion-Control Coatings" In: Intelligent Coatings for Corrosion Control* (pp. 1–15).

HINTON, B. R. W., Arnott, D. R., & Ryan, N. E. (1984). The inhibition of aluminium alloy corrosion by cerous cations. *Metals Forum*, *7*(4), 211–217.

Holmes, R. M., &Surman, D. J. (1989). *XPS and Auger investigation of mechanisms affecting corrosion inhibition of metals*. Houston, TX (USA); National Assoc. of Corrosion Engineers.

HooshmandZaferani, S., Sharifi, M., Zaarei, D., &Shishesaz, M. R. (2013). Application of Eco-Friendly Products as Corrosion Inhibitors for Metals in Acid Pickling Processes - A Review. *J. Environ. Chem. Eng.*, *1*.

Hou, B, Li, X, Ma, X, Du, C, Zhang, D, Zheng, M, Xu, W, Lu, D, &Ma, F, "The Cost of Corrosion in China," npj Mater. Degrad., 1 (1) (2017). (n.d.).

Hu, T., Shi, H., Wei, T., Liu, F., Fan, S., & Han, E. (2015). Cerium Tartrate as a Corrosion Inhibitor for AA 2024–T3. *Corros. Sci.*, *95*.

Huang, H., Wang, Z., Gong, Y., Gao, F., & Luo, Z. (2017). Water Soluble Corrosion Inhibitors for Copper in 3.5 wt % Sodium Chloride Solution. *Corros. Sci.*, *123*.

Huang, J., Lister, D., & Uchida, S. (2020). The Corrosion of Aluminum Alloy and Release of Hydrogen in Nuclear Reactor Emergency Core Coolant: Implications for Deflagration and Explosion Risk. *Nucl. Eng. Des.*, *359*.

Hubbell, M., Price, C., &Heidersbach, R. (1985). Crevice and pitting corrosion tests for stainless steels: A comparison of short-term tests with longer exposures. *Laboratory corrosion tests and standards, ASTM STP*, *866*, 324-336.

Imai, T., Shiraishi, S., Saitô, H., &Otagiri, M. (1991). Interaction of Indomethacin with Low Molecular Weight Chitosan, and Improvements of Some Pharmaceutical Properties of Indomethacin by Low Molecular Weight Chitosans, *International Journal of Pharmaceutics*, *67* (1), 11–20. https://doi.org/10.1016/0378-5173(91)90260-U

Ismail, A. I. M., & El-Shamy, A. M. (2009). Engineering behaviour of soil materials on the corrosion of mild steel. *Applied clay science*, *42*(3-4), 356-362.

Izadi, M., Mohammadi, I., Shahrabi, T., &Ramezanzadeh, B. (2019a). Corrosion Inhibition Performance of Novel Eco-Friendly Nanoreservoirs as Bi-Component Active System on Mild Steel in Aqueous Chloride Solution. *J. Taiwan Inst. Chem. Eng.*, *95*.

Izadi, M., Shahrabi, T., Mohammadi, I., &Ramezanzadeh, B. (2019a). Synthesis of Impregnated Na+ - Montmorillonite as an Eco-Friendly Inhibitive Carrier and Its Subsequent Protective Effect on Silane Coated Mild Steel. *Prog. Org. Coat.*, *135*.

Jacobs, R. L. (2011). "Developing a Research Problem and Purpose Statement", ***In the*** Handbook of Scholarly Writing and Publishing**,** T. S. Rocco and T. Hatcher (eds.), San Francisco: Jossey-Bass, pp. 125–141

Jafari, H., Akbarzade, K., &Danaee, I. (2019). Corrosion Inhibition of Carbon Steel Immersed in a 1 M HCl Solution Using Benzothiazole Derivatives. *Arab. J. Chem.*, *12*.

JafarMazumder, M. A. (2020). A review of green scale inhibitors: Process, types, mechanism and properties. In *Coatings* (Vol. 10, Issue 10, pp. 1–29). MDPI AG. https://doi.org/10.3390/coatings10100928

Javaherdashti, R. E. Z. A. (2016, September). Corrosion knowledge management for managers. In *NACE International Corrosion Conference Proceedings* (Vol. 55, pp. 945-950).

Jeannin, M., Calonnec, D., Sabot, R., &Refait, P. (2010). Role of a clay sediment deposit on the corrosion of carbon steel in 0.5 mol L− 1 NaCl solutions. *Corrosion Science*, *52*(6), 2026-2034.

Jing, C., Wang, Z., Gong, Y., Huang, H., Ma, Y., &Xie, H. (2018). Photo and Thermally Stable Branched Corrosion Inhibitors Containing Two Benzotriazole Groups for Copper in 3.5 wt % Sodium Chloride Solution. *Corros. Sci.*, *138*.

Jones, D. (1992). Principles and prevention of corrosion. *Macmillan Publishing Company (USA)*, *1992*,568.

Kaco, H., Talib, N. A. A., Zakaria, S., Jaafar, S. N. S., Othman, N. K., Chia, C. H., & Gan, S. (2018). Enhanced corrosion inhibition using purified tannin in HCl medium. *Malaysian Journal of Analytical Sciences*, *22*(6), 931-942.

Kaczerewska, O., Leiva-Garcia, R., Akid, R., Brycki, B., Kowalczyk. I & Pospieszny, T. (2018). Effectiveness of O -Bridged Cationic Gemini Surfactants as Corrosion Inhibitors for Stainless Steel in 3 M HCl: Experimental and Theoretical Studies, *Journal of Molecular Liquids*, *249*, 1113–1124. https://doi.org/10.1016/j.molliq.2017.11.142

Kadhim, A., Al-Okbi, A. K., Jamil, D. M., Qussay, A., Al-Amiery, A. A., Gaaz, T. S., Kadhum, A. A. H., Mohamad, A. B., & Nassir, M. H. (2017). Experimental and Theoretical Studies of Benzoxazines Corrosion Inhibitors. *Results Phys.*, *7*.

Kalajahi, S. T., Mofradnia, S. R., Yazdian, F., Rasekh, B., Neshati, J., Taghavi, L., Pourmadadi, M., &Haghirosadat, B. F. (2022). Inhibition performances of graphene oxide/silver nanostructure for the microbial corrosion: molecular dynamic simulation study. *Environmental Science and Pollution Research*.

Kamburova, K.; Boshkova, N.; Boshkov, N.; Atanassova, G &Radeva, T. (2018). Hybrid Zinc Coatings for Corrosion Protection of Steel Using Polyelectrolyte

Nanocontainers Loaded with Benzotriazole. *Colloids and Surfaces A: Physicochemical and Engineering Aspects***2018**, *559*, 243–250.

Kaushal, V.& Najafi, M. (2021). Microbiologically influenced corrosion of concrete in sanitary sewers: Processes and control mechanisms, in Proceedings of the 1st Corrosion and Materials Degradation Web Conference, 17–19, MDPI: Basel, Switzerland, doi:10.3390/CMDWC2021-09931

Keyvani, A., Yeganeh, M., &Rezaeyan, H. (2017). Application of Mesoporous Silica Nanocontainers as an Intelligent Host of Molybdate Corrosion Inhibitor Embedded in the Epoxy Coated Steel. *Prog. Nat. Sci. Mater. Int., 27*.

Khanna, A. S. (2002). *Introduction to high temperature oxidation and corrosion*. ASM international.

Khanna, A. S. (2012). Indian Initiatives for Corrosion Protection. *Green Corrosion Chemistry and Engineering*.

Kim, K. T., Kim, H. W., Chang, H. Y., Lim, B. T., Park, H. B., & Kim, Y. S. (2015). Corrosion Inhibiting Mechanism of Nitrite Ion on the Passivation of Carbon Steel and Ductile Cast Iron for Nuclear Power Plants. *Adv. Mater. Sci. Eng., 2015*.

King, A. D., & Scully, J. R. (2011). Sacrificial anode-based galvanic and barrier corrosion protection of 2024-T351 by a Mg-rich primer and development of test methods for remaining life assessment. *Corrosion*, *67*(5), 055004-1.

Kofstad, P. (1989). Fundamental aspects of corrosion by hot gases. *Materials Science and Engineering: A*, *120*, 25-29.

Koleva, D., Boshkov, N., Raichevski, G., &Veleva, L. (2005). Electrochemical corrosion behaviour and surface morphology of electrodeposited zinc, zinc–cobalt and their composite coatings. *Transactions of the IMF*, *83*(4), 188-193.

Kulakovskaya, T. v, Vagabov, V. M., &Kulaev, I. S. (2012). Inorganic Polyphosphate in Industry, Agriculture and Medicine: Modern State and Outlook. *Process Biochem.*, *47*.

Laboureur, D., Glabeke, G., &Gouriet, J. B. (2021). Validation of Cabrera-Mott model for low-temperature oxidation of aluminum nanoparticles. *Journal of Nanoparticle Research*, *23*(3), 1-11.C

Lafront, A. M., Safizadeh, F., Ghali, E., &Houlachi, G. (2010). Study of the copper anode passivation by electrochemical noise analysis using spectral and wavelet transforms. *Electrochimica acta*, *55*(7), 2505-2512.

Lai, C., Xie, B., Zou, L., Zheng, X., Ma, X., & Zhu, S. (2017). Adsorption and Corrosion Inhibition of Mild Steel in Hydrochloric Acid Solution by S-Allyl-O, O′-Dialkyldithiophosphates. *Results Phys.*, *7*.

Larsen, D. (2023). Libre Texts: Lewis Concept ofAcids andBases(2023,January30) by LibreTexts licensed under CC Y-NC-SA. (https://chem.libretexts.org/@go/page/1282)

Lefrou, C., Fabry, P., &Poignet, J. C. (2012). *Electrochemistry: the basics, with examples*. Springer Science & Business Media.

Lei, Y. H., Sheng, N., Hyono, A., Ueda, M., &Ohtsuka, T. (2014). Effect of Benzotriazole (BTA) Addition on Polypyrrole Film Formation on Copper and Its Corrosion Protection. *Prog. Org. Coat.*, *77*.

Li, D. G., Feng, Y. R., Bai, Z. Q., Zhu, J. W., & Zheng, M. S. (2007). Influence of temperature, chloride ions and chromium element on the electronic property of passive film formed on carbon steel in bicarbonate/carbonate buffer solution. *Electrochimica Acta*, *52*(28), 7877-7884.

Li, L., Mo, S., Qun, H., Jun, Y., Yao, H., & Bing, N. (2017). Relationship between Inhibition Performance of Melamine Derivatives and Molecular Structure for Mild Steel in Acid Solution. *Corros. Sci.*, *124*.

Li, S. Y., Kim, Y. G., Jeon, K. S., Kho, Y. T., & Kang, T. (2001). Microbiologically influenced corrosion of carbon steel exposed to anaerobic soil. *Corrosion*, *57*(9), 815-828.

Li, X., Deng, S., & Fu, H. (2011a). Sodium Molybdate as a Corrosion Inhibitor for Aluminum in H3PO4 Solution. *Corros. Sci.*, *53*.

Li, X., Deng, S., & Fu, H. (2011b). Triazolyl blue tetrazolium bromide as a novel corrosion inhibitor for steel in HCl and H2SO4 solutions. *Corrosion Science*, *53*(1), 302-309.

Likhanova, N. v, Arellanes-Lozada, P., Olivares-Xometl, O., Hernández-Cocoletzi, H., Lijanova, I. v, Arriola-Morales, J., & Castellanos-Aguila, J. E. (2019). Effect of Organic Anions on Ionic Liquids as Corrosion Inhibitors of Steel in Sulfuric Acid Solution. *J. Mol. Liq.*, *279*.

Lin, B., Tang, J., Wang, Y., Wang, H., &Zuo, Y. (2020). Study on Synergistic Corrosion Inhibition Effect between Calcium Lignosulfonate (CLS) and Inorganic Inhibitors on Q235 Carbon Steel in Alkaline Environment with Cl. *Molecules (Basel, Switzerland)*, *25*(18), 4200. https://doi.org/10.3390/molecules25184200

Little, B., Wagner, P., &Mansfeld, F. (1991). Microbiologically influenced corrosion of metals and alloys. *International Materials Reviews*, *36*(1), 253-272.

Liu, H., Haixian, L., &Yuxuan, Z. (2020). Galvanic Corrosion Due to a Heterogeneous Sulfate Reducing Bacteria Biofilm. *Coatings* 10, no. 11: 1116. https://doi.org/10.3390/coatings10111116

Liu, T., & Weyers, R. W. (1998). Modeling the dynamic corrosion process in chloride contaminated concrete structures. *Cement and Concrete research*, *28*(3), 365-379.

Liu, X., Gu, C., Wen, Z., & Hou, B. (2018). Improvement of Active Corrosion Protection of Carbon Steel by Water-Based Epoxy Coating with Smart CeO2 Nanocontainers. *Prog. Org. Coat.*, *115*.

Lopez-Garrity, O., & Frankel, G. S. (2014). Corrosion Inhibition of AA2024-T3 By Sodium Silicate. *Electrochim. Acta*, *130*.

López-Ortega, A., Bayón, R., & Arana, J. L. (2018). Evaluation of Protective Coatings for Offshore Applications. Corrosion and Tribocorrosion Behavior in Synthetic Seawater. *Surf. Coatings Technol.*, *349*.

Lorenson, T.D., Leifer, I., Wong, F.L., Rosenbauer, R.J., Campbell, P.L., Lam, A., Hostettler, F.D., Greinert, J., Finlayson, D.P., Bradley, E.S., &Luyendyk, B.P. (2011). Biomarker chemistry and flux quantification methods for natural petroleum seeps and produced oils, offshore southern California: U.S. Geological Survey Scientific Investigations Report 2011–5210, 45 p., 4 data files and OCS Study BOEM 2011–016, available at http://pubs.usgs.gov/sir/2011/5210/.

Lu, W., Liu, G., Gao, S., Xing, S., & Wang, J. (2008). Tyrosine-assisted preparation of Ag/ZnO nanocomposites with enhanced photocatalytic performance and synergistic antibacterial activities. *Nanotechnology*, *19*(44), 445711.

Luna, M. C., Le, T., Sierra, R. C., Flores, J. V. M., Rojas, L. L., & Estrada, E. M. A. (2019). Study of Corrosion Behavior of API 5L X52 Steel in Sulfuric Acid in the Presence of Ionic Liquid 1-Ethyl 3-Methylimidazolium Thiocyanate as Corrosion Inhibitor. *J. Mol. Liq.*, *289*.

LYNES, W., 1951. Some historical developments relating to corrosion. Journal of the Electrochemical Society, 98C, p. 3-10.

Ma, I. A. W., Ammar, S., Bashir, S., Selvaraj, M., Assiri, M. A., Ramesh, K., & Ramesh, S. (2020). Preparation of Hybrid Chitosan/Silica Composites via Ionotropic Gelation and Its Electrochemical Impedance Studies. *Prog. Org. Coat.*, *145*.

Ma, I. A. W., Ammar, Sh., Kumar, S. S. A., Ramesh, K., & Ramesh, S. (2022a). A concise review on corrosion inhibitors: types, mechanisms and electrochemical evaluation studies. *Journal of Coatings Technology and Research*, *19*(1), 241–268. https://doi.org/10.1007/s11998-021-00547-0

Ma, L., Zhang, C., Wu, Y., & Lu, Y. (2022b). Comparative review of different influence factors on molten salt corrosion characteristics for thermal energy storage. *Solar Energy Materials and Solar Cells*, *235*, 111485.

Ma, Q., Qi, S., He, X., Tang, Y., & Lu, G. (2017). 1, 2, 3-Triazole Derivatives as Corrosion Inhibitors for Mild Steel in Acidic Medium: Experimental and Computational Chemistry Studies. *Corros. Sci.*, *129*.

Machado, C., Alvarez, L. X., Escarpini, N., Maldonado, A. C., & Ariel, E. (2019). Green Synthesis of 1-Benzyl-4-Phenyl-1 H -1, 2, 3-Triazole, Its Application as Corrosion Inhibitor for Mild Steel in Acidic Medium and New Approach of Classical Electrochemical Analyses. *Corros. Sci.*, *149*.

MacKAY, R.J. & WORTHINGTON, R. (1936). Corrosion Resistance of Metals and Alloys. Reinhold, New York.

MacMillan, J. C., Morrison, P. J., Nevin, N. C., Shaw, D. J., Harper, P. S., Quarrell, O. W., & Snell, R. G. (1993). Identification of an expanded CAG repeat in the Huntington's disease gene (IT15) in a family reported to have benign hereditary chorea. *Journal of medical genetics*, *30*(12), 1012-1013.

Markley, T., Blin, F., Forsyth, M., & Hinton, B. (2014). *[Multifunctional rare earth organic corrosion inhibitors], in Rare Earth-Based Corros*. Woodhead Publishing Limited.

Marti, M., Fabregat, G., Azambuja, D. S., Aleman, C., & Armelin, E. (2012). Evaluation of an environmentally friendly anticorrosive pigment for alkyd primer. *Progress in Organic Coatings*, *73*(4), 321-329.

Maruthamuthu, S., Nagendran, T., Anandkumar, B., Karthikeyan, M. S., Palaniswamy, N., & Narayanan, G. (2011). Microbiologically influenced corrosion on rails. *Current Science*, *100*(6), 870-880.

Marzorati, S, Verotta, L, &Trasatti, SP, "Green Corrosion Inhibitors from Natural Sources and Biomass Wastes." Molecules, 24 (1) (2019). (n.d.).

Matter, E. A., Kozhukharov, S., Machkova, M., &Kozhukharov, V. (2012). Comparison Between the Inhibition Efficiencies of Ce(III) and Ce(IV) Ammonium Nitrates Against Corrosion of AA2024 Aluminum Alloy in Solutions of Low Chloride Concentration. *Corros. Sci., 62*.

Mehanna, M., Basseguy, R., Delia, M. L., &Bergel, A. (2009). Role of direct microbial electron transfer in corrosion of steels. *Electrochemistry communications*, *11*(3), 568-571.

Miklas, P. N., Pastor-Corrales, M. A., Jung, G., Coyne, D. P., Kelly, J. D., McClean, P. E., &Gepts, P. (2002). Comprehensive linkage map of bean rust resistance genes. *ANNUAL REPORT-BEAN IMPROVEMENT COOPERATIVE*, *45*, 125-129.

Miles, D.A. (2017). A Taxonomy of Research Gaps: Identifying and Defining the Seven Research Gaps, Doctoral Student Workshop: Finding Research Gaps – Research Methods and Strategies, Dallas, Texas, 2017

Miley, H. A. (1942). Theory of oxidation and tarnishing of metals: I. The linear, parabolic and logarithmic laws. *Transactions of The Electrochemical Society*, *81*(1), 391.

Miller, D. (1990). Corrosion Control on Aging Aircraft: What is being done ?, Materials Performance, pp.10-11

Miller, J. W. (1990). Chloride removal and corrosion protection of reinforced concrete. *VTI Rapport*, (352A).

Milo, I., &Kokalj, A. (2017). How Relevant Is the Adsorption Bonding of Imidazoles and Triazoles for Their Corrosion Inhibition of Copper? *Corros. Sci., 124*.

Mir, S. H., Nagahara, L. A., Thundat, T., Mokarian-Tabari, P., Furukawa, H., & Khosla, A. (2018). Review—Organic-Inorganic Hybrid Functional Materials: An Integrated Platform for Applied Technologies. *J. Electrochem. Soc., 165*.

Mobin, M., Basik, M., &Shoeb, M. (2019). A Novel Organic-Inorganic Hybrid Complex Based on CissusQuadrangularis Plant Extract and Zirconium Acetate as a Green Inhibitor for Mild Steel in 1 M HCl Solution. *Appl. Surf. Sci.*, *469*.

Mohamed, K. E. M., Ibrahim, O. H., El-Bedawy, M. E., & Ali, A. H. (2020). Synergistic Effect of Different Zn Salts with Sodium Octanoate on the Corrosion Inhibition of Carbon Steel in Cooling Water. *J. Radiat. Res. Appl. Sci.*, *13*.

Molina, F. J., Alonso, C., & Andrade, C. (1993). Cover cracking as a function of rebar corrosion: Part 2—Numerical model. *Materials and structures*, *26*(9), 532-548.

Montemor, M. F., & Ferreira, M. G. S. (2007). Cerium salt activated nanoparticles as fillers for silane films: Evaluation of the corrosion inhibition performance on galvanised steel substrates. *Electrochimica Acta*, *52*(24), 6976-6987.

Montemor, MF. (2016). "Hybrid Nanocontainer-Based Smart Self-Healing Composite Coatings for the Protection of Metallic Assets." In: Smart Composite Coatings and Membranes Transport, Structural, Environmental and Energy Applications. Elsevier Ltd. (n.d.).

Morinaga, S. (1988). Prediction of service lives of reinforced concrete buildings based on rate of corrosion of reinforcing steel. *Special report of institute of technology, Shimizu corporation*, *23*.

Morozov, Y., Calado, L. M., Shakoor, R. A., Raj, R., Kahraman, R., &Taryba, M. G. (2019). Epoxy Coatings Modified with a New Cerium Phosphate Inhibitor for Smart Corrosion Protection of Steel. *Corros. Sci.*, *159*.

Morsch, S., Emad, S., Farren, L. A., Goodall, M. D., Lyon, S. B., & Gibbon, S. R. (2018). The Unexpected Role of Carbonate Impurities in Polyphosphate Corrosion Inhibition. *Sci. Rep.*, *8*.

Mouanga, M., Andreatta, F., Druart, M., Marin, E., Fedrizzi, L., Olivier, M., & Al, A. (2015). A Localized Approach to Study the Effect of Cerium Salts as Cathodic Inhibitor on Iron/Aluminum Galvanic Coupling. *Corros. Sci.*, *90*.

Mu, G. N., Li, X., & Li, F. (2004). Synergistic inhibition between o-phenanthroline and chloride ion on cold rolled steel corrosion in phosphoric acid. *Materials Chemistry and Physics*, *86*(1), 59-68.

Müller, W. (1927). I. übereineeigenartigedoppelseitigeVeränderung des Osnaviculare pedis beimErwachsenen. *Deutsche ZeitschriftFürChirurgie*, *201*(1), 84-89.

Müller-Bloch, C. & Kranz, J., (2014). A Framework for Rigorously Identifying Research Gaps in Qualitative Literature Reviews, The Thirty Sixth International Conference on Information Systems, Fort Worth2015, pp. 1–19

Munis, A., Zhao, T., Zheng, M., Ur, A., & Wang, F. (2020). A Newly Synthesized Green Corrosion Inhibitor Imidazoline Derivative for Carbon Steel in 7.5% NH4Cl Solution. *Sustain. Chem. Pharm.*, *16*.

Muster, T. H., Sullivan, H., Lau, D., Alexander, D. L. J., Sherman, N., Garcia, S. J., Harvey, T. G., Markley, T. A., & Hughes, A. E. (2012). A Combinatorial Matrix of Rare Earth Chloride Mixtures as Corrosion Inhibitors of AA2024-T3: Optimisation Using PotentiodynamicPolarisation and EIS. *Electrochim. Acta, 67*.

Naderi, R., & Attar, M. M. (2008). Electrochemical Assessing Corrosion Inhibiting Effects of Zinc Aluminum Polyphosphate (ZAPP) as a Modified Zinc Phosphate Pigment. *Electrochim. Acta, 53*.

Naderi, R., Mahdavian, M., & Attar, M. M. (2009). Electrochemical Behavior of Organic and Inorganic Complexes of Zn (II) as Corrosion Inhibitors for Mild Steel: Solution Phase Study. *Electrochim. Acta, 54*.

National Oceanic and Atmospheric Administration. (2023, March 28). *Seawater*. https://www.noaa.gov/jetstream/ocean/sea-water

National Transport Safety Board. (2023). Public Inquiries Section, RE-51 490 L' Enfant Plaza, S. W Washington, DC 20594 (800) 877- 6799 or (202) 314-6551

Nazeer, A. A., &Madkour, M. (2018). Potential Use of Smart Coatings for Corrosion Protection of Metals and Alloys: A Review. *J. Mol. Liq., 253*.

Neff, D., Bellot-Gurlet, L., Dillmann, P., Reguer, S., & Legrand, L. (2006). Raman imaging of ancient rust scales on archaeological iron artefacts for long-term atmospheric corrosion mechanisms study. *Journal of Raman Spectroscopy: An International Journal for Original Work in all Aspects of Raman Spectroscopy, Including Higher Order Processes, and also Brillouin and Rayleigh Scattering*, *37*(10), 1228-1237.

Ngobiri, N. C. (2019). Comparative Study on the Inhibitive Effect of Sulfadoxine – Pyrimethamine and an Industrial Inhibitor on the Corrosion of Pipeline Steel in Petroleum Pipeline Water. *Arab. J. Chem., 12*.

Noor, N. M., Ozman, N. A. N., & Yahaya, N. O. R. D. I. N. (2011). Deterministic prediction of corroding pipeline remaining strength in marine environment using DNV RP-F101 (Part A). *Journal of Sustainability Science and Management*, *6*(1), 69-78.

Oguzie, E. E., Okolue, B. N., Ebenso, E. E., Onuoha, G. N., &Onuchukwu, A. I. (2004). Evaluation of the inhibitory effect of methylene blue dye on the corrosion of aluminium in hydrochloric acid. *Materials Chemistry and Physics*, *87*(2-3), 394-401.

Oguzie, E., Akalezi, C., &Enenebeaku, C. (2009). Inhibitive effect of methyl green dye on the corrosion of low carbon steel in acidic media. *Pigment & Resin Technology*.

Olasunkanmi, L. O., &Ebenso, E. E. (2020). Experimental and Computational Studies on Propanone Derivatives of Quinoxalin-6-Yl-4, 5-Dihydropyrazole as Inhibitors of Mild Steel Corrosion in Hydrochloric Acid. *J. Colloid Interface Sci., 561*.

Onyeachu, I. B., Bassey, I., Sorour, A. A., & Abdul-rashid, M. I. (2019). Green Corrosion Inhibitor for Oil Field Application I: Electrochemical Assessment of 2- (2-

Pyridyl) Benzimidazole for API X60 Steel under Sweet Environment in NACE Brine ID196. *Corros. Sci., 150*.

Osella, A., Favetto, A., & López, E. (1998). Currents induced by geomagnetic storms on buried pipelines as a cause of corrosion. *Journal of applied geophysics*, *38*(3), 219-233.

Ostapenko, G. I., Gloukhov, P. A., &Bunev, A. S. (2014). Investigation of 2-Cyclohexenylcyclohexanone as Steel Corrosion Inhibitor and Surfactant in Hydrochloric Acid. *Corros. Sci., 82*.

Othaki, E.P. &Ngobiri, Nnaemeka. (2020). Inhibition of Pipeline Steel Corrosion in 0.5 M H2SO4 Using Cotyledon of ChrysophyllumAlbidum. Journal of Applied Sciences and Environmental Management. 24. 691-697. 10.4314/jasem.v24i4.22.

Othman, M. H., Al-amiery, A. A., Al-majedy, Y. K., Amir, A., Kadhum, H., Bakar, A., & Sumer, T. (2018). Synthesis and Characterization of a Novel Organic Corrosion Inhibitor for Mild Steel in 1 M Hydrochloric Acid. *Results Phys., 8*.

Otieno, M. B., Beushausen, H. D., & Alexander, M. G. (2011). Modelling corrosion propagation in reinforced concrete structures–A critical review. *Cement and Concrete composites*, *33*(2), 240-245.

Ouddai, R., Chabane, H., Boughaba, A., &Frah, M. (2012). The Skikda LNG accident: losses, lessons learned and safety climate assessment. *International journal of global energy issues*, *35*(6), 518-533.

Palmer, J. D. (1989). *Environmental characteristics controlling the soil corrosion of ferrous piping*. ASTM International.

Papavinasam, S. (2011). Corrosion Inhibitors. In *Uhlig's Corrosion Handbook* (pp. 1021–1032). John Wiley & Sons, Ltd. https://doi.org/https://doi.org/10.1002/9780470872864.ch71

Papavinasam, S., & Revie, R. W. (2008). Review of standards for evaluating coatings to control external corrosion of pipelines.

Parker, M., & Peattie, E. G. (1984). *Pipeline Corrosion and Cathodic Protection: A Practical Manual for Corrosion Engineers, Technicians, and Field Personnel*. Gulf Professional Publishing.

Patni, N., Agarwal, S., & Shah, P. (2013). Greener Approach Towards Corrosion Inhibition. *Chin. J. Eng., 2013*.

Payne, K. A. (1999). *The Corrosion of High Temperature Alloys by Molten Glass* (Doctoral dissertation).

Pereira, R. F. D. C., Oliveira, E. S. D. D., Lima, M. A. G. D. A., &Brasil, S. L. D. C. (2015). Corrosion of galvanized steel under different soil moisture contents. *Materials Research*, *18*, 563-568.

Perez, N. (2004). Mixed Potential Theory. In: Perez, N. (eds) Electrochemistry and Corrosion Science. Springer, Boston, MA. https://doi.org/10.1007/1-4020-7860-9_5

PERRIGO, L.D. (Editor), 1993. A History of the Technical Practices Committee and Technical Committees. NACE.

Pezzani, R.; Salehi, B.; Vitalini, S.; Iriti, M.; Zuñiga, F.A.; Sharifi-Rad, J.; Martorell, M. & Martins, N. (2019). Synergistic Effects of Plant Derivatives and Conventional Chemotherapeutic Agents: An Update on the Cancer Perspective. *Medicina , 55*, 110. https://doi.org/10.3390/medicina55040110

Phear, A., Dew, C., Ozsoy, B., Wharmby, N. J., Judge, J., & Barley, A. D. (2005). *Soil nailing-best practice guidance* (No. C637).

Pilling, N. B., &Bedworth, R. E. (1923). Substrate Depletion Analysis and Modeling of the High Temperature Oxidation of Binary Alloys. *Journal of the Institute of Metals, 29*, 529.

Popov, B. N. (2015). *Corrosion engineering: principles and solved problems*. Elsevier.

Popov, BN, Popov, BN, "Chapter 14 – Corrosion Inhibitors." In: Corrosion Engineering, pp. 581–597. 2015. (n.d.).

Portes, E., Gardrat, C., Castellan, A and Coma, V. (2009). Environmentally Friendly Films Based on Chitosan and Tetrahydrocurcuminoid Derivatives Exhibiting Antibacterial and Antioxidative Properties. *Carbohydrate Polymers, 76* (4), 578–584. https://doi.org/10.1016/j.carbpol.2008.11.031

Portevin, A. M., Pretet, E., & Jolivet, H. (1934). Methods for corrosion study of metals and alloys in gases at elevated temperatures and their applications. *Rev. met, 31*, 101-115.

POURBAIX, M. (1945). Thermodynamics of Dilute Solutions with Applications to Electrochemistry and Corrosion. Centre Belged'Etude de la Corrosion, Brussels.

Pour-Ghaz, M., Isgor, O. B., &Ghods, P. (2009). The effect of temperature on the corrosion of steel in concrete. Part 1: Simulated polarization resistance tests and model development. *Corrosion Science*, *51*(2), 415-425.

Pritchard, O., Hallett, S. H., & Farewell, T. S. (2013). Soil corrosivity in the UK–Impacts on Critical Infrastructure. *ITRC–Infrastructure Transition Research Consortium, Cranfield University*.

Punckt, C., Bolscher, M., Rotermund, H. H., Mikhailov, A. S., Organ, L., Budiansky, N…& Hudson, J. L. (2004). Sudden onset of pitting corrosion on stainless steel as a critical phenomenon. *Science*, *305*(5687), 1133-1136.

Qiang, Y., Zhang, S., Tan, B., & Chen, S. (2018). Evaluation of Ginkgo Leaf Extract as an Eco-Friendly Corrosion Inhibitor of X70 Steel in HCl Solution. *Corros. Sci., 133*.

Qiang, Y., Zhang, S., Yan, S., Zou, X., & Chen, S. (2017). Three Indazole Derivatives as Corrosion Inhibitors of Copper in a Neutral Chloride Solution. *Corros. Sci., 126*.

Ralkhal, S., Shahrabi, T., &Ramezanzadeh, B. (2019). Synthesis and Construction of a Highly Potent Hybrid Organic/Inorganic Anti-Corrosive Pigment for Effective Corrosion Control of Mild Steel in Simulated Seawater. *Constr. Build. Mater.*, *222*.

Ramezanzadeh, M., Bahlakeh, G., &Ramezanzadeh, B. (2019a). Adsorption Mechanism and Synergistic Corrosion-Inhibiting Effect between the Green Nettle Leaves Extract and Zn2+ Cations on Carbon Steel. *J. Ind. Eng. Chem.*, *77*.

Ramezanzadeh, M., Bahlakeh, G., &Ramezanzadeh, B. (2019b). Elucidating Detailed Experimental and Fundamental Understandings Concerning the Green Organic-Inorganic Corrosion Inhibiting Molecules onto Steel in Chloride Solution. *J. Mol. Liq.*, *290*.

Rangel, C. M., De Damborenea, J., De Sa, A. I., &Simplicio, M. H. (1992). Zinc and polyphosphates as corrosion inhibitors for zinc in near neutral waters. *British Corrosion Journal*, *27*(3), 207-212.

Raupach, M. (2006). Models for the propagation phase of reinforcement corrosion–an overview. *Materials and Corrosion*, *57*(8), 605-613.

Refait, P., Rahal, C., &Masmoudi, M. (2020). Corrosion Inhibition of Copper in 0.5 M NaCl Solutions by Aqueous and Hydrolysis Acid Extracts of Olive Leaf. *J. Electroanal. Chem.*, *859*.

Rezaee, N., Attar, M. M., &Ramezanzadeh, B. (2013). Studying Corrosion Performance, Microstructure and Adhesion Properties of a Room Temperature Zinc Phosphate Conversion Coating Containing Mn 2 + on Mild Steel. *Surf. Coat. Technol.*, *236*.

Richards, C. A. J., McMurray, H. N., & Williams, G. (2019). Smart-Release Inhibition of Corrosion Driven Organic Coating Failure on Zinc by Cationic Benzotriazole Based Pigments. *Corros. Sci.*, *154*.

Roberge, P. R., &Eng, P. (2005). Corrosion engineering. *Principles and Practice*, *1*.

Rodriguez, J. (1996). Physical and chemical properties of bimetallic surfaces. *Surface Science Reports*, *24*(7-8), 223-287.

Rodriguez, J., Mouanga, M., Roobroeck, A., Cossement, D., Mirisola, A., & Olivier, M. (2018). Study of the Inhibition Ability of Benzotriazole on the Zn-Mg Coated Steel Corrosion in Chloride Electrolyte. *Corros. Sci.*, *132*.

Roy, P., Karfa, P., Adhikari, U., &Sukul, D. (2014). Corrosion inhibition of mild steel in acidic medium by polyacrylamide grafted Guar gum with various grafting percentage: Effect of intramolecular synergism. *Corrosion Science*, *88*, 246-253.

S…& El Gouri, M. (2020b), "Epoxy resin and TiO2 composite as anticorrosive material for carbon steel in 3 % NaCl medium: experimental and computational studies," J Mol Liq317(114249). https:// doi. org/ 10. 1016/j. molliq. 2020. 114249.

Saadawy, M. (2016). Effect of Inorganic Anions on the Pitting Behaviour of Austenitic Stainless Steel 304 in H2SO4 Solution Containing Chloride Ion. *Int. J. Electrochem. Sci., 11*.

Sadeghi, R., Amirnasr, M., Meghdadi, S., &Talebian, M. (2019). Carboxamide Derivatives as New Corrosion Inhibitors for Mild Steel Protection in Hydrochloric Acid Solution. *Corros. Sci., 151*.

Saei, E., Ramezanzadeh, B., Amini, R., &Kalajahi, M. S. (2017). Effects of Combined Organic and Inorganic Corrosion Inhibitors on the Nanostructure Cerium Based Conversion Coating Performance on AZ31 Magnesium Alloy: Morphological and Corrosion Studies. *Corros. Sci., 127*.

Saifi, H, Ouchenane, S, Bourenane, R, Boukerche, S, Joiret, S, &Takenouti, H, "Electrochemical Behavior Investigation of Cysteine on Nickel Corrosion in Acidic Medium." J. Fail. Anal. Prev., (2019). (n.d.).

Saifi, H., Bernard, M. C., Joiret, S., Rahmouni, K., Takenouti, H., &Talhi, B. (2010). Corrosion inhibitive action of cysteine on Cu–30Ni alloy in aerated 0.5 M H2SO4. *Materials Chemistry and Physics*, *120*(2-3), 661-669.

Salazar-bravo, P., Ángel-lópez, D. D. e. l., Torres-huerta, A. M., & Domínguez-crespo, M. A. (2019). Corrosion Investigation of New Hybrid Organic/Inorganic Coatings for Carbon Steel Substrates: Electrochemical and Surface Characterizations. *Prog. Org. Coat., 135*.

Salehi, E., Naderi, R., &Ramezanzadeh, B. (2017). Synthesis and Characterization of an Effective Organic/Inorganic Hybrid Green Corrosion Inhibitive Complex Based on Zinc Acetate/UrticaDioica. *Appl. Surf. Sci., 396*.

Samantara, M. K., Padhi, R. K., Sowmya, M., Kumaran, P., &Satpathy, K. K. (2017). Heavy metal contamination, major ion chemistry and appraisal of the groundwater status in coastal aquifer, Kalpakkam, Tamil Nadu, India. *Groundwater for sustainable development*, *5*, 49-58.

Sanaei, Z., Ramezanzadeh, M., Bahlakeh, G., &Ramezanzadeh, B. (2019). Use of Rosa canina fruit extract as a green corrosion inhibitor for mild steel in 1 M HCl solution: A complementary experimental, molecular dynamics and quantum mechanics investigation. *Journal of industrial and engineering chemistry*, *69*, 18-31.

Sanni, O., Fayomi, O. S. I., & Popoola, A. P. I. (2019, December). Eco-friendly inhibitors for corrosion protection of stainless steel: an overview. In *Journal of physics: conference series* (Vol. 1378, No. 4, p. 042047). IOP Publishing.

Saranya, J., Sowmiya, M., Sounthari, P., Parameswari, K., Chitra, S., &Senthilkumar, K. (2016). N-heterocycles as corrosion inhibitors for mild steel in acid medium. *Journal of Molecular Liquids*, *216*, 42-52.

Sarmiento, E., González-Rodriguez, J. G., Ramirez-Arteaga, A. M., &Uruchurtu, J. (2013). Corrosion Inhibition of 316L Stainless Steel in LiBr+Etileneglycol+H2O by Using Inorganic Inhibitors. *Int. J. Electrochem. Sci., 8*.

Sastri, V. S. (2010). Corrosion Inhibitors: Other Important Applications." In: Cottis, B, Graham, M, Lindsay, R, Lyon, S (eds.) Shreir's Corrosion, pp. 2990–3000. Elsevier(n.d.).

Sastri, V. S., Perumareddi, J. R., Rao, V. R., Rayudu, G. V. S., &Bunzli, J.-C. (2003). *Modern aspects of rare earths and their complexes*. Elsevier.

Satapathy, A. K., Gunasekaran, G., Sahoo, S. C., Amit, K., & Rodrigues, P. v. (2009). Corrosion Inhibition by *Justicia gendarussa* Plant Extract in Hydrochloric Acid Solution. *Corros. Sci., 51*.

Sayin, K., &Karakaş, D. (2013). Quantum chemical studies onsome inorganic corrosion inhibitors. *Corrosion science*, *77*, 37-45.

Schaschl, E., & Marsh, G. A. (1963). The effect of soil conditions on corrosion of steel by oxygen. *Int. Congr. Metallic Corrosion, Trans. 2nd Congr.*, 104.

Sebastian, D. (2016). *Fabrication and Analysis of Super Hydrophobic Metal Surfaces* (Doctoral dissertation, Lamar University-Beaumont).

Sendall, B. C., Kong, G. A., Goulter, K. C., Aitken, E. A. B., Thompson, S. M., Mitchell, J. H. M., ... & Gulya, T. J. (2006). Diversity in the sunflower: Puccinia helianthipathosystem in Australia. *Australasian Plant Pathology*, *35*(6), 657-670.

Shao, Y., Jia, C., Meng, G., Zhang, T., & Wang, F. (2009). The Role of a Zinc Phosphate Pigment in the Corrosion of Scratched Epoxy-Coated Steel. *Corros. Sci., 51*.

Shaw, P., Obot, IB.,&Yadav, M. (2019). Functionalized 2-Hydrazinobenzothiazole with Carbohydrates as a Corrosion Inhibitor: Electrochemical, XPS, DFT and Monte Carlo Simulation Studies. Mater. Chem. Front., 1–10 (2019). (n.d.).

Sheikholeslami, S.; Williams, G.; McMurray, H. N.; Gommans, L.; Morrison, S.; Ngo, S.; Williams, D. E & Gao, W. (2021). Cut-Edge Corrosion Behavior Assessment of Newly Developed Environmental-Friendly Coating Systems Using the Scanning Vibrating Electrode Technique (SVET). *Corrosion Science*, *192*, 109813

Shreir, L. L. (2010). 1.05-Basic Concepts of Corrosion. *Shreir's Corrosion. Oxford: Elsevier*, 89-100.

Sı, G., & Erbil, M. (2016). Assessment of the Inhibition Efficiency of 3, 4-Diaminobenzonitrile Against the Corrosion of Steel. *Corros. Sci., 102*.

Siamphukdee, K., Collins, F., & Zou, R. (2013). Sensitivity analysis of corrosion rate prediction models utilized for reinforced concrete affected by chloride. *Journal of materials engineering and performance*, *22*(6), 1530-1540

Singh, A., Ansari, K. R., Singh, D., Quraishi, M. A., Lgaz, H., & Chung, I. (2020). Comprehensive Investigation of Steel Corrosion Inhibition at Macro/Micro Level by Ecofriendly Green Corrosion Inhibitor in 15% HCl Medium. *J. Colloid Interface Sci., 560*.

Singh, D., Mazumder, M. A. J., Quraishi, M. A., Ansari, K. R., & Suleiman, R. K. (2020). Microwave-Assisted Synthesis of a New Piperonal-Chitosan Schiff Base as a Bio-Inspired Corrosion Inhibitor for Oil-Well Acidizing. *Int. J. Biol. Macromol.*, *158*.

Singh, V., Paul, V. K., & Solanki, S. K. (2022). Feasibility Study of Adaptive Reuse of Old Buildings. *International Journal of Housing and Human Settlement Planning*, *8*(1), 10-31p.

Singla, A. K & Chawla, M. (2010). Chitosan: Some Pharmaceutical and Biological Aspects - an Update. *Journal of Pharmacy and Pharmacology*, *53* (8), 1047–1067. https://doi.org/10.1211/0022357011776441

Soestbergen, M. V. a. n., Baukh, V., Erich, S. J. F., Huinink, H. P., & Adan, O. C. G. (2014). Release of Cerium Dibutylphosphate Corrosion Inhibitors from Highly Filled Epoxy Coating Systems. *Prog. Org. Coat.*, *77*.

Solmaz, R. (2020). Institute of Chemical Engineers Dardagan Fruit Extract as Eco-Friendly Corrosion Inhibitor for Mild Steel in 1 M HCl: Electrochemical and Surface Morphological Studies. *J. Taiwan Inst. Chem. Eng.*, *107*.

Solomon, M. M., Gerengi, H., &Umoren, S. A. (2017a). Carboxymethyl Cellulose/Silver Nanoparticles Composite: Synthesis, Characterization and Application as a Benign Corrosion Inhibitor for St37 Steel in 15% H_2SO_4 Medium. *ACS Appl. Mater. Interfaces*, *9*.

Solomon, M. M., Gerengi, H., Kaya, T., &Umoren, S. A. (2017b). Enhanced Corrosion Inhibition Effect of Chitosan for St37 in 15% H_2SO_4 Environment by Silver Nanoparticles. *Int. J. Biol. Macromol.*, *104*.

Song, Y., Jiang, G., Chen, Y., Zhao, P., & Tian, Y. (2017). Effects of chloride ions on corrosion of ductile iron and carbon steel in soil environments. Scientific Reports, 7(1). https://doi.org/10.1038/s41598-017-07245-1

Song, Y., Liu, J., Wang, H., & Shu, H. (2019). Research Progress of Nitrite Corrosion Inhibitor in Concrete. *Int. J. Corros.*, *2019*.

Soriano, C., &Alfantazi, A. (2016). Corrosion behavior of galvanized steel due to typical soil organics. *Construction and Building Materials*, *102*, 904-912.

Spangberg, D. (2003). Cation Solvation in Water and Acetonitrile from Theoretical Calculations. Acta Universitatis Upsaliensis. Comprehensive Summaries of Uppsala Dissertations from the Faculty of Science and Technology 892. 50pp. Uppsala. ISBN 91-554-5751-7

Stansbury, E. E., & Buchanan, R. A. (2000). *Fundamentals of electrochemical corrosion*. ASM international*Steel, PIM, Stranick, MA, "The Corrosion Inhibition of Metals by Molybdate." Corrosion, 296–302 (1984)*. (n.d.).

Sun, H., Jin, Z., Yang, C., Akkermans, R., Robertson, S., Spenley, N., Miller, S., Todd, S. (2016). COMPASS II: extended coverage for polymer and drug-like molecule databases. *Journal of molecular modeling*. 22. 47. 10.1007/s00894-016-2909-0.

Swain, P. A. (2005). Bernard Courtois (1777-1838) famed for discovering iodine (1811) and his life in Paris from 1798. *Bull. Hist. Chem*, *30*(2), 103.

Synergistic Effect of Imidazoline Derivative and Benzimidazole as Corrosion Inhibitors for Q235 Steel: An Electrochemical, XPS, FT-IR and MD Study. *Arabian Journal for Science and Engineering*, *47*(6), 7123–7134. https://doi.org/10.1007/s13369-021-06540-4

Tamilselvi, M., Kamaraj, P., Arthanareeswari, M., &Devikala, S. (2015). Nano Zinc Phosphate Coatings for Enhanced Corrosion Resistance of Mild Steel. *Appl. Surf. Sci.*, *327*.

Tan, B., Zhang, S., Qiang, Y., Guo, L., Feng, L., Liao, C., Xu, Y., & Chen, S. (2018). A Combined Experimental and Theoretical Study of the Inhibition Effect of Three Disulfide-Based Flavouring Agents for Copper Corrosion in 0.5 M Sulfuric Acid. *J. Colloid Interface Sci.*, *526*.

Tanane, O., Abboud, Y., Aitenneite, H., &Bouari, A. E. l. (2016). Corrosion Inhibition of the 316L Stainless Steel in Sodium Hypochlorite Media by Sodium Silicate. *J. Mater. Environ. Sci.*, *7*.

Tang, Z, "A Review of Corrosion Inhibitors for Rust Preventative Fluids." Curr. Opin. Solid State Mater. Sci., 23 (4) 100759 (2019). (n.d.).

Tao, S., & Huang, H. (2019). Study on Corrosion Inhibition Performance of 1, 2-Dithiolane-3- Pentanoicacid on X65 Steel in 0. 5 M Sulfuric Acid. *Int. J. Electrochem. Sci.*, *14*.

The frontier orbital approach considers Lewis acid-base reactions in terms of the donation of electrons from the base's highest occupied orbital into the acid's lowestunoccupied orbital. (2022, September 27). https://chem.libretexts.org/@go/page/ 162900

Thiel, A., &Luckmann, H. (1928). Studienüber das Indium. III. Abhandlung. *Zeitschriftüranorganische und allgemeineChemie*, *172*(1), 353-371.

Thomas, S., Thomas, R., Zachariah, A. K., Mishra, R. K., (2017). Eds.; Micro and Nano Technologies; Elsevier, pp 173–195. https://doi.org/10.1016/B978-0-323-46139-9.00008-6

Thompson, A. W., & Bernstein, I. M. (1981). Reviews on Coatings and Corrosion 4.

THOMPSON, PE. (1947). The dissolution of gold in cyanide solution. Transactions of Electrochemical Society, 91, p. 41-71

Tiba, C., & De Oliveira, E. M. (2012). Utilization of cathodic protection for transmission towers through photovoltaic generation. *Renewable energy*, *40*(1), 150-156.

TOMASHOV, N.D. (1966). Theory of Corrosion and Protection of Metals. MacMillan, New York.

Trethewey, K. R., & Chamberlain, J. (1995). Corrosion for science and engineering.

Trueman, B. F., Krko, W. H., & Gagnon, G. A. (2018). Effects of Ortho- and Polyphosphates on Lead Speciation in Drinking Water. *Environ. Sci. Water Res. Technol., 4*.

Tullmin, M., & Roberge, P. R. (2000). Atmospheric corrosion. *Uhlig's Corrosion Handbook*, 305.

Tveten, B., Hultquist, G., & Norby, T. (1999). Hydrogen in chromium: influence on the high-temperature oxidation kinetics in O2, oxide-growth mechanisms, and scale adherence. *Oxidation of Metals*, *51*(3), 221-233.

UHLIG, H. (2000). Corrosion Handbook. Wiley, New York (Second edition edited by W. Revic in 2000).

Ulaeto, S. B., Pancrecious, J. K., Rajan, R., Rajan, T. P. D., & Pai, B. C. (2018). Role of Nanodispersoids on Corrosion Inhibition Behavior of Smart Polymer Nanocomposite Coatings. In *Advanced Polymeric Materials for Sustainability and Innovations* (pp. 303-348). CRC Press.

Umoren, S, A.; Solomon, M. M.&Saji, V. S. (2022). Fundamentals of Corrosion Inhibition. In *Polymeric Materials in Corrosion Inhibition*; Elsevier, pp 103–127. https://doi.org/10.1016/B978-0-12-823854-7.00026-6.

Umoren, S. A., & Solomon, M. M. (2017). Synergistic corrosion inhibition effect of metal cations and mixtures of organic compounds: a review. *Journal of environmental chemical engineering*, *5*(1), 246-273.

Umoren, S. A., & Solomon, M. M. (2017). Synergistic Corrosion Inhibition Effect of Metal Cations and Mixtures of Organic Compounds: A Review. *Biochem. Pharmacol., 5*.

Umoren, S. A., &Eduok, U. M. (2016). Application of Carbohydrate Polymers as Corrosion Inhibitors for Metal Substrates in Different Media: A Review. *Carbohydr. Polym., 140*.

Umoren, S. A., Solomon, M. M., Obot, I. B., & Suleiman, R. K. (2019). A Critical Review on the Recent Studies on Plant Biomaterials as Corrosion Inhibitors for Industrial Metals. *J. Ind. Eng. Chem., 76*.

Valle-Molina, C., Alamilla, J. L., Sánchez-Moreno, J., Najjar, S. S., & López-Acosta, N. P. (2014). Reliability functions for buried submarine pipelines in clay subjected to upheaval buckling. *Applied Ocean Research*, *48*, 308-321

Vanmarcke, E. (2010). *Random fields: analysis and synthesis*.

Verma, C., Ebenso, E. E., & Quraishi, M. A. (2017a). Corrosion Inhibitors for Ferrous and Non-Ferrous Metals and Alloys in Ionic Sodium Chloride Solutions: A Review. *J. Mol. Liq., 248*.

Verma, C., Ebenso, E. E., & Quraishi, M. A. (2017b). Ionic liquids as green and sustainable corrosion inhibitors for metals and alloys: an overview. *Journal of Molecular Liquids*, *233*, 403-414.

Verma, C., Ebenso, E. E., Bahadur, I., & Quraishi, M. A. (2018). An Overview on Plant Extracts as Environmentally Sustainable and Green Corrosion Inhibitors for Metals and Alloys in Aggressive Corrosive Media. *J. Mol. Liq.*, *266*.

Verma, C., Ebenso, E. E., Quraishi, M. A & Hussain, C. M. (2021). Recent Developments in Sustainable Corrosion Inhibitors: Design, Performance and Industrial Scale Applications, *Mater. Adv.*, *2* (12), 3806–3850. https://doi.org/10.1039 /D0MA00681E

Verma, C., Lgaz, H., Verma, D. K., Ebenso, E. E., Bahadur, I., & Quraishi, M. A. (2018). Molecular dynamics and Monte Carlo simulations as powerful tools for study of interfacial adsorption behavior of corrosion inhibitors in aqueous phase: A review. *Journal of Molecular Liquids*, *260*, 99–120. https://doi.org/10.1016/j.molliq.2018.03.045

Verma, C., Obot, I. B., Bahadur, I., Sherif, E. S. M & Ebenso, E. E. (2018). Choline Based Ionic Liquids as Sustainable Corrosion Inhibitors on Mild Steel Surface in Acidic Medium: Gravimetric, Electrochemical, Surface Morphology, DFT and Monte Carlo Simulation Studies, *Applied Surface Science*, *457*, 134–149. https://doi.org/10.1016/j.apsusc.2018.06.035

Verma, C., Olasunkanmi, L. O., Ebenso, E. E., & Quraishi, M. A.(2018). Substituents Effect on Corrosion Inhibition Performance of Organic Compounds in Aggressive Ionic Solutions: A Review. *J. Mol. Liq.*, *251*.

Verma, C., Olasunkanmi, L. O., Ebenso, E. E., Quraishi, M. A., &Obot, I. B. (2016). Adsorption Behavior of Glucosamine-Based, Pyrimidine-Fused Heterocycles as Green Corrosion Inhibitors for Mild Steel: Experimental and Theoretical Studies. *J. Phys. Chem. C*, *120*.

Verma, C., Quraishi, M. A & Ebenso, E. E. (2018). Microwave and Ultrasound Irradiations for the Synthesis of Environmentally Sustainable Corrosion Inhibitors: An Overview, *Sustainable Chemistry and Pharmacy*, *10*, 134–147. https://doi.org/10.1016/j.scp.2018.11.001

Verma, C., Quraishi, M. A., & Singh, A. (2015). 2-Amino-5-Nitro-4,6-Diarylcyclohex-1-Ene-1,3,3-Tricarbonitriles as New and Effective Corrosion Inhibitors for Mild Steel in 1 M HCl: Experimental and Theoretical Studies. *J. Mol. Liq.*, *212*.

Verma, C., Saji, V. S., Quraishi, M. A., &Ebenso, E. E. (2020). Pyrazole Derivatives as Environmental Benign Acid Corrosion Inhibitors for Mild Steel: Experimental and Computational Studies. *J. Mol. Liq.*, *298*.

Verma, C., Sorour, A. A., Ebenso, E. E., & Quraishi, M. A. (2018). Inhibition Performance of Three Naphthyridine Derivatives for Mild Steel Corrosion in 1 M HCl: Computation and Experimental Analyses. *Results Phys.*, *10*.

Verma, D. K., & Khan, F. (2016). Green Approach to Corrosion Inhibition of Mild Steel in Hydrochloric Acid Medium Using Extract of Spirogyra Algae. *Green Chem. Lett. Rev.*, *9*.

Vermilyea, D. A. (1972). A theory for the propagation of stress corrosion cracks in metals. *Journal of the Electrochemical Society*, *119*(4), 405.

von WolzogenKuhr, C. A. H. (1961). Unity of anaerobic and aerobic iron corrosion process in the soil. *Corrosion*, *17*(6), 293t-299t.

Vu, K. A. T., & Stewart, M. G. (2000). Structural reliability of concrete bridges including improved chloride-induced corrosion models. *Structural safety*, *22*(4), 313-333.

Vu, T. V., Nguyen, T. V., Tabish, M., Ibrahim, S., Hoang, T. H. T., Gupta, R. K., ... & Yasin, G. (2021). Water-borne ZnO/acrylic nanocoating: fabrication, characterization, and properties. *Polymers*, *13*(5), 717.

Vukasovich, M. S., Arbor, A., & Farr, J. P. G. (1986). Molybdate in Corrosion Inhibition-A Review. *Polyhedron*, *5*.

Wan, Hongxia& Song, Dongdong& li, Xiaogang& Zhang, Dawei& Gao, Jin& Du, Cuiwei. (2017). Effect of Zinc Phosphate on the Corrosion Behavior of Waterborne Acrylic Coating/Metal Interface. Materials. 10. 654. 10.3390/ma10060654.

Wang, P., Xiong, L., He, Z., Xu, X., Hu, J., Chen, Q., Zhang, R., Pu, J., & Guo, L. (2022).

Wang, X., Yang, H., & Wang, F. (2011). An Investigation of Benzimidazole Derivative as Corrosion Inhibitor for Mild Steel in Different Concentration HCl Solutions. *Corros. Sci.*, *53*.

Wanhill, R, J, H., Molent, L. & Barter, S, A. (2021). milestone case histories in aircraft structural integrity: Draft 2021. https://doi.org/10.13140/RG.2.2.11758.74562.

Wen, X., Bai, P., Luo, B., Zheng, S., & Chen, C. (2018). Review of Recent Progress in the Study of Corrosion Products of Steels in a Hydrogen Sulphide Environment. *Corros. Sci.*, *139*.

Wildey, J, F II. (1990). Aging Aircraft, Materials Performance, March 1990, pp.80-85.

Williams, L. P. (1965). Michael Faraday (1791–1867). *The Physics Teacher*, *3*(2), 64-70.

Winkler, D. A.; Breedon, M.; Hughes, A. E.; Burden, F. R.; Barnard, A. S.; Harvey, T. G. & Cole, I. (2014). Towards Chromate-Free Corrosion Inhibitors: Structure–Property Models for Organic Alternatives. *Green Chem*, *16* (6), 3349–3357

Witte, F., Kaese, V., Haferkamp, H., Switzer, E., Meyer-Lindenberg, A., Wirth, C. J., &Windhagen, H. (2005). In vivo corrosion of four magnesium alloys and the associated bone response. *Biomaterials*, *26*(17), 3

Wonnie Ma, I. A., Shafaamri, A., Kasi, R., Zaini, F. N., Balakrishnan, V., Subramaniam, R., &Arof, A. K. (2017). Anticorrosion Properties of Epoxy/Nanocellulose Nanocomposite Coating. *Bioresources*, *12*.

Wu, L., Wang, C., Pokharel, D, B., Etim, I, N., Zhao, L., Dong, J., Ke, W., & Chen, N. (2018) Effect of applied potential on the microstructure, composition and corrosion resistance evolution of fluoride conversion film on AZ31 magnesium alloy[J]. J. Mater. Sci. Technol., 34(11): 2084-2090

Yan, M., Sun, C., Xu, J.,&Ke, W. (2014). Anoxic Corrosion Behavior of Pipeline Steel in Acidic Soils. Industrial & Engineering Chemistry Research 53 (45), 17615-17624

Yoganandan, G.; Pradeep Premkumar, K &Balaraju, J. N. (2015). Evaluation of Corrosion Resistance and Self-Healing Behavior of Zirconium–Cerium Conversion Coating Developed on AA2024 Alloy. *Surface and Coatings Technology, 270*, 249–258.

Yohai, L., Schreiner, W., Vázquez, M., &Valcarce, M. B. (2016a). Phosphate Ions as Effective Inhibitors for Carbon Steel in Carbonated Solutions Contaminated with Chloride Ions. *Electrochim. Acta, 202*.

Yohai, L., Valcarce, M. B., & Vázquez, M. (2016b). Testing Phosphate Ions as Corrosion Inhibitors for Construction Steel in Mortars. *Electrochim. Acta, 202*.

Yuhuan, B., Wenxiang, D (2020). IOP Conf. Ser.: Mater. Sci. Eng. 772 012099

Yurt, A., Duran, B., & Dal, H. (2014). An Experimental and Theoretical Investigation on Adsorption Properties of Some Diphenolic Schiff Bases as Corrosion Inhibitors at Acidic Solution/Mild Steel Interface. *Arab. J. Chem., 7*.

Zhang, D., Tang, Y., Qi, S., Dong, D., Cang, H., & Lu, G. (2016a). The Inhibition Performance of Long-Chain Alkyl-Substituted Benzimidazole Derivatives for Corrosion of Mild Steel in HCl. *Eval. Program Plann., 102*.

Zhang, D., Wang, L., Qian, H., & Li, X. (2016b). Superhydrophobic surfaces for corrosion protection: a review of recent progresses and future directions. *Journal of Coatings Technology and Research*, *13*(1), 11-29.

Zhang, F., Liu, Z. G., Zeng, R. C., Li, S. Q., Cui, H. Z., Song, L., & Han, E. H. (2014). Corrosion resistance of Mg–Al-LDH coating on magnesium alloy AZ31. *Surface and Coatings Technology*, *258*, 1152-1158.

Zhang, G., Wu, L., Tang, A., Ma, Y., Song, G. L., Zheng, D., ... & Pan, F. (2018). Active corrosion protection by a smart coating based on a MgAl-layered double hydroxide on a cerium-modified plasma electrolytic oxidation coating on Mg alloy AZ31. *Corrosion Science*, *139*, 370-382.

Zhang, Y., Cheng, Y., Ma, F., & Cao, K. (2019). Corrosion Inhibition of Carbon Steel by 1-Phenyl-3-Amino-5- Pyrazolone in H2SO4 Solution. *Int. J. Electrochem. Sci., 14*.

Zhu, Z., Fu, J., Pei, F., Tan, Z., Tian, X., Mao, R., & Wang, L. (2013). Influence of moisture on corrosion behaviour of steel ground rods in mildly desertified soil. *Anti-Corrosion Methods and Materials*, *60*(3), 148-152.

Zhuang, J. J., Guo, Y. Q., Xiang, N., Xiong, Y., Hu, Q.,& Song, R. G. (2015). A study on microstructure and corrosion resistance of ZrO2-containing PEO coatings formed

on AZ31 Mg alloy in phosphate-based electrolyte. *Applied Surface Science, 357*, 1463-1471.

Zoran, C, P. (2016). Corrosion in airframes, Serbian Armed Forces, AF and AD, 204th Aviation Brigade, Batajnica, Republic of Serbia

APPENDICES

Activities/experimental procedures being carried out at theACE-FUELS General Purpose Research Laboratory

Plate 7.1: Test running the Metallographic Lapping/Polishing machine (UNIPOL 820)

Plate 7.2: Mr. IdemaOsuaniFyneface Using the Metallographic Lapping and Polishing machine(UNIPOL 820)to polish test coupons.

Plate 7.3: Using the FA2104 Electronic weighing balance to measure grinded MPL samples for preparation of extract-based corrosion inhibitor.

Plate 7.4: Using the magnetic stirrer to stir the the sample of MPL in ethanol to extract the inhibitor

Plate 7.5: Determining the inhibitor concentrations, with Idema Osuani Fyneface is Dr. I. Arukalam (Supervisor)

Plate 7.6: MPL extract-based inhibitor concentrations determined and poured out in various containers getting ready to be used.

Plate 7.7: Mr. Idema Osuani Fyneface(PhD Research Student) and Dr. I. Arukalam (Project Supervisor) Simulating the test environment.

Plate 7.8: Coupons immersed in 3.5wt.% NaCl test environment.